HEALTH MONITORING OF SACRIFICIAL ANODE THROUGH PZT TRANSDUCER

A Dissertation Report Submitted in Partial Fulfilment of the Requirement

For the Award of Degree of

MASTER OF ENGINEERING

IN

STRUCTURAL ENGINEERING

Submitted by-

SAHIL KUMAR

802224017

Under the supervision of

Dr. Shweta Goyal

Professor, CED

Dr. Arpit Goyal

Assistant Professor, CED

THAPAR INSTITUTE
OF ENGINEERING & TECHNOLOGY
(Deemed to be University)

Department Of Civil Engineering

Thapar Institute of Engineering and Technology

(Deemed To Be University)

Patiala-147004 (Punjab)

September 2024

DECLARATION

I hereby declare that the work which is presented in this Dissertation Report entitled **"HEALTH MONITORING OF SACRIFICIAL ANODE THROUGH PZT TRANSDUCER"** as per the requirement for the award of Master of Engineering in Structures, submitted in the Department of civil engineering, Thapar Institute of Engineering & Technology (Deemed to be University), Patiala, is a review carried out by me under the guidance of Dr. Shweta Goyal, professor, Department of Civil Engineering, Thapar Institute of Engineering & Technology, Patiala. Dr. Arpit Goyal, Assistant professor, Department of Civil Engineering, Thapar Institute of Engineering & Technology, Patiala.

DATE: 19/9/24

SAHIL KUMAR
802224017

Certificate

This is to certify that the above declaration made by the student concerned is correct according to the best of my knowledge and belief.

Dr. Shweta Goyal
Professor, CED

Dr. Arpit Goyal
Assistant Professor, CED

Thapar Institute of Engineering & Technology, Patiala

ACKNOWLEDGEMENT

I wish to express my deep gratitude to **Dr. Shweta Goyal, Professor,** Department of Civil Engineering, Thapar Institute of Engineering and Technology (Deemed to be University), Patiala, and **Dr. Arpit Goyal, Assistant Professor,** Department of Civil Engineering, Thapar Institute of Engineering and Technology (Deemed to be University), Patiala, for providing guidance, support, and patience in listening to my ideas and suggesting me with new ways for implementation and for the motivation and inspiration that encouraged me throughout my work. I would also like to thank all my colleagues for providing me with all the help and facilities required for completing this Dissertation report.

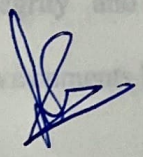

SAHIL KUMAR

82224017

ABSTRACT

This research investigates the long-term viability and effectiveness of sacrificial galvanic anodes in reinforced concrete structures, employing advanced testing, monitoring, and analysis techniques. By focusing on potential difference measurements, health monitoring using PZT transducers, and conductance data, the study provides comprehensive insights into the corrosion protection mechanisms offered by galvanic anodes. Results reveal a high initial rate of corrosion protection, with effectiveness diminishing over time as the anode nears the end of its service life. Continuous monitoring is emphasized as critical for maintaining corrosion protection and ensuring the durability of reinforced concrete. The research compares the performance of two anode types, with Anode A demonstrating superior stability and resistance to degradation compared to Anode B. Furthermore, the study identifies RMSD% as an effective indicator of anode degradation and potential life span, while conductance measurements provide real-time insights into corrosion progression. The findings also confirm the efficacy of cathodic protection through 100 mV depolarization testing. Overall, this study underscores the importance of advanced, non-destructive monitoring techniques to ensure the structural integrity and long-term durability of critical infrastructure, particularly in high-risk environments like bridges and marine installations.

TABLE OF CONTENT

LIST OF FIGURE

LISTS OF TABLES

CHAPTER 1 INTRODUCTION

1.1 GENERAL

The natural and spontaneous process of corrosion causes pure metals and their alloys to react chemically or electrochemically with their surroundings, transforming them into a variety of stable forms including sulfides, oxides, hydroxides, etc. Industrial assets, structures, railroad bridges, transportation, and residential areas are all negatively impacted by corrosion. In the world, corrosion results in economic losses of almost 2.5 trillion USD, or nearly 3.4 percent of GDP, according to a NACE 2016 research. It is possible to decrease corrosion expenses by 15-35% ($375-875 billion) by effectively utilizing the current anti-corrosion technologies. The significant financial and safety risks linked to corrosion make it a crucial subject for scientists and engineers operating in the field of corrosion science and technology worldwide(Verma *et al.*, 2018)**.**

Metallic and non-metallic materials are destroyed by corrosion over time as a result of chemical and electrochemical reactions with their surroundings. Ores and stable compounds are the result of refined metals being released from their higher energy state and back into their lower energy state by natural chemical recombination. Although many other metals can also corrode, iron and steel corrosion accounts for a large portion of this damage. Leaks of liquid or gas can result from corrosion damage. The structure's deterioration from corrosion and eventual structural breakdown are even more harmful. Thus, metal corrosion is a major industrial and economic issue for which there is a constant need for study into potential remedies. In building sites, petrochemical processing, and other industries, corrosion results in structural damage to metal and alloy-based equipment and components.(Aslam *et al.*, 2022).

Steel reinforcement in concrete is done to strengthen the structural element in tension, because concrete is weak in it, but as a result of steel corrosion, structures break. It has grown to be a significant and global issue, requiring costly repairs that now cost billions of dollars annually.

Numerous intangible losses also exist, such as the energy needed to make replacements for rusted objects. Steel corrosion in reinforced concrete shortens the structure's lifespan and possibly has the potential to collapse it.(Qureshi *et al.,* 2019).

1.2 IMPACT OF CORROSION

Corrosion is a major challenge in terms of its economic, environmental, safety and public health implications. Available data indicate that corrosion losses are significant, with annual costs in the billions of dollars in several industries, including, but not limited to, oil and gas, aerospace, marine and agriculture. In addition, corrosion is a continuous process that affects the longevity and efficiency of structures, equipment and industrial equipment. In general, corrosion is a serious problem that requires effective preventive measures to protect materials from its harmful effects and minimize the resulting economic and environmental losses. Among the various strategies available to prevent or mitigate the degradation or depreciation of metal surfaces, the use of corrosion inhibitors (CI) is one of the most powerful methods to protect metal surfaces from the harmful effects of corrosion. Due to its ease of use and cost-effectiveness, this method has gained significant traction and is rapidly growing in popularity(Elyoussfi *et al.*, 2023).

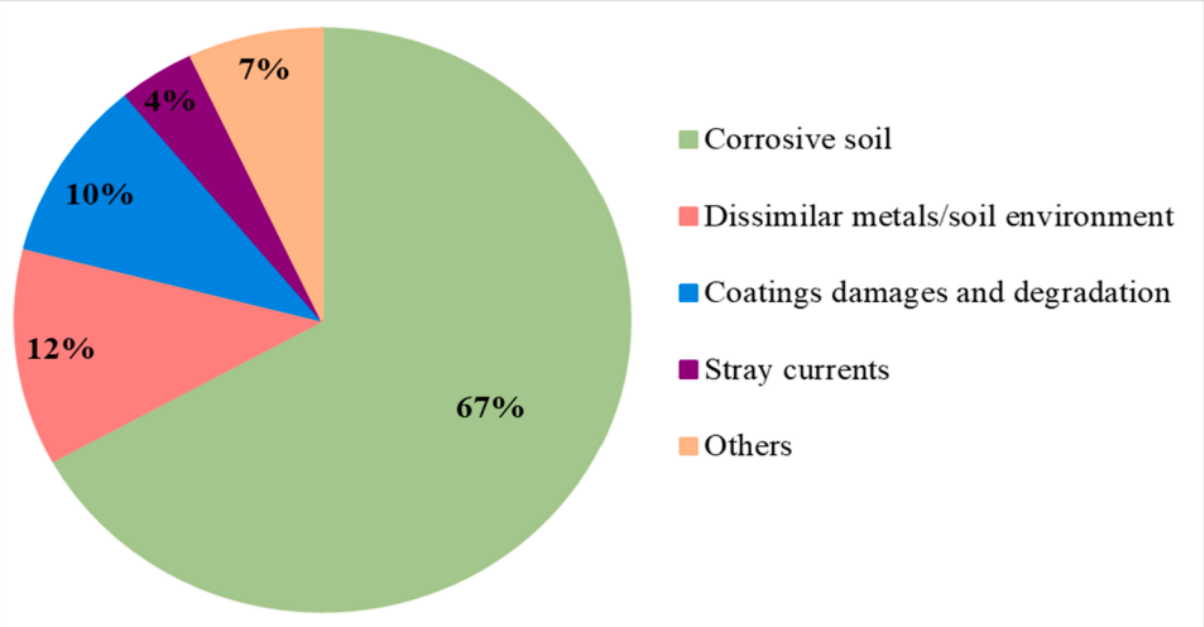

Figure 1. 1 Primary Factors Contributing to Corrosion in Metal Pipelines (Farh, Ben Seghier and Zayed, 2023).

1.1.1. IMPACT OF CORROSION ON REINFORCEMENT

One of the most significant harms to reinforced concrete worldwide during its life cycle is reinforcement corrosion. Damage to reinforced concrete structures is commonly attributed to harsh weather conditions and aggressive chemical agents. Numerous vital energy and transportation facilities are located in coastal locations, where they are subjected to high humidity and chloride concentrations, making reinforcement corrosion a serious risk. This calls for modernizing techniques that guarantee the corrosion-weakened reinforced concrete structures' strength and longevity.(Zabihi-Samani *et al.*, 2018).

An increasing number of concrete structures are vulnerable to embedded reinforcement corrosion. Long-term exposure to harsh factors, such as ocean chlorides and de-icing salts or compounds combined with chlorides, is the cause of this; carbonation will rise in both situations. Because of the lesser quality concrete and thinner cover depth, many older structures are often more vulnerable than those built today. When the cross section of the steel and concrete is lost due to corrosion of the reinforcement, the structure's serviceability and

eventually its safety are reduced. As a result, during the past 30 years, concrete structure preservation and repair have grown to be significant industries. However, traditional methods of repairing concrete have frequently failed to show themselves to be reliable or long-lasting.(Polder and Peelen, 2018).

Surface losses occur when metals and alloys interact with their surroundings chemically, biochemically, or electrochemically. This results in the formation of more thermodynamically stable oxides, hydroxides, or carbonates. We refer to this process as corrosion. The anodic and cathodic regions of the steel, together with the pore water of the hardened cement paste acting as the electrolyte, combine to form the concrete on the surface of the embedded steel bar, which functions as an electrochemical cell under an electric potential difference. As a result, a current flows across the system, attacking the metal that has a higher electrode potential—the anode—while sparing the cathode. Consequently, long-term armature corrosion starts.(Goyal *et al.*, 2018).

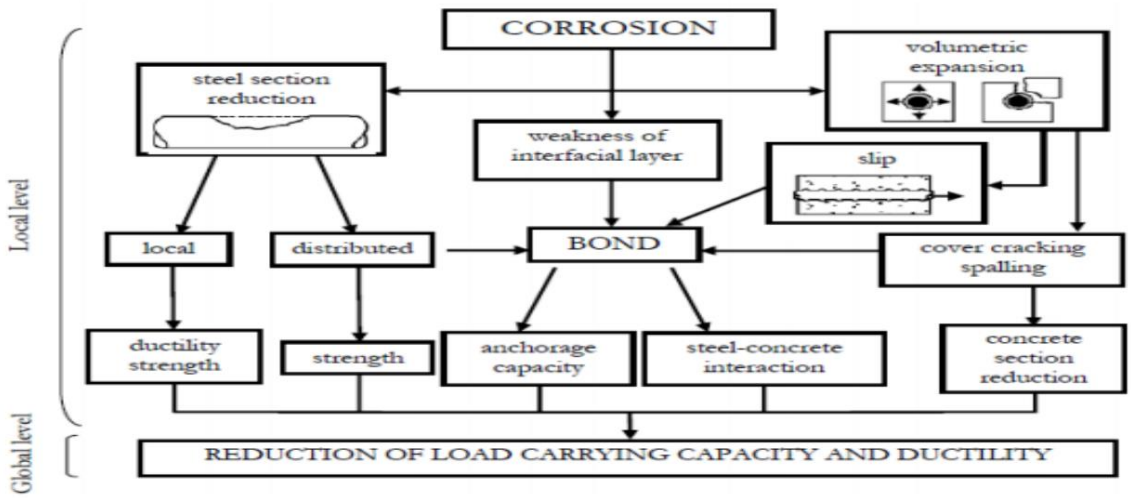

Figure 1. 2 Impact of Corrosion on Structural Performance (Goyal et al., 2018)

1.3 MECHANISM OF CORROSION IN STRUCTURE

Chloride-induced corrosion in concrete requires priority research in aggressive environments beyond the effects of carbonation. When chloride ions migrate into the concrete surface, passivation occurs, increasing corrosion. In particular, an anode cavity is formed on the surface of the steel during this process, where chloride ions work exclusively as catalysts without wear. The basic principle of steel corrosion, which is the process by which iron at the anode loses electrons and becomes iron oxide. The steel matrix loses mass as a result of this corrosion process, and corrosion products show up on the surface of the reinforcement. Once corrosion has started, the volume expansion of these corrosion products, which varies by a factor of 2–6, produces a propagation stress that leads to cracking. After that, the microcracks offer an avenue for rapid ion migration. There are three stages to the complete corrosion process: (A) As corrosion ions seep into the concrete, they build up until a certain level of chloride is present. (b) Microcracks are caused by corrosion. (c) Cracks propagate to the code-imposed width limit. When this width is exceeded, there is a risk.

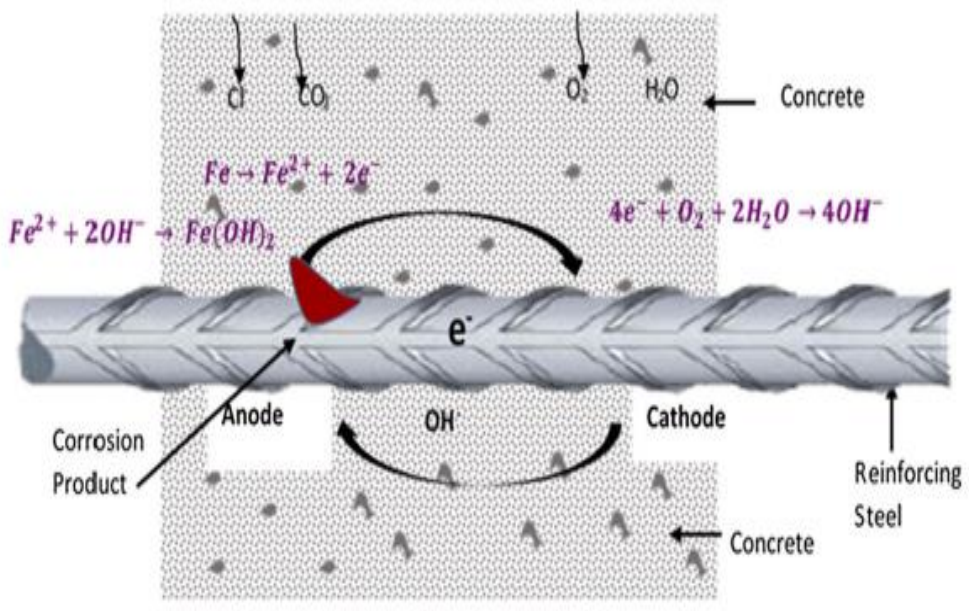

Figure 1. 3 Diagram of the Corrosion Process in Concrete (Goyal et al., 2018)

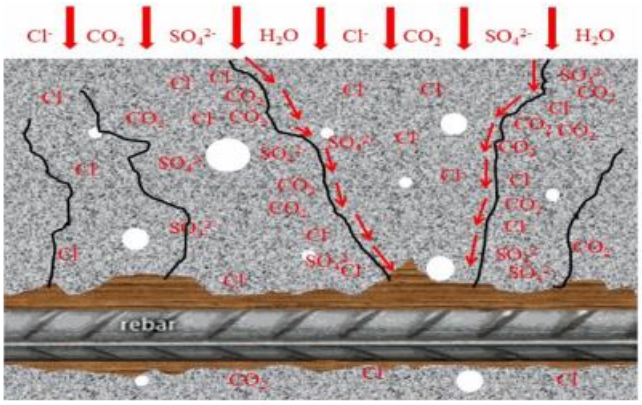

Figure 1. 4 Illustration of Reinforcement Corrosion in Concrete (Li et al., 2021)

Pouring the steel into the concrete as soon as the cement starts to hydrate creates a passive layer of protection on the surface that is between 10−3 and 10−1 μm thick and is made of γ-Fe2O3 that is securely linked to the steel. This layer slows down the pace of corrosion by obstructing the flow of ions between the steel and the surrounding concrete. This oxide coating shields the steel from deterioration. The only pH range at which it is stable is 12–14. This layer has to be disrupted in order for corrosion to happen. Corrosion happens when water and oxygen are present, and this happens when carbonate or chloride ions are present or when the concrete is of low quality.

Anodic Reaction

$Fe \rightarrow Fe^{2+} + 2e^{-}$ (1)

$Fe^{2+} + 2OH^{-} \rightarrow Fe(OH)_2$

(Ferrous hydroxide) (2)

$4Fe(OH)_2 + 2H_2O + O_2 \rightarrow 4Fe(OH)_3$

(Ferric hydroxide) (3)

$2Fe(OH)_3 \rightarrow Fe_2O_3 \cdot H_2O + 2H_2O$

(Hydrated Ferric oxide) (4)

Cathodic Reaction

4e− + O2 + 2H2O → 4OH− (5)

These processes result in the production of rust, or hydrogenated iron oxide, which is very porous and has a volume six to ten times that of steel. Rust causes spalling and cracking. In Figure 3, the overall response mechanism is described. Every reaction listed in Equations 6 and 7 results in the reduction of iron at the anode and oxygen at the cathode:

Fe → Fe2+ + 2e− eo = −0.688 VSCE (6)

Fe + OH− → [Fe(OH)]ads + e− →

Fe(OH) + + H+ + 2e− eo = −0.404 VSCE (7)

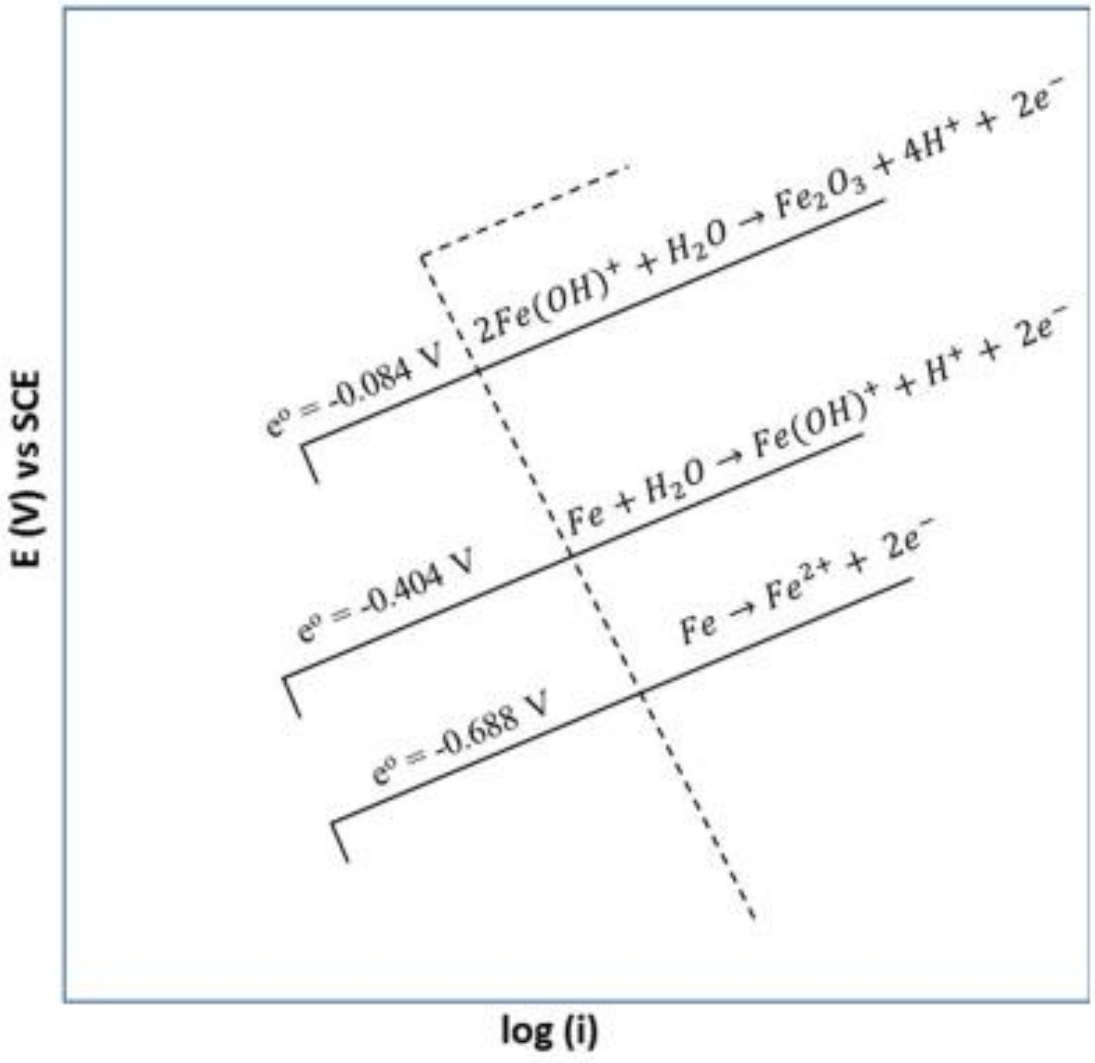

Figure 1. 5 Corrosion reaction mechanism (Goyal et al., 2018)

The presence of OH− ions is necessary for the production of Fe(OH)+. During the production of Fe2+ ions, OH− ions migrate from the bulk to the surface in order to preserve electrical neutrality. Equation 7 is better for the iron surface at high pH than Equation 6. The electrode potential shifts to a more anodic direction and raises the concentration of Fe(OH)+ on the steel surface as a result of collecting Fe(OH)+ ions. Equation 8 states that Fe(OH)+ oxidizes to iron oxide and forms a barrier oxide layer. It shields the steel in a passive manner. Corrosion cannot start until aggressive materials, such as chloride ions or a pH decrease, pass through this passive layer.

$$Fe(OH) + + H2O \rightarrow Fe2O3 + 4H+ + 2e-$$

$$eo = -0.084 \text{ VSCE} \quad (8)$$

(Goyal *et al.*, 2018)

1.4 CORROSION PROTECTION AND CONTROL TECHNIQUES

The two primary categories of corrosion protection and control techniques are internal and exterior corrosion protection.

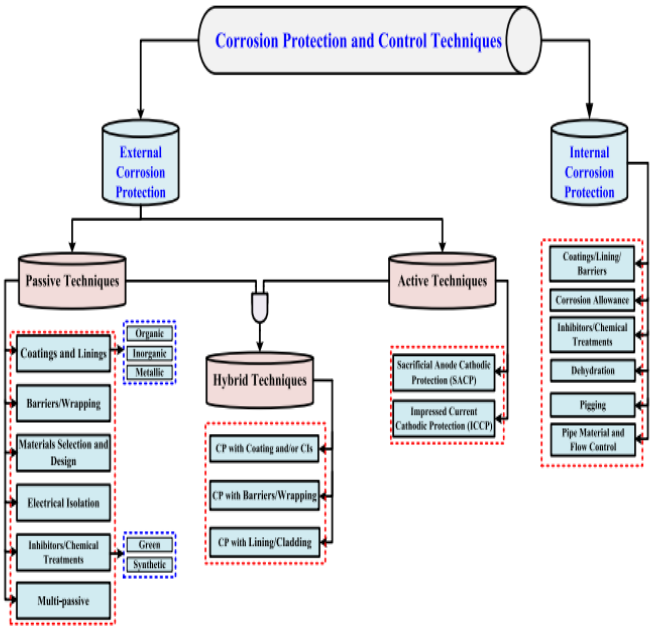

Figure 1. 6 Categories of Corrosion Protection and Control Techniques(Farh, Ben Seghier and Zayed, 2023)

1.5 PZT

Lead Zirconate Titanate (PZT) is a widely used piezoelectric material recognized for its high piezoelectric coefficients and exceptional electromechanical coupling capabilities, making it ideal for various applications, particularly in structural health monitoring systems. Operating on the principle of the piezoelectric effect, PZT generates an electric field in response to mechanical stress and vice versa, which enables its use in both sensors and actuators for assessing structural health. In concrete structures, PZT transducers are employed to monitor critical properties such as early age hydration, stiffness development, and compressive strength gain, thereby contributing significantly to effective structural evaluation. Additionally, when combined with Electro-Mechanical Impedance (EMI) techniques, PZT sensors provide real-time damage detection, concrete strength assessment, and corrosion monitoring, underscoring their versatility in structural health monitoring applications.(Shi *et al.*, 2019)

1.6 WORKING OF PZT

Lead Zirconate Titanate (PZT) operates on the principle of the piezoelectric effect, where mechanical stress induces an electric field and an applied electric field generates mechanical strain. This dual functionality makes PZT a vital material for sensors and actuators, particularly in structural health monitoring systems. When subjected to a variable electric field, PZT transducers undergo axial vibrations, leading to changes in impedance that can be meticulously analyzed to detect alterations in the material's properties. The effectiveness of PZT in damage detection is rooted in its sensitivity to shifts in the peak frequencies of the impedance spectrum, with the resonant modes of the material significantly enhancing the sensitivity to minute changes, thereby providing highly accurate assessments of structural integrity.(Hire, Hosseini and Moradi, 2021)

1.7 PZT ON ANODE

PZT transducers are strategically attached to sacrificial anodes to monitor corrosion levels by analyzing changes in conductance spectra over time as the anode undergoes accelerated corrosion, typically induced by the application of impressed current. The PZT transducer is securely affixed to the polished surface of the anode using instant adhesive, enabling it to accurately measure the electromechanical impedance of the anode during corrosion monitoring experiments. To safeguard the transducer from the corrosive effects of the liquid electrolyte used in these experiments, a protective layer of waterproofing epoxy is applied, ensuring the durability and reliability of the PZT during prolonged exposure. The interaction between the PZT transducer and the surrounding environment plays a crucial role in the monitoring process. When the smart anode, embedded with the PZT transducer, is placed within a conductive mortar or concrete block, the quality factor of the electromechanical resonances is altered, which in turn impacts the conductance spectra and impedance measurements. This setup allows the PZT transducer to provide detailed insights into the corrosion process, making it an effective tool for real-time structural health monitoring. (Talakokula *et al.*, 2016) (Tamhane *et al.*, 2022)

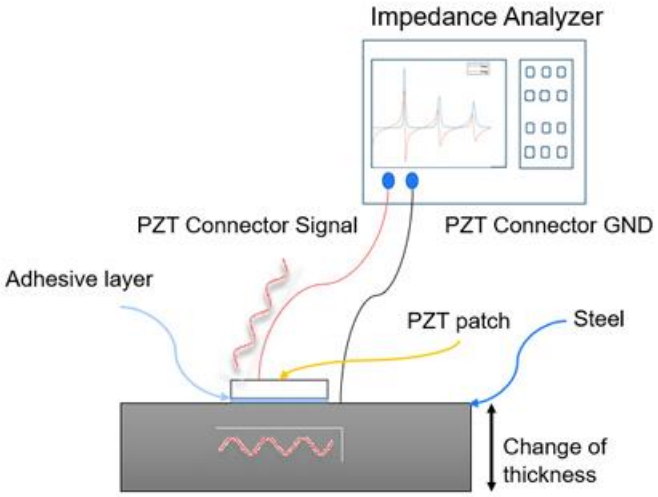

Figure 1. 7 Working of PZT

1.8 SCOPE OF THE STUDY

This study investigates the long-term viability and effectiveness of sacrificial anodes in reinforced concrete structures, focusing on potential difference measurements, health monitoring, and the use of advanced sensors. It aims to develop and validate methods to ensure the durability and performance of sacrificial anodes over extended periods. The research examines the longevity of anodes under various environmental conditions, analyzing their ability to prevent corrosion in steel reinforcements over time. By measuring the potential difference between the anode and steel, the study assesses the anode's effectiveness in maintaining protection against corrosion. Health monitoring techniques are implemented using PZT transducers and LCR meters to continuously evaluate the condition of the anodes, enabling early detection of degradation. The study also analyzes corrosion patterns to identify vulnerable areas within the concrete structure and enhance non-destructive testing methods to provide real-time data for timely maintenance. Additionally, it explores the applicability of these findings to different types of reinforced concrete structures, such as bridges and marine installations, to improve their long-term durability and safety. This research aims to contribute to effective corrosion management strategies and extend the service life of critical infrastructure.

1.9 OBJECTIVES

- Develop and evaluate a method to monitor the health and effectiveness of sacrificial anodes in reinforced concrete structures.
- Measure potential differences of steel to assess protection levels.
- Use PZT transducers and LCR meters to continuously monitor anode health and identify degradation patterns for timely maintenance.

CHAPTER 2 LITERATURE REVIEW

2.1 CATHODIC PROTECTION

Goyal *et al.*, 2020 Cathodic protection (CP) is widely used to protect reinforced concrete structures exposed to aggressive environments against corrosion. Cathodic protection works by directing a small electric current from the anode to the corroding steel, protecting it from further damage by locally adding hydroxyl ions. Cathodic protection of concrete was developed in the United States in the 1970s and was introduced in Europe in the 1980s. (Sadeghi, Musa and Nassrullah, 2019)Cathodic protection system is very expensive, so it is mostly used in the oil sector to protect oil pipelines against corrosion. The method is only applied to some special and very important RC structures due to high implementation, design and monitoring costs. If used correctly, the method completely prevents corrosion of reinforcement and can also stop corrosion where it is already present.

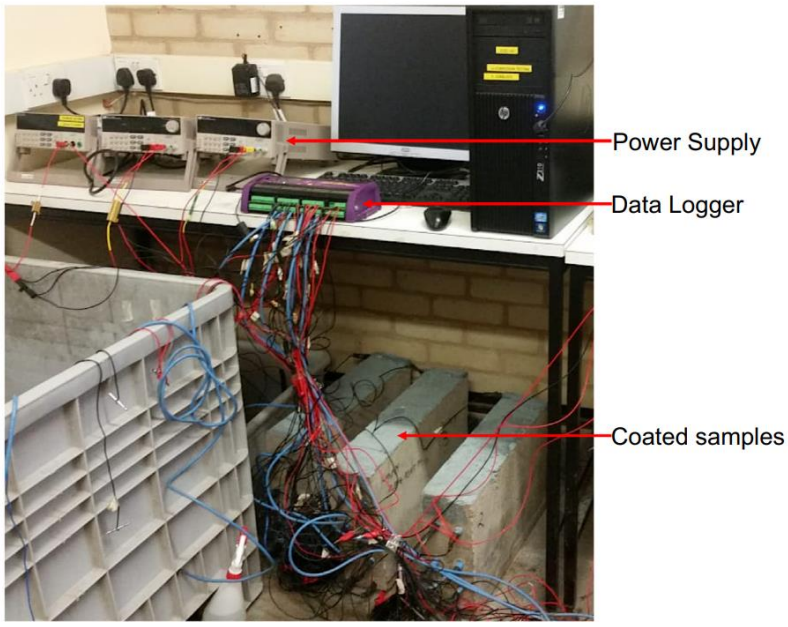

Figure 2. 1 Configuration and Connections for Cathodic Polarization of Beam Specimens (Goyal et al., 2020)

Preston 2019 When compared to concrete site repairs and cathodic protection renewals during the structure's life, cathodic protection systems for new construction are more ecologically

friendly, use less material due to reduced current needs, and have cheaper installation and operating costs.

2.2 MECHANISM OF CATHODIC PROTECTION

Martinelli-orlando, Mundra and Angst, 2023 Studied that there is still disagreement around the basic process of CP, especially when it comes to metals in porous medium like soil. By using in-situ and ex-situ characterization approaches in conjunction with electrochemical measurements to characterize the spatiotemporal changes happening at the steel-electrolyte interface, we provide a resolution to the long-standing issue. We demonstrate that the interfacial electrolyte experiences both deoxygenation and alkalinization following CP, and that an iron oxide coating may develop concurrently on the steel surface depending on polarization circumstances. In the study further show that these modifications to the interfacial electrolyte chemistry and the surface state of the steel lead to differences in the kinetics of anodic and cathodic processes.

Büchler, 2020 studied that the cathodic current-driven activation polarization can result in a shift and lower rates of corrosion, new research has shown that concentration polarization can also change the composition of soil. While ISO 8044 recognizes the importance of cathodic current in attaining activation polarization, its effectiveness is questioned due to practical difficulties in reaching large current densities. Protection criteria highlight the combined function of both polarization processes in providing efficient corrosion protection in underground pipes by correlating the consequent pH and potential changes with passivation. This growing knowledge opens the door to a more complex understanding of the electrochemical processes involved in CP by challenging an oversimplified interpretation of the material.

Polder and Peelen, 2018 According to studies, the notion of cathodic protection entails changing the steel surface's potential to greater negative values, which speeds up reduction

reactions and slows down oxidation reactions. Positive effects of the current include an increase in cathodic processes, which produce hydroxyl ions and boost pH at the steel/concrete interface. Furthermore, the negatively charged chloride ions are repelled by the steel's negative charge.

2.2.1 TYPES OF CATHODIC PROTECTION

Farh, Ben Seghier and Zayed, 2023 studied that the active corrosion prevention strategies encompass a range of methods that actively work to prevent corrosion on metal surfaces. The task involves converting all active anodic locations on the metallic pipeline to passive cathodic areas by applying a protective current. The galvanic or sacrificial anode cathodic protection (SACP) and impressed current cathodic protection (ICCP) are two widely recognized methods for corrosion prevention.

Harahap *et al.*, 2023 studied that the reinforced concrete structures frequently employ two types of cathodic protection systems: sacrificial anode cathodic protection (SACP) and impressed current cathodic protection (ICCP). The selection of the cathodic protection system is typically impacted by various considerations. This paper includes a literature review on the use of SACP (Self-Adaptive Control Parameters) and ICCP (Iterative Cross-Correlation Procedure). This article aims to compare the SACP and ICCP methodologies for reinforced concrete elements, specifically focusing on structure condition, budget, service life, maintenance, and monitoring requirements.

Polder and Peelen, 2018 researched and found that impressed current CP (ICCP) and galvanic or sacrificial CP (GCP) are the two main types of CP systems. In order to create an electric current flow, ICCP uses a low voltage direct current power supply. The anode is made up of a substance, like a conductive coating, that is either completely eaten or consumed extremely slowly. Concrete surfaces are coated with conductive coatings, which are carbon-filled

polymers that are frequently covered with a top layer for protection. Metallic conductors called primary anodes are used to supply electricity to the active anode material.

Goyal *et al.*, 2018 It was found that there are two ways to apply cathodic protection: impressed current cathodic protection, which is driven by an external power source, and sacrificial anode cathodic protection, which is a passive system. Additionally, a hybrid system that incorporates the best features of both approaches has been unveiled.

Byrne, Norton and Holmes, 2015 SACP don't last long or are unsure how long they'll work. They rely on how much electric current they give and the materials they use, like metals that wear away. When they stop working, the concrete might start to get worse. Common materials used are zinc, aluminium, and magnesium. These metals are mixed to work better and last longer. Zinc and its mixtures are often used in concrete. Aluminium and magnesium and their mixtures are used less because they can damage the concrete. Different kinds of these quick protection materials are explained next. This method is often used more than the other one because it's better for bigger and longer-lasting structures. It works well against corrosion caused by things like chloride. It can adjust to different needs. In this method, there's a special power source connected to a non-consumable anode and the metal. This makes a reaction that helps protect the metal. There are different kinds of materials used for the anode like magnetite, graphite, and more.

Table 2.1 The comparison between SACP and ICCP (Harahap *et al.*, 2023)

	Indicators	SACP	ICCP
1	Mechanism	a protection method by offering a sacrificial anode to the protected metal	a protection method that gives electrons a more negative potential so that the metal will move to the immune zone
2	Attachment to a resource	does not depend on external power sources	Depend on external power sources
3	Energy scale used	ease of installation	ICCP involves the permanent installation of a low voltage, controlled electrical system which passes direct current to the steel so that all of the steel is made into a cathode, thus preventing the steel from corroding
4	Maintenance plan	repairs can be targeted	maintenance and inspection are recommended every 20 years
5	Interactions caused by the used of cathodic protection	do not affect other structures or interaction problems	can targeted a wrong structure
6	Administrative affairs of the use	SACP is much easier and requires less involvement, as it does not require handover of documents, data turnover or transfer of knowledge	ICCP needs a regular inspection so that it makes there are several documents and data needed to to be administrative completeness
7	Cost	SACP systems are cost - effective, easy to install, do not require close supervision, and are faster in terms of the time it takes to get to an object's location, thus minimizing disruption	requires a fairly high cost, starting from installation, maintenance and routine monitoring, ongoing electricity costs, as well as the procurement of equipment and materials needed to optimize the performance of the ICCP system
8	Age of use	the anode life depends on the average amount of flow leaving the anode	selection of the right anode in the ICCP system can support long -term structural corrosion protection, which is 10 to 120 years
9	The condition of the anode	the anode connection is also protected	connected to an external power source
10	Risk of using	no chance of crop damage due to wrong connection	the risk of ICCP is stray current corrosion
11	Application of cathodic protection system	Underground protection, water heaters, above ground tanks, hulls, pipelines	Above -ground structures such as bridges car parks, marine structures and buildings

2.3 ICCP ANODES IN CATHODIC PROTECTION

Goyal, Pouya and Ganjian, 2023 Anode Material Modification: To increase the ZRP anode's electrical conductivity, graphite powder was added. The underlying material's specifics are still under wraps, but graphite powder was combined with it using naptha mild aromatic as a solvent. The powdered graphite had a specific gravity of 1.9 and a particle size of less than 53 um. Using the same methodology as in a prior study, electrical conductivity testing was used to establish the number of coats applied.

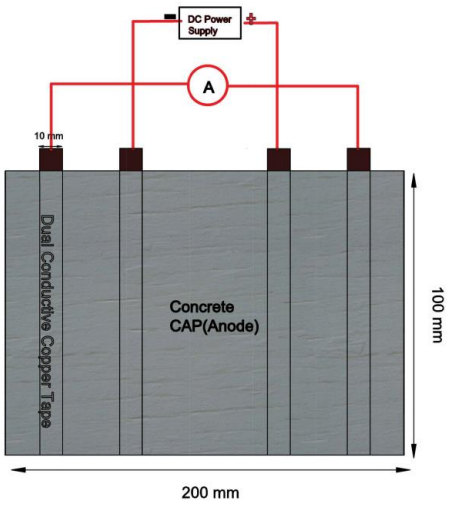

Figure 2. 2 Setup for an electrical conductivity test.(Goyal, Pouya and Ganjian, 2023; Sadeghi et al., 2023)

Electrical Conductivity Test: By varying the graphite percentage by ZRP weight from 2% to 20% and changing the solvent percentage for the appropriate consistency, the ZRP's performance was improved and concrete CAP was created. The measurements of conductance were done after NACE TM0105. Resistance was measured using dual conductive copper tape strips on plastic board specimens, and resistivity and conductivity were computed from there. Test Method: In accordance with NACE TM0294 (NACE 2007), service life testing was carried out. An uncoated titanium rod was used as the cathode, and a 20 × 20 mm Concrete CAP anode block was constructed. To polarize the anode, a continuous current of 17.8 mA was supplied through it. The electrolyte in the test was a 3% NaCl solution. A titanium rod was

utilized as the cathode for anode life testing after the anode had first been polarized under cathodic polarity. Up until anode failure, which was identified by a considerable increase in anode potential (a rise of 4.0V) and cell voltage, data were continually logged on anode potential, current, and electrolyte pH.

Analysis of Electrical Conductivity: It was discovered that the graphite content had a significant impact on the anode paint's electrical conductivity. The conductivity significantly improved with an increase in graphite from 5% to 10%; subsequent increases had little effect. Approximately 10% graphite was present in the optimum mixture for the concrete CAP anode, which provided a 99.7% reduction in resistivity when compared to the ZRP anode without graphite. Because fewer coats were required as a result of this innovation, costs were reduced. Concrete CAP was shown in the study as a useful ICCP anode system for RC constructions. It met the required standards for electrochemical performance and demonstrated satisfactory performance. With 10% graphite and 10% solvent, the final formulation provided the best electrical conductivity and ease of application. For effective ICCP, the study suggested spacing primary anode conductors at 0.70–0.8 m. With a current density of 20 mA/m^2, the concrete CAP anode's predicted service life was 45 years, suggesting that it is a viable option for prolonging the life of RC structures polluted with chloride.

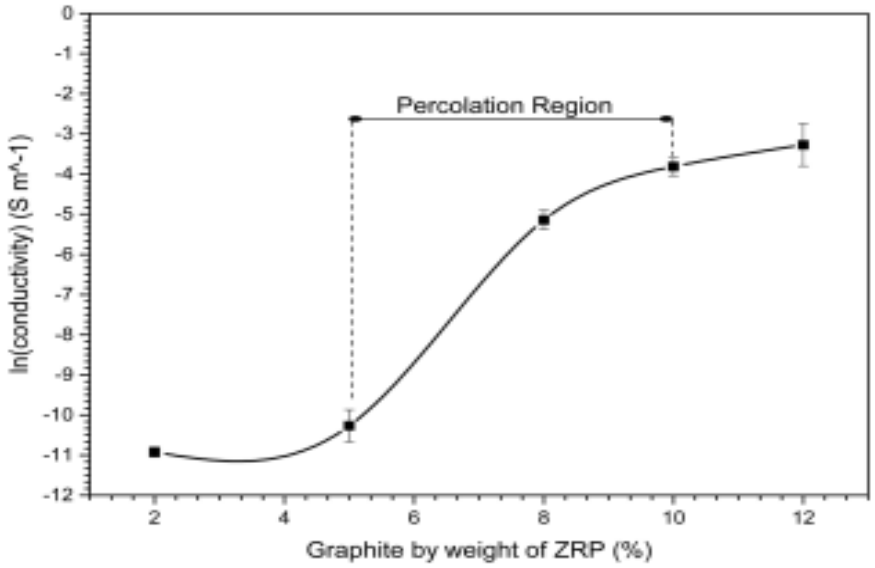

Figure 2. 3 Influence of Graphite Percentage on Anode Paint Conductivity, Highlighting the Percolation Region (Sadeghi et al., 2023)

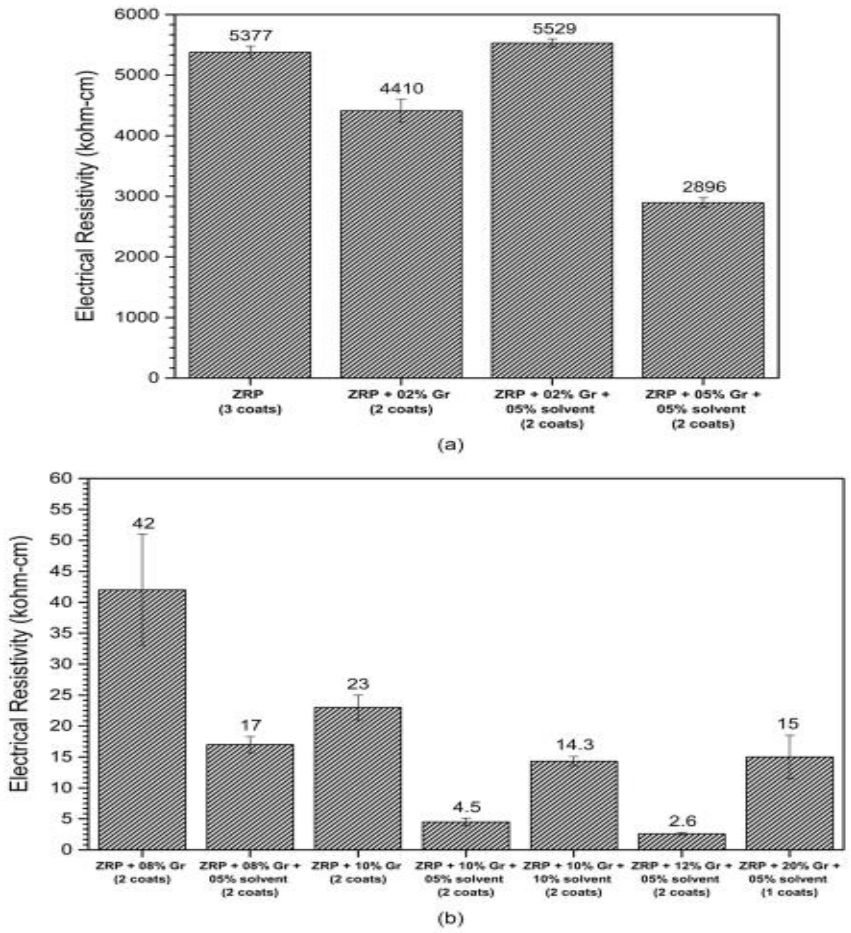

Figure 2. 4 Variation in Electrical Resistivity for Anode Paint Formulations: (a) Graphite Powder 0% to 5% and (b) Graphite Powder 8% to 10% (Sadeghi et al., 2023)

Deshpande *et al.*, 2021 utilized a solvent-based epoxy ester resin in the creation of model anticorrosion paints while studying the ICCP of mild steel in relation to zinc-based paint coatings. The binder is made of epoxy resin with a medium molecular weight that has been altered by fatty acids from tung oil. This solution has a 60% concentration. The binder's acidity is indicated by its acid number of 4. Its flow duration is 250 s, and its viscosity range, which quantifies its resistance to flow, is 2.5–5.0 Pas. Both painted and uncoated mild steel samples were submerged in a 3.5% NaCl solution and subjected to cathodic polarization experiments using an electrochemical cell fitted with a potentiostat/galvanostat. The experiments' potential range was established between 0V and 2V

Table 2.2 Cathodic polarization (Deshpande et al., 2021)

Sample	Oxygen ionization potential, mV	Concentration polarization or corrosion protection potential range		Hydrogen evolution current density
		Start, mV	End, mV	End, mA per cm ^{2}
Uncoated mild steel	687.7	699.8	990.3	458.2
Painted mild steel containing spherical zinc PVC = 61%	681.6	693.7	984.3	309.3

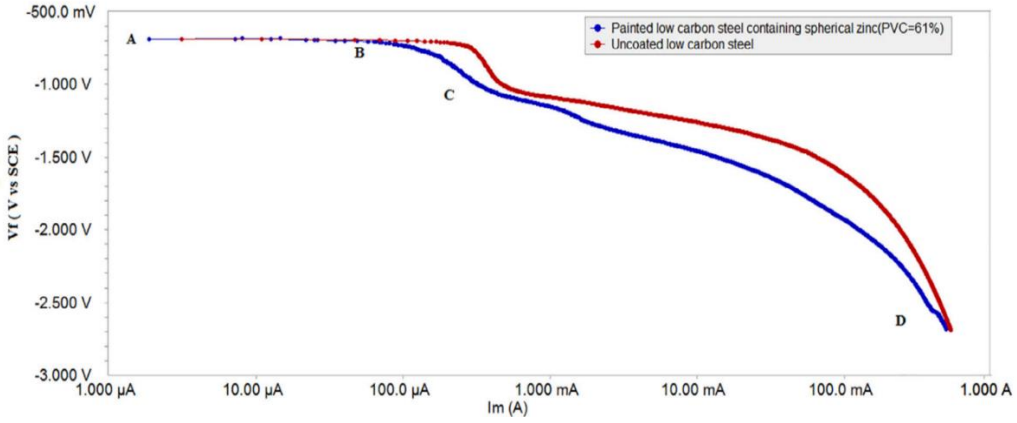

Figure 2. 5 Cathodic Polarization Curves for Mild Steel and Painted Samples in 3.5% NaCl Solution (Deshpande et al., 2021)

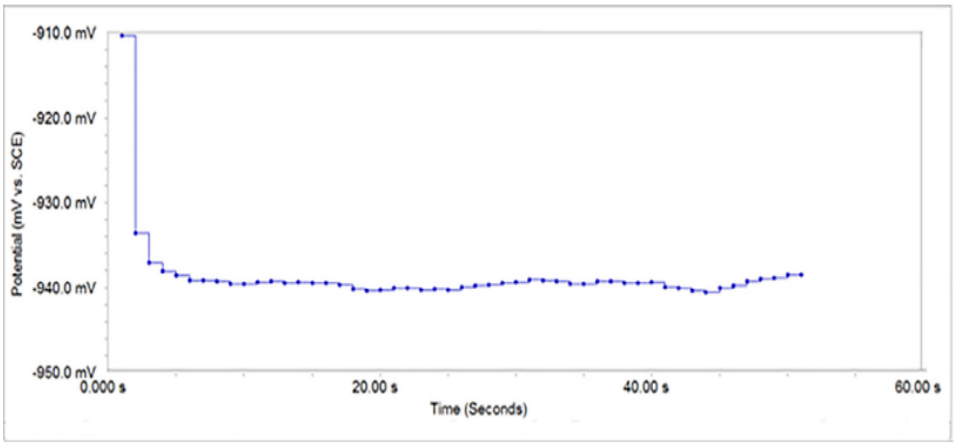

Figure 2. 6 Reduction in Cathodic Potential for Painted Mild Steel with Spherical Zinc PVC (61%) Under Impressed Current in 3.5% NaCl Solution (Deshpande et al., 2021)

Table 2.3 *Iron loss in 3.5 % NaCl solution: Samples with and without cathodic protection.*

Samples	Without cathodic protection in ppm	With cathodic protection in ppm
Mild steel	3.28	2.56
Painted mild steel containing spherical zinc PVC = 61%	2.36	0.48

Goyal, Sadeghi and Ganjian, 2019 designing a long-lasting, easily installable, and effective anode system for protection. Commercially accessible zinc-rich paint with a solvent basis that combines a binder, aromatic hydrocarbons, and zinc powder. Applyable in different air conditions by brushing, rollerblading, spraying, or dipping. Commercial confidentiality prevents the disclosure of specific paint information. C32/40 grade concrete specimens cast at a 0.5 water-to-cement ratio. according to BS 1881-125:2013, mix proportioning. During casting, 3% NaCl solution is applied by weight of cement. Specimen sizes varied according to the type of experiment..

Table 2.4 Coating layers

SLAB	DRY COAT			TOTAL THICKNESS (mm)
	1^{ST} COAT (mm)	2^{ND} COAT (mm)	3^{RD} COAT (mm)	
SLAB 1	110	99	73	282
SLAB 2	97	92	94	275
SLAB 3	99	94	88	281

Demolded after a day and allowed to cure for 28 days at 20 ± 1 °C in a salt solution. For every test, three specimens were examined. The surface was wire-brushed for 15–20 minutes to reveal the aggregates and eliminate the laitance layer. Use pure compressed air to clean the surface. paint with a high zinc content combined to create a smooth liquid. applied with a paint roller in three coats, keeping the thickness between 200 and 350 μm overall. Give each layer a full day to dry completely before adding the next.

100x100x100 mm concrete cubes were cast and allowed to cure. Epoxy was used to affix metallic discs with a diameter of 20 mm to the specimens. To evaluate the strength of the binding between the anode overlay and substrate, a pull-off test was conducted. The ability to permeate Characteristic of Coating Standards-compliant measurements are made of water vapor transmission and absorption. The coating exhibited a low water vapor transmission rate and decreased water absorption.

Test for Polarization conducted using steel bars implanted in slab specimens. Anomet platinum covered wire and MMO coated titanium mesh ribbon are the two main anode conductors that are utilized. Better current distribution and a smaller potential drop across the coating were

demonstrated with anomet wire. It was established what current density was needed to achieve cathodic protection requirements.

Test of Service Life Accelerated test with ZRP block acting as the anode in an aqueous solution. Anode potential was recorded up until the point of failure.

X-ray diffraction (XRD) is used to assess oxidation products in the coating and coating-concrete interface characterization process. Utilizing Field Emission Scanning Electron Microscopy (FE-SEM) to examine zinc oxidation products and microstructure. Bond strength, with an average pull-off failure stress of 2.73 MPa, satisfied requirements. The coating exhibited a low water vapor transmission rate and decreased water absorption. Compared to MMO Coated Titanium Mesh Ribbon, Anomet Platinum Clad Wire demonstrated superior current distribution and a reduced potential drop across the coating. For ZRP to be successfully applied in ICCP, the ideal current density was determined to be 40 mA/m^2 of steel surface area. Potential shift and decay were shown to have a linear relationship.

Up until failure, the anode was polarized at a steady 17.8 mA current until the anode potential increased by 4.0 V. Twelve days were needed for total polarization before failure. Anode performance at 20 mA/m^2 current density is predicted to last for about 15 years. Microstructural examination showed that during polarization, zinc oxide/hydroxide was formed. ZRP coating thickness was found to be between 200 and 350 μm by SEM examination. Products of zinc

corrosion found on the zinc particle surface. Zinc and oxygen were detected by EDS analysis, indicating the possibility of zinc oxide/hydroxide production.

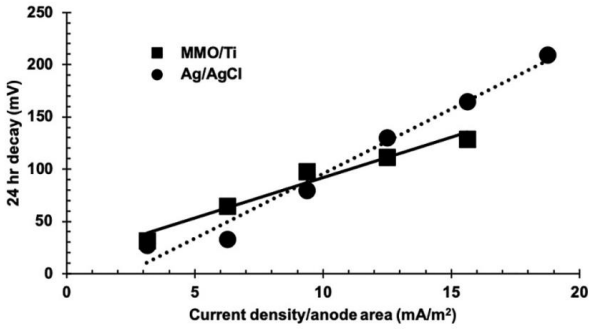

Figure 2. 7 Relationship Between Potential Decay Over 24 Hours and Polarization Current Density (Goyal, Sadeghi, and Ganjian, 2019)

Table 2.5 Summary of polarization test results. (Goyal, Sadeghi and Ganjian, 2019)

Current density/steel area mA/m^2	Current density/anode area mA/m^2	Pre energization Potential (mV)	'Instant off' potential (mV) Vs		4 h decay (mV) Vs		24 h decay (mV) Vs		Voltage across anode (V)
			MMO/Ti	Ag/AgCl/0.5MKCl	MMO/Ti	Ag/AgCl/0.5MKCl	MMO/Ti	Ag/AgCl/0.5MKCl	
10	3.13	−323	−462	−411	28	13	32	16	1.5–2.5
20	6.25	−320	−414	−376	60	41	67	48	2–3
30	9.38	−318	−432	−383	83	57	98	80	2.5–4
40	12.50	−300	−546	−486	94	108	130	181	3–4
50	15.63	−342	−525	−498	143	110	164	153	4–5
60	18.75	−338	−641	−630	175	168	209	200	5–7

ZRP coating met performance requirements and proved to be an excellent ICCP anode system. bond strength at the anode-concrete interface that is satisfactory. A primary anode using Anomet platinum-clad wire displayed superior current distribution. With a projected 15-year service life, the coating avoided premature failure. Zinc oxide/hydroxide formation was noted during polarization. Additional durability testing and cross-comparison with alternative anodes are required to determine feasibility.

Oleiwi *et al.*, 2018 To attain a 28-day compressive strength of 38 N/mm², concrete specimens were constructed in accordance with the British Building Research Establishment's (BRE) specifications. 390 kg/m³ of locally made limestone Portland cement (CEM I/A-LL) was utilized. Fine aggregates weighing 1125 kg/m³ were made of natural sands with a maximum size of 4.75 mm and a specific gravity of 2.47. Limestone with a maximum size of 10 mm and

a specific gravity of 2.49 was utilized as coarse aggregate at a rate of 580 kg/m³. To develop specimens with variable levels of chloride contamination, different amounts of pure NaCl (0%, 1%, 2%, 3.5%, and 5% of the cement weight) were added to the mix water. The water-to-cement ratio in the concrete mixtures was 4.

Two instances of reinforced concrete for each chloride content totaled ten. The specimen measured 150 x 93 × 90 mm³. To replicate local rebar cluster structures, three standard 10 mm diameter reinforcing bars were added in each specimen. Three electrically connected rebars were measured, and their average response was used to account for changes in oxygen access caused by rebar position. To enable electrical connections, a 3 mm diameter by 5 mm deep hole was bored into one end of each rebar. A 73 mm section of the steel rebars was left exposed to the concrete environment, giving them an overall exposed surface area of 6880 mm². The ends of the rebars were coated with epoxy resin to protect them from environmental exposure.

Each specimen had an integrated woven carbon fiber (CF) sheet that functioned as the anode. The sheet had a nominal surface size of 144 × 93 mm². For electrical connection, the carbon fiber anode protruded from the specimen by about 30 mm. After casting, epoxy glue was applied to the exposed steel bars of each reinforced concrete specimen. The linear polarization method outlined by Stern and Geary was used to evaluate the rates of rebar corrosion in the reinforced concrete specimens. Equations that were appropriate were used to determine corrosion current and polarization resistance (R). Two electrodes were subjected to a sinusoidal alternating current in order to measure the electrical resistivity of concrete. For cathodic protection, galvanostatic polarization was employed, giving the rebars in each specimen varying CP current densities.

Corrosion Rate and Chloride Content: The specimens' chloride contents were calculated as a percentage of their cement weight. Higher rates of reinforcement corrosion were found to be directly correlated with either a lower resistivity of the concrete or a higher chloride content. Low (corrosion rate < 5 mA/m2), moderate (corrosion rate between 5-10 mA/m2), and high (corrosion rate > 10 mA/m2) were the three categories used to categorize corrosion risk levels. In accordance with earlier literature guidelines, a threshold chloride level of 0.45% by the mass of cement indicated a low corrosion rate.

Concrete Resistivity: The risk of corrosion was evaluated using figures for concrete resistivity. If the concrete resistivity was more than 17 kΩ·cm, the reinforcements were expected to experience a low corrosion rate; if the resistivity was less than 12.5 kΩ·cm, the corrosion rate was expected to be significant. These results were in line with earlier studies, which indicated that very high corrosion occurs below 10 kΩ·cm.

CP Operation Time and Instant-Off Potential: Under different current densities, the first three hours of CP operation showed notable variations in the instant-off potential, which was measured immediately following CP stoppage. The potential showed signs of stability after three hours, suggesting that the system was in a stable state. The CP performance assessment metrics were all measured 24 hours after the CP was put into practice.

Influence of Chloride Content and CP Current Density on Instant-Off Potential Higher applied CP current density resulted in an increase in the absolute value of the instant-off potential; however, this effect was less pronounced with higher concrete chloride content. The British standards-recommended criteria of -720 mV was not always met, even at the maximum applied current density of 75 mA/m².

4-Hour Potential Decay:

4-Hour Potential Decay: The efficacy of CP was assessed using 4-hour potential decay, which calculates the difference between instant-off potential and potential following four hours of CP cessation. For CP effectiveness, a 100 mV depolarization in 4 hours is deemed adequate.The 4-hour potential decay curve for specimens free of chloride was continuously higher than the 100 mV threshold, suggesting that reinforcements in these conditions are immune to corrosion in the absence of CP. A -500 mV 24-hour CP instant-off potential was sufficient to safeguard reinforcements in all examined contaminated concretes, as determined by the 100 mV 4-hour potential decay requirement. In cases with a high chloride content or a high starting corrosion rate, the needed protective current density was more than the rate of corrosion. According to the study's findings, CP current density should be determined by chloride content and concrete resistivity.

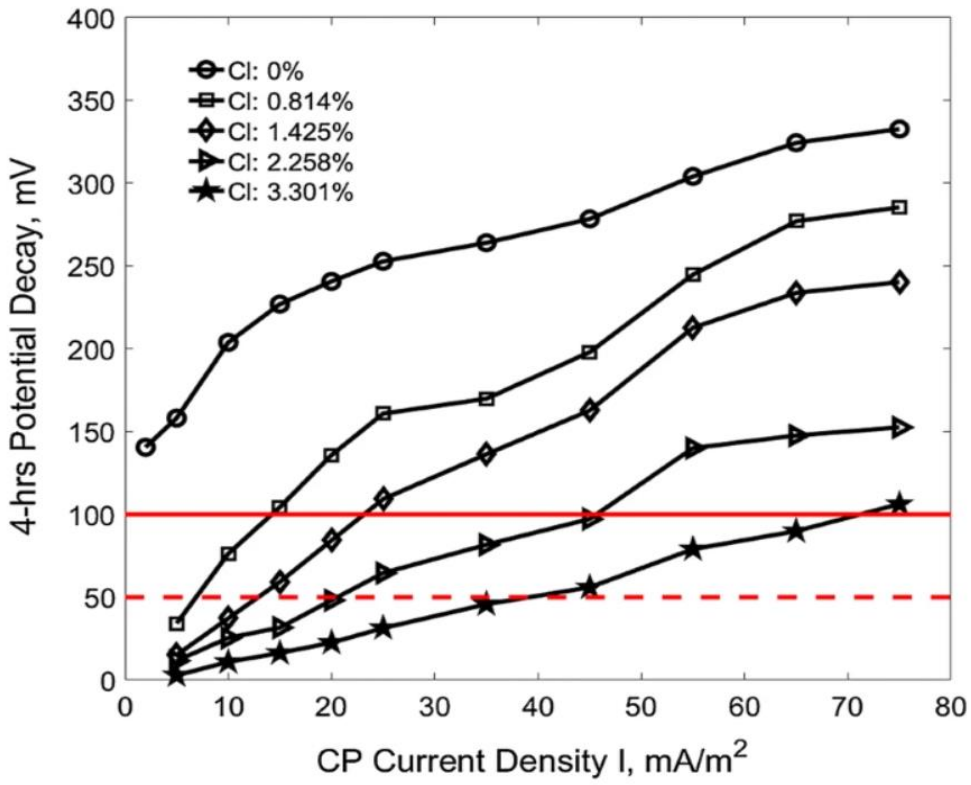

Figure 2. 8 Reinforcement Depolarization as a Function of CP Current Density (Oleiwi et al., 2018)

Comparison of Criteria: To prevent the reinforcements in Portland concrete from corroding, a threshold for the application of CP may be set at a total chloride concentration of 0.31% by weight of cement or 17 k cm concrete electrical resistivity. For reinforced concrete with up to 3.4% chloride contamination by weight of cement, an instant-off potential of -500 mV with respect to Ag/AgCI/0.5KCI electrode can offer sufficient protection, in relation to the 100 mV depolarization requirement, or concrete resistivity is at least 6.7 kM cm.

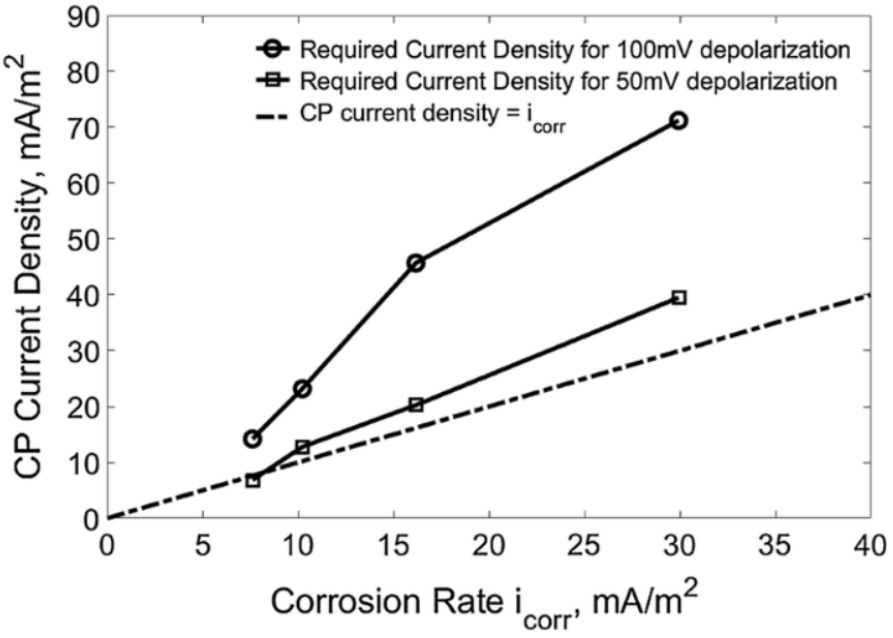

Figure 2. 9 Required CP Current Density for Various Depolarization Levels (Oleiwi et al., 2018)

Concrete resistivity, chloride concentration, and CP current demand were found to be well correlated, and characterization modeling was recommended.

Poltavtseva, Ebell and Mietz, 2015 In ICCP systems, which are composed of binders and conductive pigments, CBCCs are employed as secondary anodes. They are necessary to keep the steel reinforcing in concrete constructions from corroding. For efficient protection, the potential of the reinforcing steel should be decreased below -720 mV (vs. Ag/AgCl/0.5 M KCl).

The study aims to comprehend deterioration behavior through morphological and electrochemical investigations.

Three distinct CBCCs with various conductive pigments and binders were examined. Tests for galvanostatic polarization, open-circuit potential, and electrical impedance were performed. In test solutions, the concentrations of dissolved organic and inorganic carbon were measured.

The electrical impedance of CBCCs is affected by humidity, with higher humidity leading to increased impedance. CBCC 1 exhibits low resistance and stable behavior, while CBCC 3 has higher initial resistance due to porosity. CBCC 3, with NiCCF, shows improved conductivity and stable impedance over time. CBCC 3 with an organic polymer binder showed significantly higher dissolved organic carbon (TOC) in the test solution. CBCC 1 exhibited volume changes due to the reaction of magnesium carbonate with concrete pore water. CBCC 3 showed large cavities and increased porosity, likely due to the dissolution of the organic polymer binder.

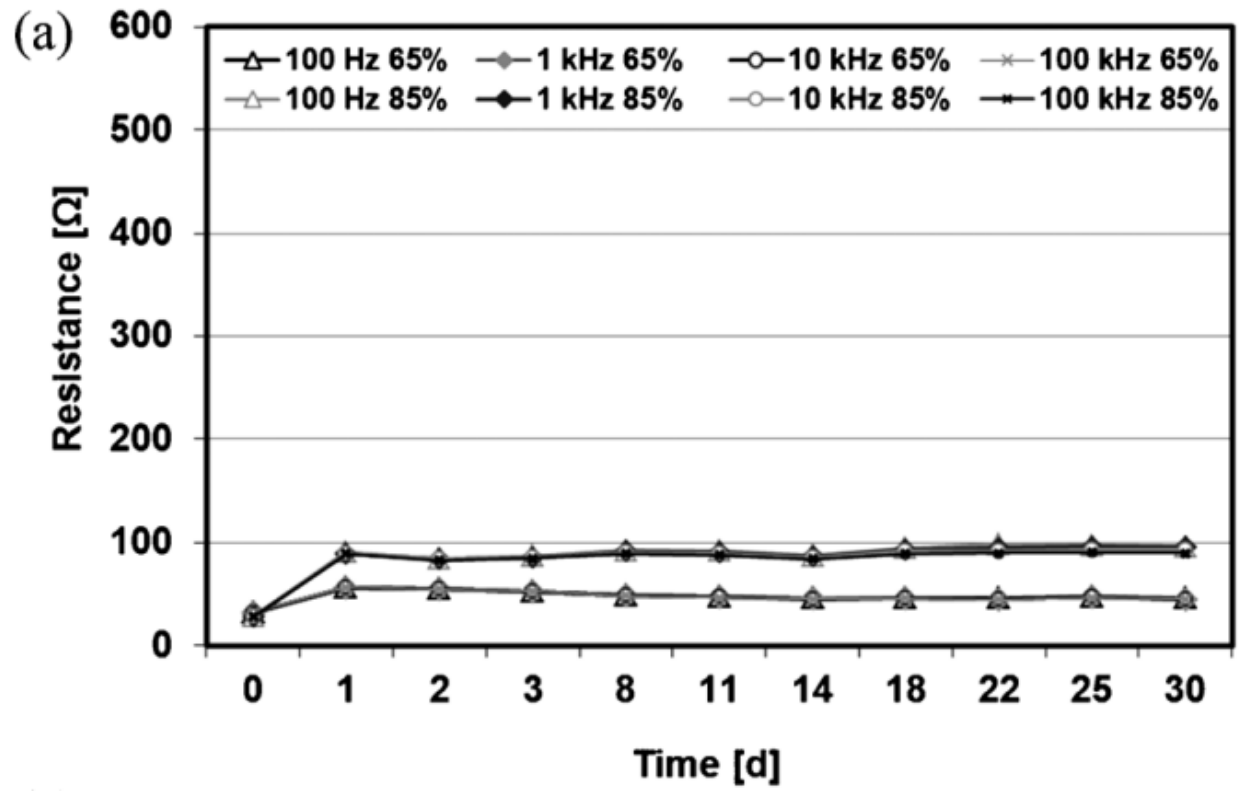

(b)

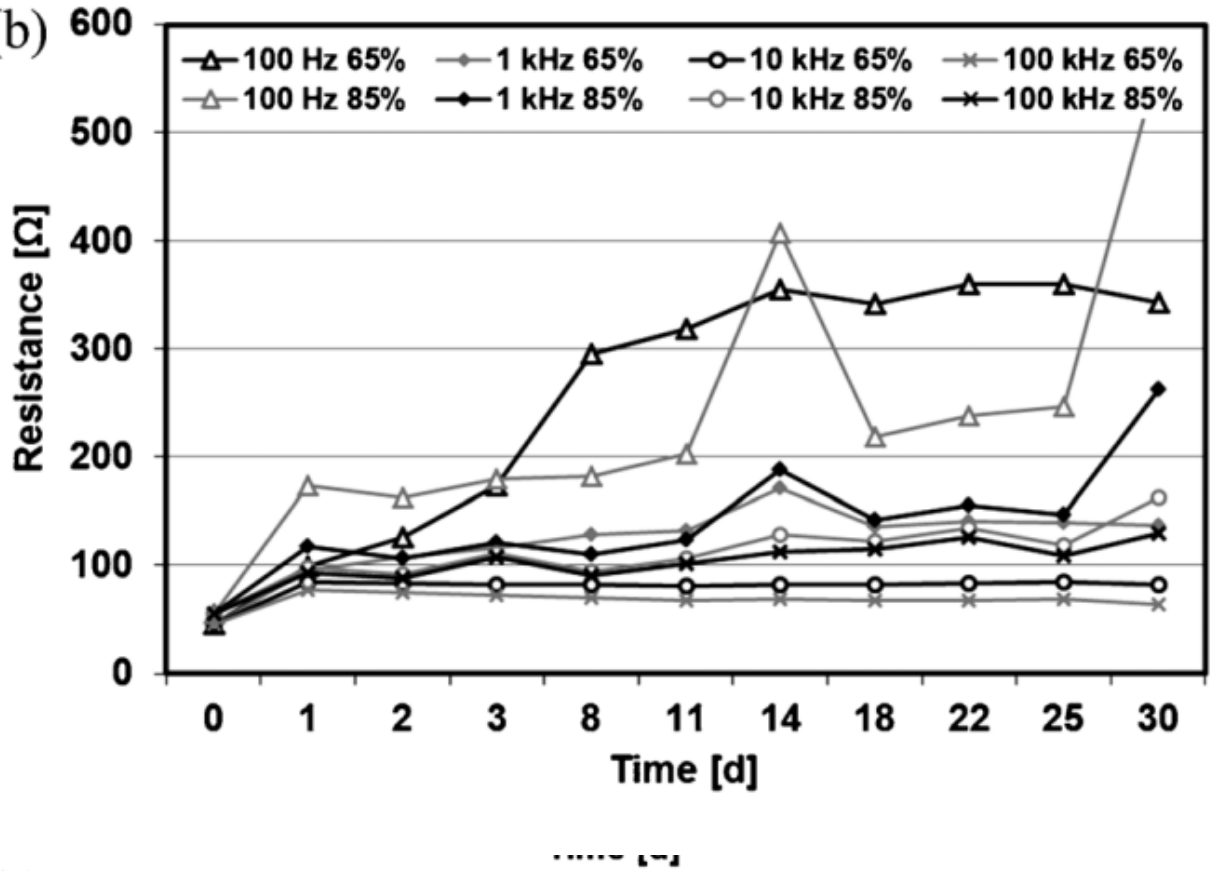
100 Hz 65%
1 kHz 65%
10 kHz 65%
100 kHz 65%
100 Hz 85%
1 kHz 85%
10 kHz 85%
100 kHz 85%
Resistance [Ω]
0
100
200
300
400
500
600
0
1
2
3
8
11
14
18
22
25
30
Time [d]

(c)

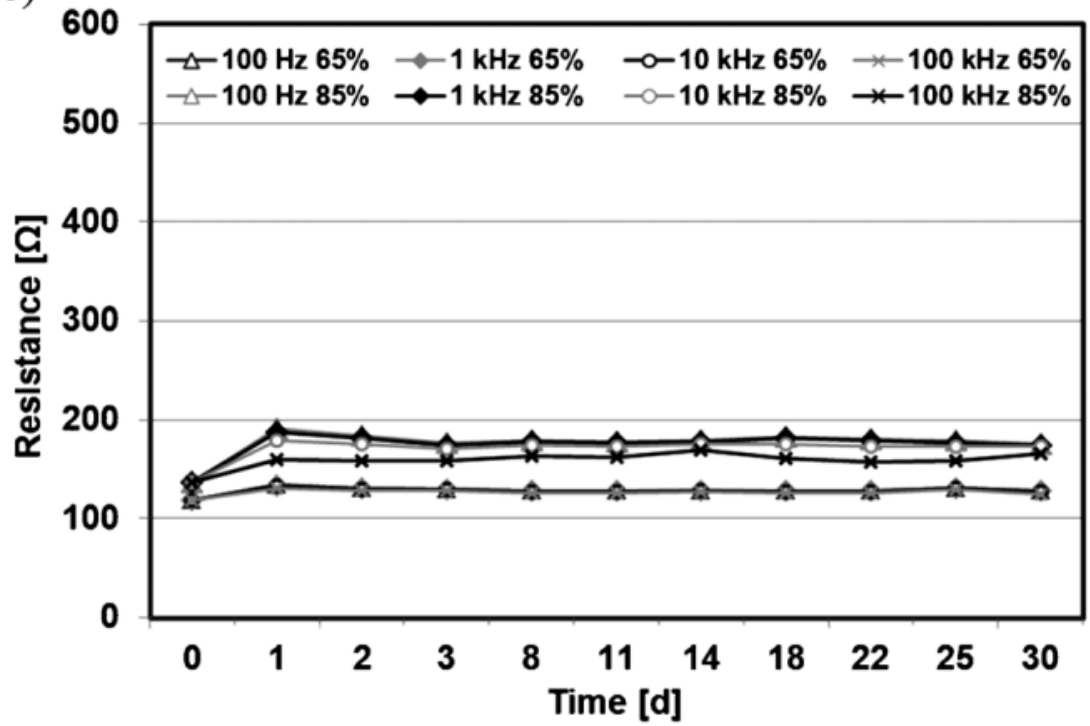
100 Hz 65%
1 kHz 65%
10 kHz 65%
100 kHz 65%
100 Hz 85%
1 kHz 85%
10 kHz 85%
100 kHz 85%
Resistance [Ω]
0
100
200
300
400
500
600
0
1
2
3
8
11
14
18
22
25
30
Time [d]

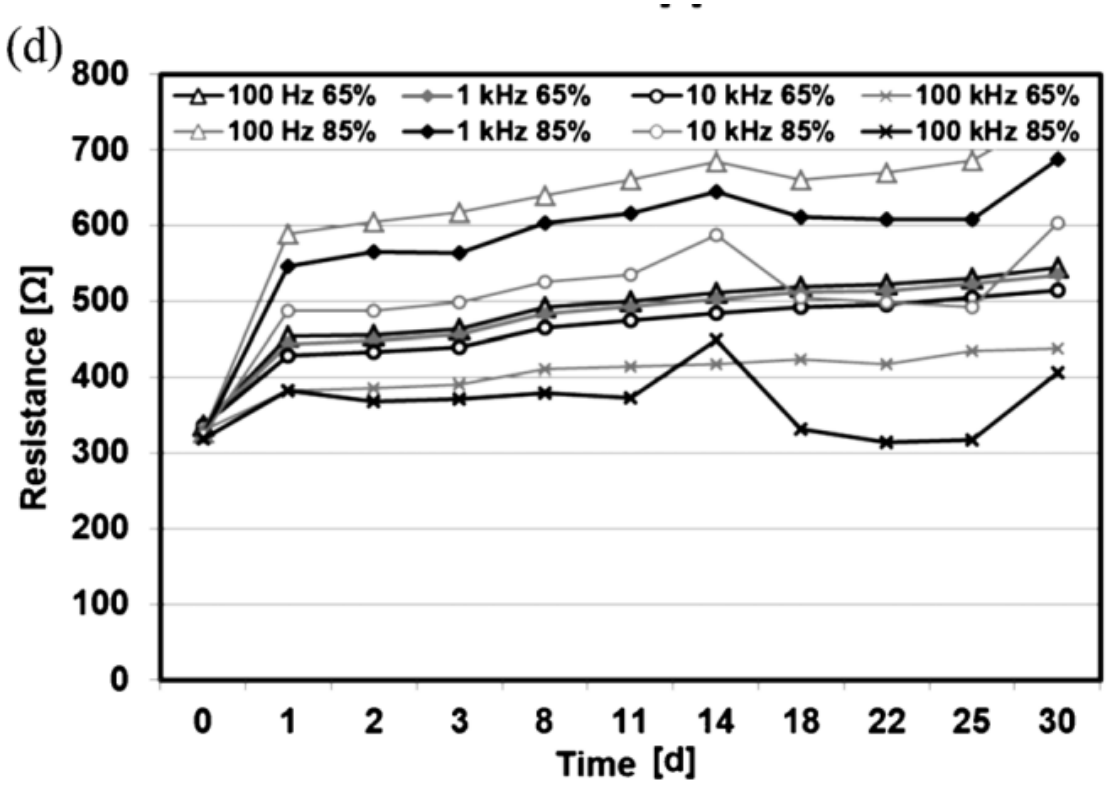

Figure 2. 10 Impedance Variation of Coatings Over Time: (a) CBCC 1, (b) CBCC 2, (c) CBCC 3 with Nickel-Coated Carbon Fibers, (d) CBCC 3 without Nickel-Coated Carbon Fibers (Poltavtseva, Ebell, and Mietz, 2015)

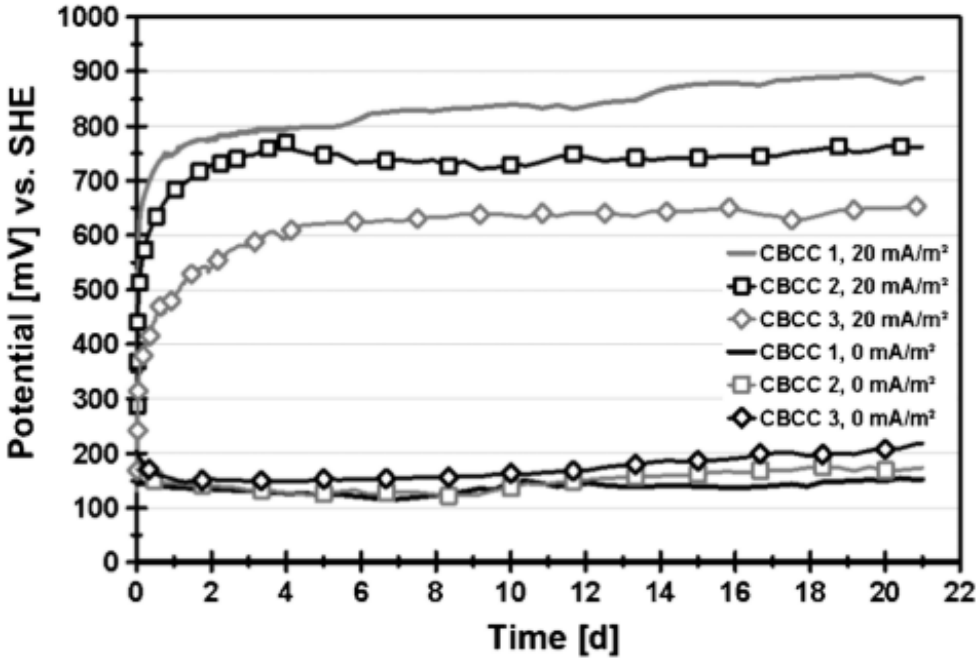

Figure 2. 11 Potential–Time Curves for Three Coatings at Open-Circuit and Anodic Polarization with i_o 20 mA/m² (Poltavtseva et al., 2015)

CBCC 1 and CBCC 2 exhibit better electrochemical properties and low carbon dissolution. CBCC 3 has good anode potential control but suffers from organic binder dissolution, leading to increased porosity. Protecting coatings from moisture penetration is crucial for long-term performance.

Syaiful, Sujitha and Vedalakshmi, 2014 Carbon fibers, activated charcoal, and graphite powder are used as conductive fillers in cementitious anodes. Pumice aggregate is used as lightweight aggregate in mortar mixes. Specimens are prepared with varying proportions of carbon fibers, graphite powder, and activated charcoal. Compressive strength, dry density, and electrical conductivity are measured. Accelerated galvanostatic tests are conducted to assess dissolution behavior. Electrochemical impedance spectroscopy (EIS) and polarization tests are used to analyze oxidation products and corrosion rates. Galvanostatic tests indicate the ability to maintain protection over extended periods. Conductive cementitious anodes offer an alternative to traditional anode materials.

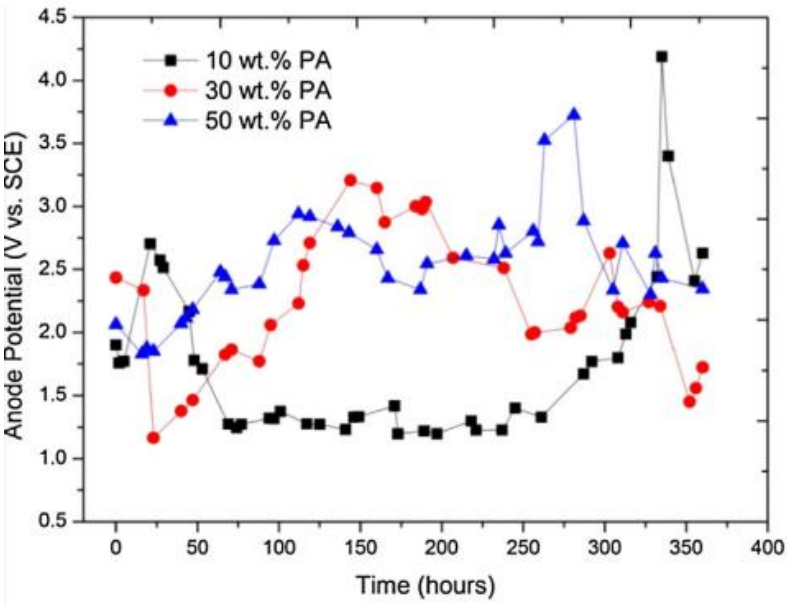

(a)

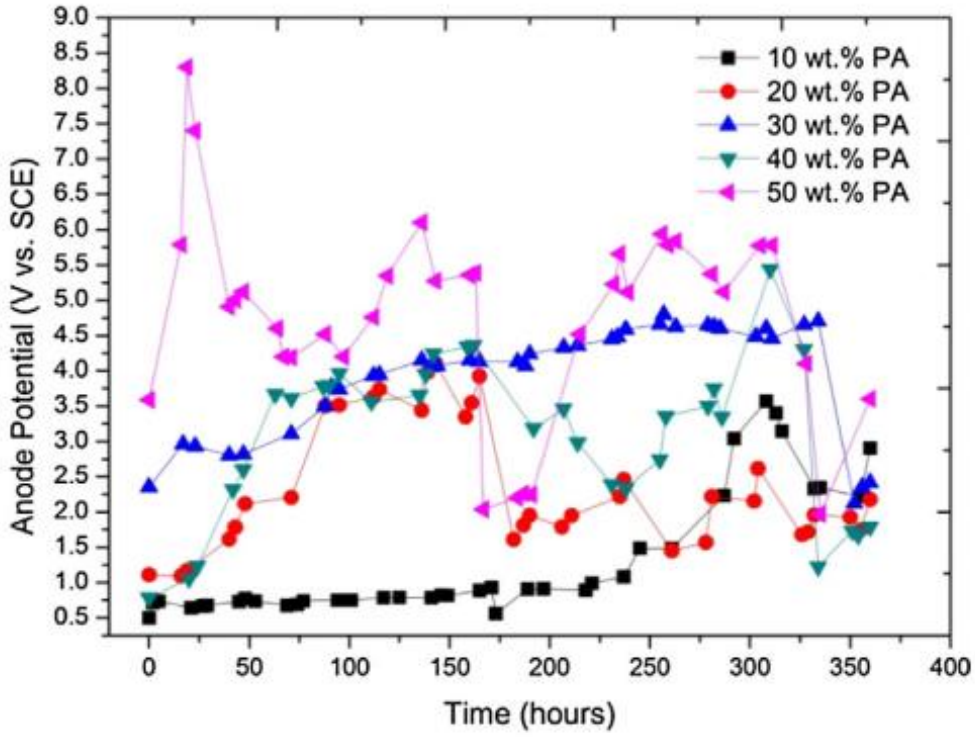
Anode Potential (V vs. SCE)
Time (hours)
10 wt.% PA
20 wt.% PA
30 wt.% PA
40 wt.% PA
50 wt.% PA

(b)

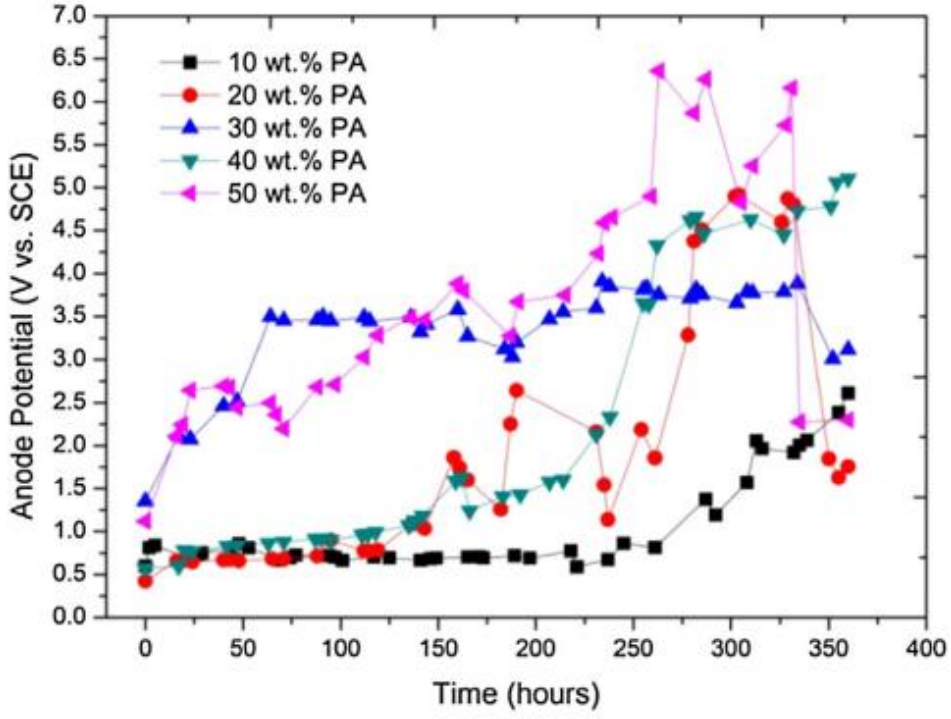
Anode Potential (V vs. SCE)
Time (hours)
10 wt.% PA
20 wt.% PA
30 wt.% PA
40 wt.% PA
50 wt.% PA

(c)

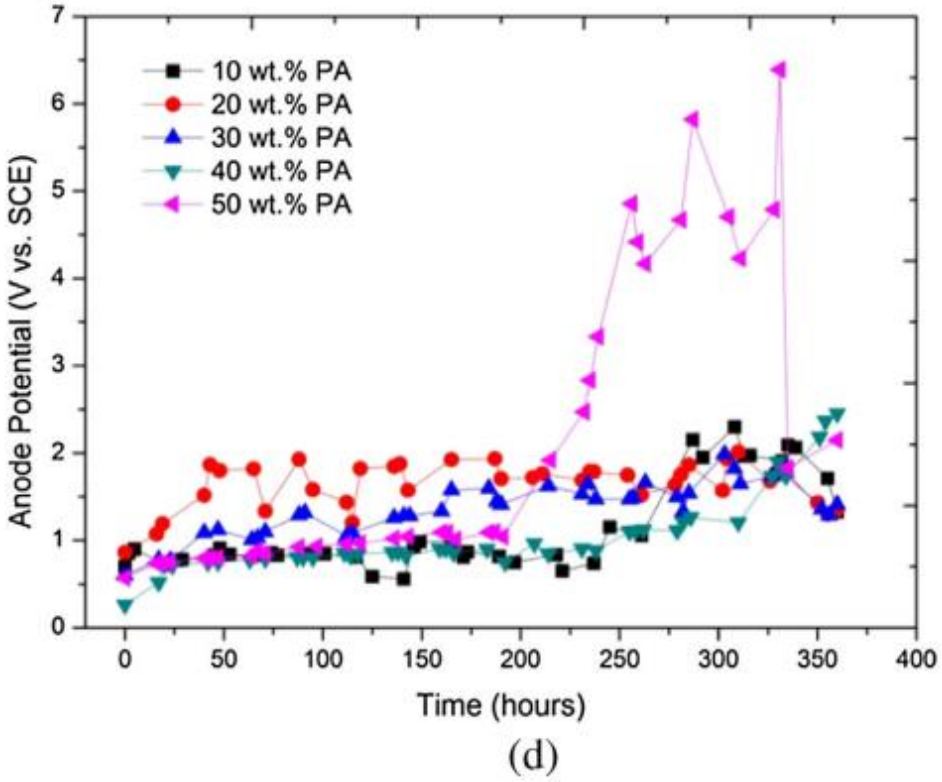

Figure 2. 12 Anode Potential of Conductive Mortar as a Function of Exposure Time: (a) SPS + 3% NaCl without CF, (b) 0.3% CF, (c) 0.7% CF, (d) 1.1% CF (Syaiful, Sujitha, and Vedalakshmi, 2014)

Conductivity Enhancement: The addition of carbon fibers (CF) significantly improved the electrical conductivity of the cementitious mortar. The highest conductivity, reaching 0.20 S/cm, was achieved in mortar with 30% pumice aggregate and 1.1% CF. This was attributed to the formation of a three-dimensional network of conductive fibers, following the percolation theory.

Weight Reduction: The lightweight conductive mortar was shown to reduce the self-weight of the anode by 50% compared to conventional anodes. This weight reduction is advantageous for preventing debonding issues due to excessive weight.

Compressive Strength: When CF content was below 0.5%, the compressive strength of the pumice mortar improved compared to cement mortar containing natural sand. However, excessive CF addition and air voids reduced the compressive strength.

Galvanostatic Testing: The conductive anode demonstrated stable passive behaviour, with a breakdown voltage exceeding 2.5 V, during 14 days of accelerated galvanostatic testing. The presence of chloride did not cause the dissolution of carbon Fibers due to the formation of stable oxidation products on the Fiber surface.

SEM Analysis: Scanning electron microscopy (SEM) images confirmed the stability of both primary and secondary anodes within the conductive mortar during the accelerated galvanic test.

ICCP Application: The lightweight conductive cementitious anode offers advantages in terms of weight reduction, lower anode potential shift, and higher conductivity, making it a potentially cost-effective solution for ICCP applications in marine substructures.

Lambert *et al.*, 2015 The CFRP fabric anode can function at extremely high current densities, specifically 128 mA/m2 of steel area, while maintaining strong mechanical bonding.

CFRP fabric can be employed to reinforce corroded reinforced concrete (RC) beams, thereby preserving their structural integrity and enhancing the final strength of the compromised beam.

When compared to conventional cathodic protection (CP) methods for reinforced concrete, the carbon fiber reinforced polymer (CFRP) anode demonstrates the ability to function at significantly greater levels of electric current.

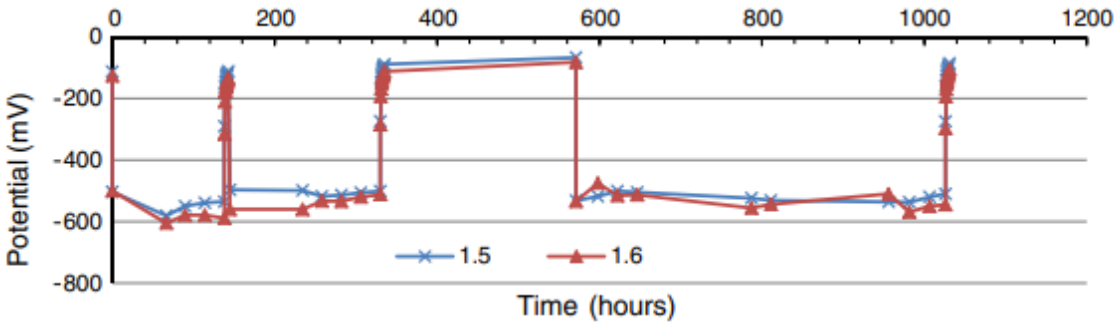

Figure 2. 13 Steel Potential During ICCP Operation (Beams 1.5, 1.6—Group 1) with Constant Applied Current Density of 128.4 mA/m² of Steel Area (Lambert et al., 2014)

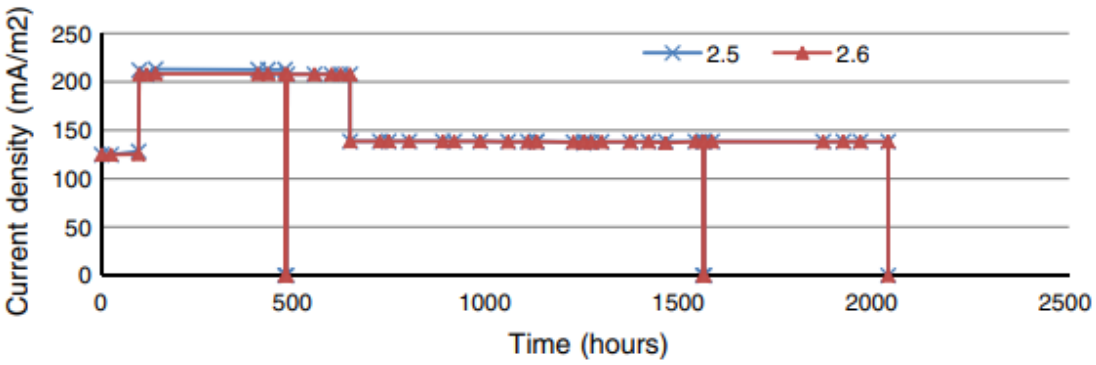

Figure 2. 14 ICCP Applied Current Density (mA/m² of Steel Surface Area) for Beams 2.5 and 2.6 (Lambert et al., 2014)

2.4 SACP ANODES IN CATHODIC PROTECTION

Quale *et al.*, 2017 Thermal spray (TS) is a versatile coating application method used for various coatings, including metallic, ceramic, cermet, and polymeric coatings. In the offshore industry, Thermal Sprayed Aluminum (TSA) coatings are commonly employed to protect steel structures, risers, pipe components, and ships in marine environments. TSA coatings, primarily composed of 99.5% aluminum or AlMg5 alloy, act as sacrificial anodes, providing cathodic protection to the underlying steel substrate. The Distributed Sacrificial Anode (DSA) concept has been proposed as an alternative to TSA. DSA coatings, using an Al-Zn-In anode alloy composition, aim to offer improved electrochemical properties and corrosion protection. Hypotheses regarding DSA's performance suggest its potential as a sacrificial anode with reduced current demand compared to traditional sacrificial anodes. This concept could result in substantial weight and cost savings in subsea applications. Objectives of further research include assessing DSA's effectiveness as a partial or full anode replacement for subsea cathodic protection, as well as exploring potential applications for sacrificial protection of creviced corrosion-resistant alloys at elevated temperatures.

In this study, wire with a specific Al-Zn-In composition was produced through the re-casting of commercial Type A High-Grade Al-Zn-In anodes. The process involved melting the anode alloy and extruding it through a 5mm die. Subsequently, the wire was drawn through multiple stages to achieve the final diameter of 2 mm, suitable for the thermal spray gun. After 20 steps, a 300m long wire was obtained. Thermal Spray Process: Both conventional TSA (Al-99.5) and DSA coatings were applied to 6 mm thick 600 x 600 mm plain carbon steel plates. The application involved electric arc thermal spray technique using a 300 A gun. Surface preparation included grit blasting to SA 2.5, and coating thicknesses were measured between 1140 – 1250 μm on seven test plates. TSA and DSA Characterization: Prior to testing, adhesion strength was assessed using pull-off tests on specially prepared steel plates. Cross-section

analysis of TSA and DSA samples was performed using optical and scanning electron microscopy. Chemical analysis was conducted using inductively coupled plasma mass spectrometry (ICS-MS) on the as-received anode, re-cast bar, drawn wire, and final DSA coating.

Long-Term Testing: Open Circuit Potential (EOC): Electrochemical behavior of freely exposed DSA-coated samples was compared with TSA, as-received anode specimens, and 5 mm wire. EOC was measured versus a Ag/AgCl reference electrode. Galvanic Corrosion: Galvanic couplings between DSA, TSA, conventional anodes, and carbon steel (CS) were tested with different area ratios. Galvanic currents and potentials were measured. Crevice Corrosion Protection: DSA coating's ability to prevent crevice corrosion was examined using creviced UNS S31603 samples exposed to seawater. Electrochemical potential and current measurements were taken during exposure. Electrochemical Testing: Polarization resistance measurements, potentiostatic cathodic polarization curves, and anodic polarization curves were conducted in accordance with ASTM G59. Results were used to calculate corrosion rates. Post-Mortem Characterization: Samples were examined for pitting or cracks using optical microscopy and SEM. The composition of intermetallic particles and surfaces in and adjacent to pits were determined using Energy Dispersive Spectroscopy (EDS).

The wire production, including re-casting, extrusion, and drawing, presented no challenges, resulting in a 2 mm wire suitable for thermal spraying (TS).

Adhesion Strength: Single layer TSA: 13.5 MPa (cohesive fracture) Dual layer TSA + DSA: 8.8 MPa (adhesive fracture between TSA and DSA)

Open Circuit Potential Measurements: EOC trends in seawater at 10°C: Rapid decrease in potential initially, stabilizing or slowly increasing afterward. DSA stabilized at -1000 mVAg/AgCl after 235 days, while TSA stabilized around -935 mVAg/AgCl after 60 days.

Galvanic Corrosion: DSA showed more negative stabilization than TSA when coupled to CS (area ratio 10:1).

Electrochemical Testing: Polarization curves of DSA-coated samples after 8, 30, and 235 days of exposure. Polarization curves of anode, DSA, and TSA-coated samples after 30 days of exposure.

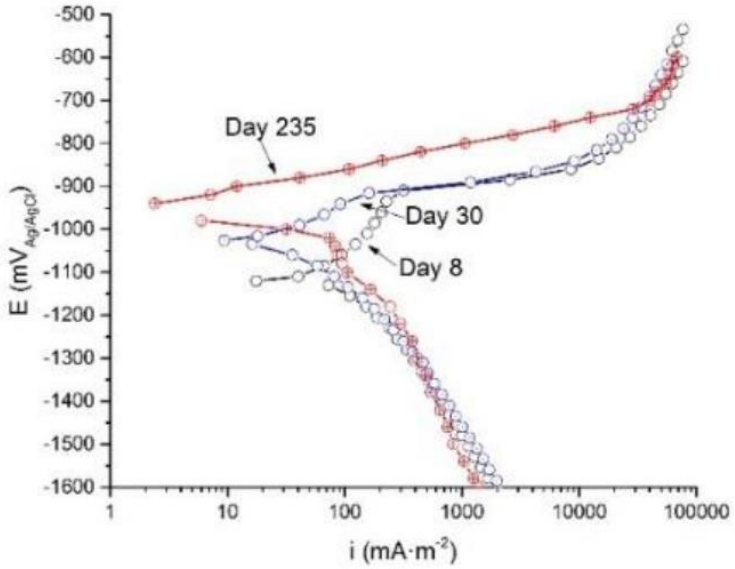

Figure 2. 15 Polarization Curves of DSA-Coated Samples at 8, 30, and 235 Days of Exposure

Surface Examination and Characterization: Visual examination after exposure showed differences between DSA-CS and TSA-CS galvanic pairs. SEM and EDS analysis of cross sections after 30 days revealed DSA surface integrity and TSA coating degradation.

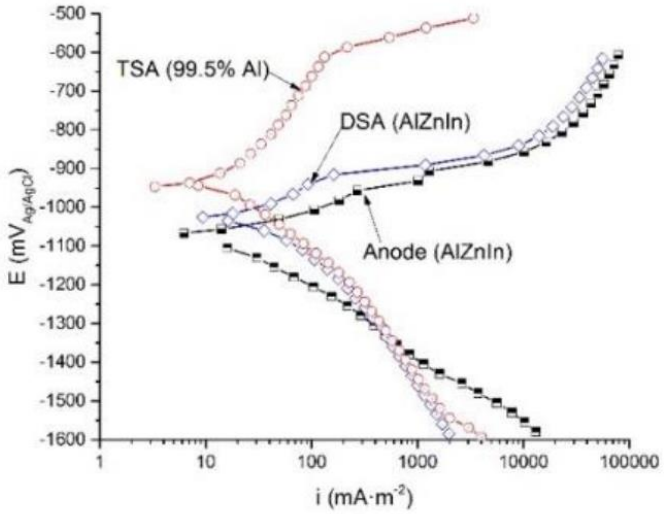

Figure 2. 16 Polarization Curves for Anode, DSA, and TSA-Coated Samples After 30 Days (Quale et al., 2017)

Astuti *et al.*, 2019 investigated zinc coating using a solution of lithium monohydrate. Two 2400 mm long and 44 years old reinforced concrete (RC) beams were used in this experiment. To protect rebars in patch and non-patch repairs, two different types of sacrificial anodes—Type A and Type B—were used. Zinc covered in a porous mortar containing a solution of lithium monohydrate was used to produce the anodes. The zinc's corrosion was aided by the application of this solution. The space that will be available for integration determines the sort of anode that is chosen. Anode Type B, which measures 140 mm in length, 45 mm in width, and 13 mm in thickness, has been selected as the anode for the patch repair. A cylindrical, ribbed sacrificial anode of 30 mm in diameter and 130 mm in length was also added and placed into the preexisting concrete. It is possible to effectively create a negative potential shift in concrete by using sacrificial anodes in both patch repair and non-patch concrete. This shift is produced by positioning the sacrificial anodes 400 mm apart, which produces a 100 mV depolarization.

(Farooq *et al.*, 2019) In order to assess the performance of aluminum and zinc sacrificial anodes in artificial seawater, this study examines their electrochemical characteristics and cathodic protection efficacy. The study highlights the significance of impressed current cathodic

protection (ICCP) and sacrificial cathodic protection (SCP) in marine conditions, where anodes based on zinc and aluminum are frequently utilized because of their current capacity and efficiency. It also talks about how high-strength steel can get embrittled by hydrogen, which is why SCP is a better option for submerged constructions.

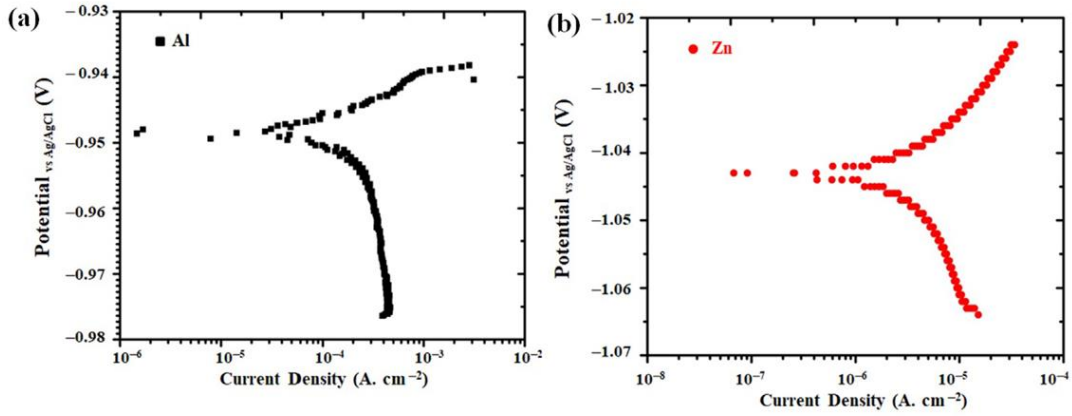

Figure 2. 17 Tafel polarization scan of Al and Zn anodes in artificial seawater. (Farooq et al., 2019)

The anode samples, cut from cast materials with a surface area of 16 cm², were made from aluminum and zinc alloys, with attention given to their microstructural characteristics, such as the formation of pure α and η phases. The samples underwent cleaning processes involving sodium hydroxide and nitric acid before being dried. The study involved electrochemical measurements using open circuit potential and polarization tests in a three-electrode cell setup with artificial seawater as the electrolyte. Mass loss and hydrogen evolution tests were conducted to determine the current efficiency of the anodes, adhering to NACE standard procedures. The impressed current method was also employed, with charge flow measured using a coulometer and hydrogen gas evolution closely monitored. The primary objective was to evaluate the current efficiency and overall effectiveness of aluminum and zinc sacrificial anodes in cathodic protection. Results showed that aluminum anodes had a current efficiency of 93.3% and an anode capacity of 2784.8 A h/kg, while zinc anodes had a current efficiency

of 66.6% and an anode capacity of 519.36 A h/kg. The hydrogen evolution test revealed efficiencies of 86.2% for aluminum and 95.3% for zinc, with both anodes shifting to more negative potentials over time. This comprehensive evaluation enhances the understanding of sacrificial anode performance in marine environments, offering valuable insights into their role in protecting metallic structures from corrosion.

Farhana Zainal *et al.*, 2020 After seven and fourteen days, the potential value of the SACP sample was lower than that of the control sample, according to the Open Circuit Potential (OCP) test procedures. The SACP sample had a potential value inside the immunity zone, while the control sample had a potential value inside the passivity region, as shown by the Pourbaix diagram.

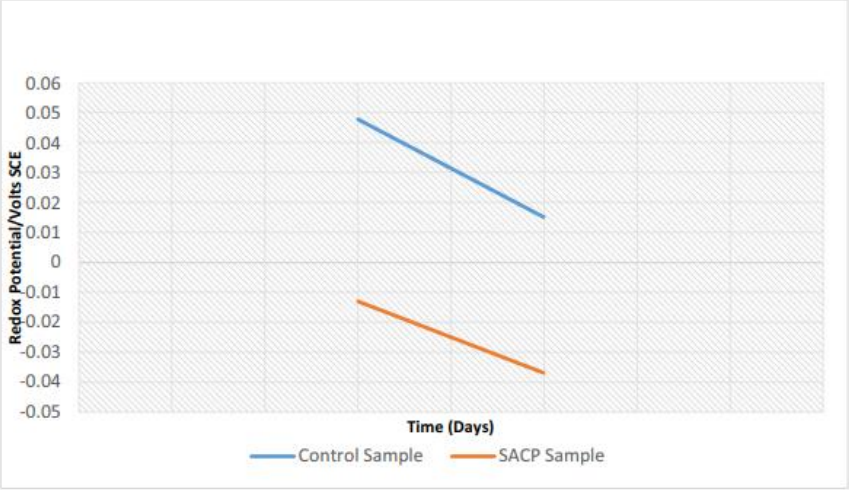

Figure 2. 18 Redox Potential vs. Time (Days) for Geopolymer Concrete Samples with and without SACP (Zainal et al., 2020)

(Jawad, Amouzad Mahdiraji and Hajibeigy, 2020) This research delves into optimizing sacrificial anode cathodic protection systems for aboveground storage tanks, with a strong emphasis on controlling the anode's current to enhance both efficiency and longevity. The study involved a series of experiments using a laboratory-based tank filled with saline water, precisely prepared with 5661 ppm salinity. Magnesium anodes, known for their effectiveness, were utilized in these experiments. The primary objective was to develop a system that could

minimize overprotection and reduce energy loss, thereby significantly extending the anode's lifespan when compared to conventional systems.

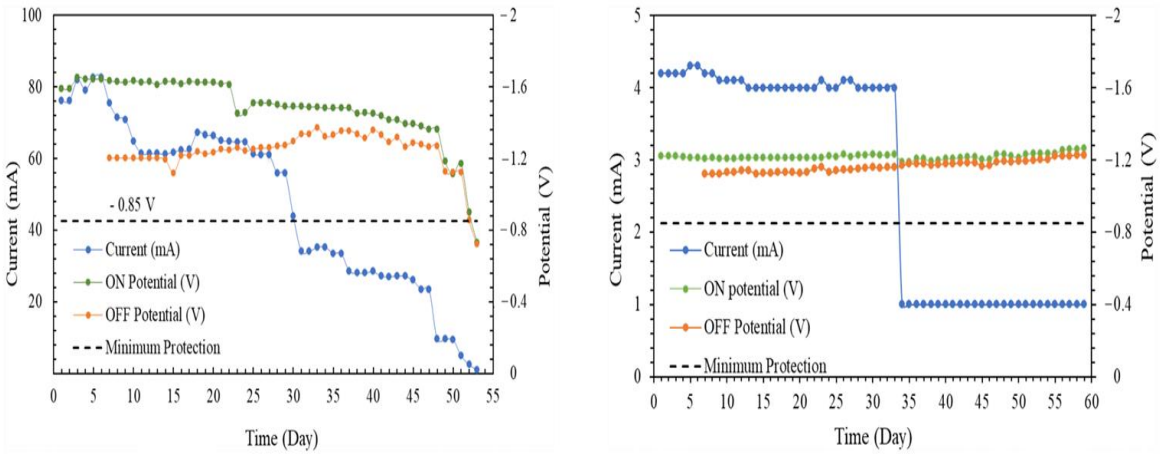

Figure 2. 19 a) Potential “ON” and current “OFF”: Measured internal tank potential for Tank-2 with the CP system proposed in the design. b) Potential “ON” and current “OFF”: Measured internal tank potential for Tank-3 with the CP system proposed in the design. (Jawad, Amouzad Mahdiraji and Hajibeigy, 2020)

The experiments focused on measuring the current and potential of the tank body by using a variable resistor to achieve the minimum protection potential. In the critical Tank-3 setup, the performance was closely monitored, with "ON" and "OFF" potentials and currents recorded using a copper/copper sulfate reference electrode and a digital multimeter. The initial current was recorded at approximately 4.2 mA during the first 12 days, eventually stabilizing at around 4 mA by the 33rd day, indicating full polarization of the tank body. The study's results were compelling, demonstrating that the proposed system could extend the anode's lifetime by an impressive 35.55 times compared to traditional methods. Additionally, the performance of the anode in Tank-3, where the remaining weight was 31 g out of the original 33 g, underscored the effectiveness of the design. Even though the coating of the tanks increased the protection level, it was still insufficient for complete self-protection against corrosion. This research offers valuable insights into the importance of controlled current management in enhancing the

performance and longevity of cathodic protection systems, providing a robust foundation for future improvements in the protection of aboveground storage tanks.

(Wang *et al.,* 2020) In order to test the efficacy of cathodic protection (CP) in reducing corrosion in reinforced concrete polluted with chloride, three different sacrificial anode types—aluminum, magnesium, and zinc—were used in this study. The purpose of the study is to evaluate the effects of these anodes on the rates of corrosion of implanted steel bars and the general resilience of concrete buildings subjected to chloride ions. The concrete slabs used in the experiments were 1.0 m x 1.0 m x 0.06 m in size. They were constructed using river sand and Ordinary Portland cement (No. 42.5) and had steel bars (HPB235) implanted in a mesh pattern. In order to replicate a chloride-contaminated environment, 5% sodium chloride was added by weight of cement to the concrete mix, which had a water/cement ratio of 0.5 and a sand/cement ratio of 2.5.

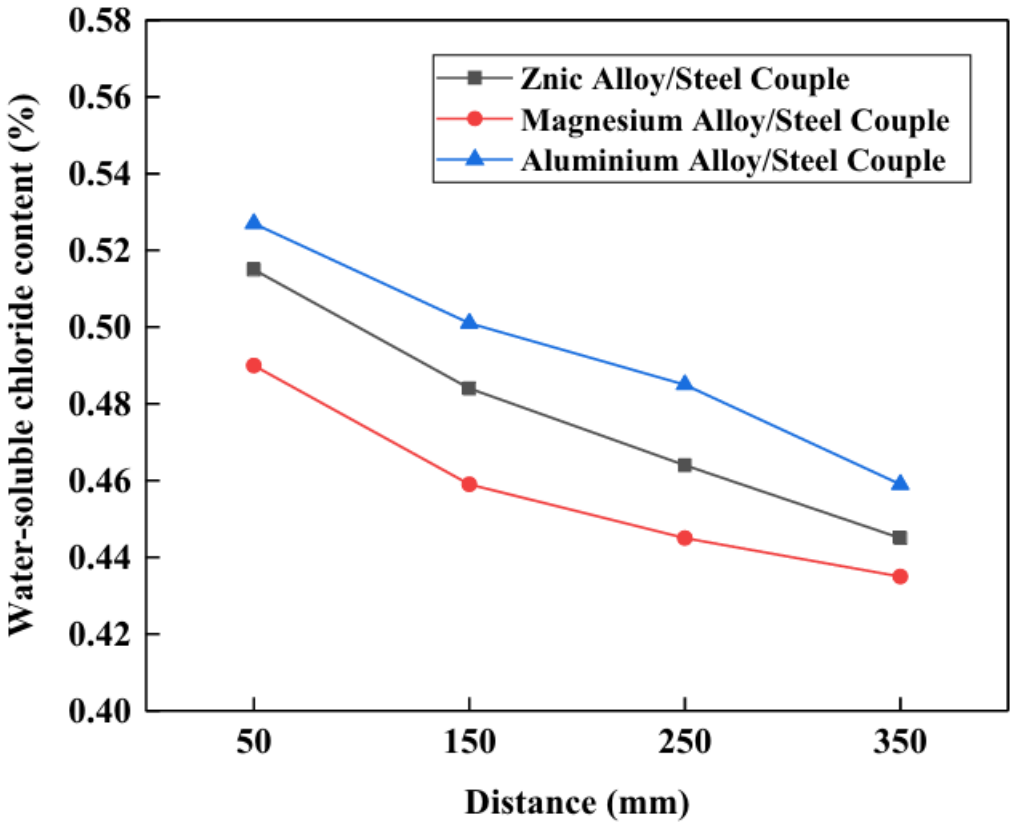

Figure 2. 20 Variations in water-soluble chlorine content with distance from the anodes in concrete slabs after a duration of 30 days. (Wang et al., 2020)

The study involved applying CP using the three types of sacrificial anodes and comparing their performance against a control specimen without anodes. Electrochemical impedance spectroscopy (EIS) tests were carried out on a regular basis to assess the steel bars' rates of corrosion. ZSimpWin software was used to analyze the results. The findings demonstrated that when corrosion products generated, the diameter of the capacitive arc in the Nyquist plot increased over time, indicating decreased corrosion rates. Furthermore, the impedance modulus rose and the resistance of the mortar pore solution reduced, indicating improved steel bar protection. This study offers important new information about how well various sacrificial anodes work to extend the longevity of reinforced concrete buildings in areas with high levels of chloride.

(Krishnan *et al.*, 2021) The study does not specify exact specimen sizes or materials, it covers the application of galvanic anodes in various concrete structures, including jetties and industrial buildings.. Although this may not always guarantee total passivation of steel rebars, it does indicate the common practice of inserting one anode per square meter of concrete surface area. The main goal was to demonstrate how CP systems can greatly extend the service life of repairs and lower overall costs by comparing the long-term performance and LCC of patch repairs with and without CP systems. Results revealed that traditional patch repairs often fail within five years, necessitating repeated repairs and leading to increased costs, whereas CP strategies can enhance service life to over 20 years and reduce LCC by up to 90%.

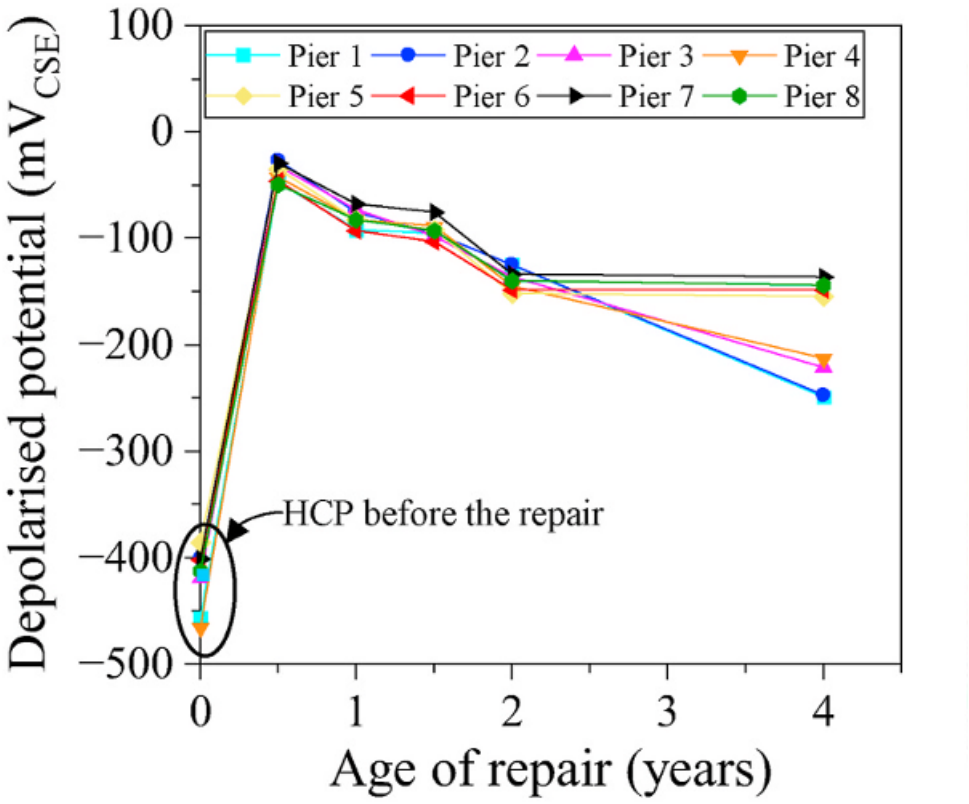

Figure 2. 21 Depolarized corrosion potential obtained from piers on finger jetty (Krishnan et al., 2021)

The paper concludes that galvanic anodes are economically advantageous and effectively control corrosion in concrete structures. It serves as a significant contribution to

understanding CP technology in the construction industry. A relevant concluding figure could compare the life-cycle costs of traditional patch repairs versus CP strategies over a 30-year period, highlighting the substantial savings achieved with galvanic anodes. This analysis underscores the potential of CP systems to enhance the durability and cost-effectiveness of concrete repairs, supporting broader adoption in the industry.

2.5 MONITORING OF CP

a. 100 mV Polarisation Development/Decay

b. Potential decay over 24 hours of at least 100 mV from instantaneous off

c. Potential decay over an extended period of 150 mV from instant off

d. Instant off potential more negative than -720 mV

e. Negative 850 mV (CSE) Polarised Potential (for buried and submerged structures)

f. E-log I Test

John P. Broomfield 2014 concepts of cathodic protection for steel in concrete have been thoroughly established by the integration of theoretical frameworks, experimental research, and vast field data. The 100 mV depolarization criterion is a highly successful standard for accomplishing corrosion control, particularly in less hostile environments. This criterion is beneficial in reducing the current flow, which is in line with the considerations for the lifespan of the anode design. The positive aspect of the 100 mV depolarization criterion is shown by its ability to lengthen the lifespan of anode systems. This criterion reduces current flow, hence fostering a more sustainable and long-lasting cathodic protection system. Nevertheless, despite the advancements achieved in this domain, obstacles continue to exist in guaranteeing precise potential control in practical applications. Further work is needed to improve the reliability and precision of reference electrodes in real-world applications, with special focus on their stability and calibration. The continuous investigation is essential for enhancing the effectiveness of cathodic protection methods and guaranteeing the enduring resilience of steel structures embedded in concrete.

2.6 MONITORING OF STRUCTURE THROUGH PZT

(Wang *et al.*, 2010) This paper investigates the application of Electromechanical Impedance (EMI) techniques for detecting damage in I-type steel beams, employing piezoelectric ceramic (PZT) transducers for comprehensive numerical and experimental analysis. The study utilized PZT patches measuring 24 mm × 12 mm with a thickness of 0.5 mm, which were bonded to the beam's surface at a distance of 350 mm from the left end. Various damage scenarios were introduced by creating gaps of 5 mm, 10 mm, 20 mm, and 40 mm using a linear cut machine. To monitor impedance variations, the research employed a WaynerKerr 6500B impedance analyzer to collect electrical admittance data. The analysis focused on calculating the root-mean-square deviation of real admittance (RMSDR) to assess the extent of damage. Findings revealed that even minimal damage (5 mm) resulted in significant changes in PZT admittance measurements, and the RMSDR index effectively indicated the extent of damage. Nonetheless, the study identified challenges related to the dense high-order modes of the beam, which can complicate the accurate detection of damage solely based on EMI admittance spectroscopy. The paper underscores the potential of EMI techniques in structural health monitoring while highlighting areas for further research to address these complexities.

(Talakokula *et al.*, 2016) The research focuses on addressing carbonation-induced corrosion in reinforced concrete structures is a serious problem in addition to corrosion caused by chloride. The scientists suggest employing piezoelectric lead zirconate titanate (PZT) ceramic patches connected to rebar as a novel, non-destructive method of identifying and measuring this kind of corrosion. Proper adherence was ensured by bonding PZT patches measuring 10 × 10 × 0.3 mm to machined flat surfaces on the rebar in cylindrical reinforced concrete examples of different diameters. The electro-mechanical admittance signatures of the PZT patches were periodically measured during the 230-day accelerated carbonation tests, which were carried

out at 5% CO2 concentration and 75% relative humidity. This was done to evaluate alterations in mechanical impedance parameters, particularly the equivalent mass parameter (EMP) and equivalent stiffness parameter (ESP). The study aimed to correlate these impedance changes with physical evidence of corrosion, validated through techniques like optical microscopy, SEM, and Raman spectroscopy. The findings revealed that ESP initially increased due to calcium carbonate formation, which stiffened the concrete, but decreased significantly after corrosion onset, indicating its progression. The results demonstrated that PZT ceramic transducers offer an effective alternative for non-destructively diagnosing carbonation-induced rebar corrosion, with the EMP providing a measure of the average corrosion rate.

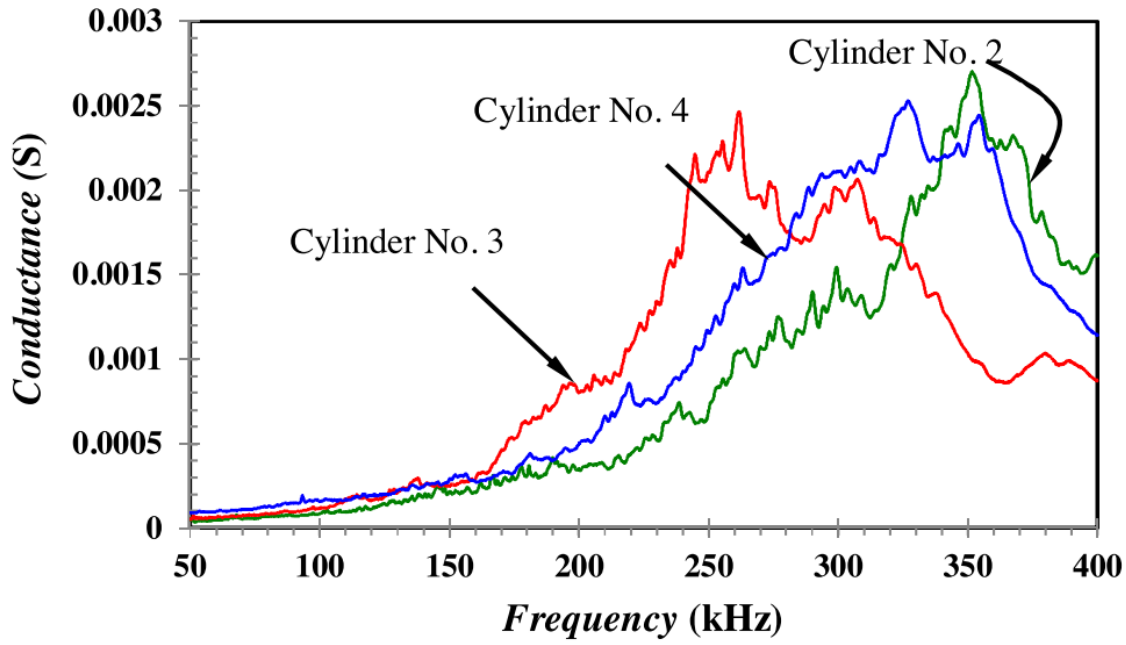

Figure 2. 22 Baseline Conductance Profiles of PZT Patches Embedded in Reinforced Concrete Cylindrical Specimens (Talakokula et al., 2016)

(Shi *et al.*, 2019) This paper investigates the use of piezoelectric impedance techniques to monitor corrosion in reinforced concrete structures, a significant concern for maintaining the integrity of civil engineering constructions, especially in coastal areas and critical

infrastructures like bridges and ports. The study used a 14 mm diameter, 340 mm long steel bar as the specimen, embedded in concrete mix C30 with a ratio of 1:2.2:3.6:0.6 for cement, sand, stone, and water. Two types of Lead Zirconate Titanate (PZT) wafers, with diameters of 12 mm and thicknesses of 2 mm and 5 mm, were employed as piezoelectric transducers. Corrosion was accelerated using an electrochemical workstation with a current density of 1 mA cm^-2, while the specimen was submerged in a 5% NaCl solution. The electrical impedance of the PZT transducers was measured to assess corrosion progression, which was categorized into initial (less than 2% mass loss), developing (2-4%), and rapid corrosion (greater than 4%). The study aimed to establish a reliable method for real-time monitoring of reinforcement bar corrosion in concrete. Results showed that corrosion significantly altered the resistance spectra of the piezoelectric transducers, demonstrating their potential for evaluating corrosion evolution and improving maintenance strategies, thereby enhancing safety in reinforced concrete structures.

(Liu *et al.*, 2020) The research explores advanced techniques for monitoring corrosion in reinforced concrete, a critical issue impacting the durability and safety of structures. Traditional electrochemical methods, while common, are often labor-intensive and influenced by external factors. This study investigates a novel approach using embedded annular piezoelectric transducers for real-time, non-destructive monitoring of corrosion. Although the paper does not specify the exact dimensions of the specimens, it notes that standard concrete and steel rebars were used, with accelerated corrosion induced through electrochemical methods. The research involved three distinct experiments: applying electrochemical methods to induce corrosion, using the ultrasonic pitch-catch method to monitor damage, and employing electrochemical impedance spectroscopy to analyze corrosion phenomena. The study aimed to develop an in-situ, non-invasive monitoring method and assess the effectiveness of the embedded piezoelectric transducers in detecting corrosion. Results indicated that the These

parameters were correlated by an increase in capacitance arc length in high-frequency zones of electrochemical impedance spectra with corrosion rate. Visible corrosion products on the surface of the concrete and two capacitance arcs in Nyquist spectra were indicators of corrosion rates more than 3%. The longitudinal mode wave packet's peak-to-peak value decreased, according to ultrasonic research over time, indicating that acoustic energy is influenced by corrosion progression. The study concluded that variations in acoustic energy and frequency components provide a qualitative assessment of corrosion extent in reinforced concrete.

(Hire, Hosseini and Moradi, 2021) The purpose of this research is to optimize the size and frequency range of lead zirconate titanate (PZT) patches for efficient monitoring. This study looks into the application of Electromechanical Impedance (EMI) techniques for corrosion detection in reinforced concrete (RC) structures. The study used PZT patches of 10 × 10 mm in length and width with thicknesses of 0.3 mm, 0.5 mm, and 1.5 mm. The findings showed that, in the 50 kHz to 400 kHz frequency range—which is crucial for corrosion detection—only the 10 × 10 × 1.5 mm patch produced a distinct peak in the impedance spectra. The patches were attached to rebars within RC structures that were subjected to induced corrosion damage. The study measured impedance changes and observed how different patch sizes and thicknesses influenced the impedance spectrum, noting that increasing patch thickness enhanced sensitivity. The experiments showed that significant corrosion damage led to noticeable changes in the impedance spectrum, including a leftward shift of the main peak and the appearance of new peaks. The primary objective was to identify the optimal PZT patch size for effective corrosion detection, and the study found that a patch thickness of 1.5 mm provided clearer and stronger peaks, improving the distinction between pristine and damaged states using metrics such as the correlation coefficient deviation (CCDM). The findings concluded that the mechanical impedance ratio between the host structure and the patch plays a crucial

role in sensitivity, and increasing patch thickness can reduce sensitivity loss due to large impedance ratios.

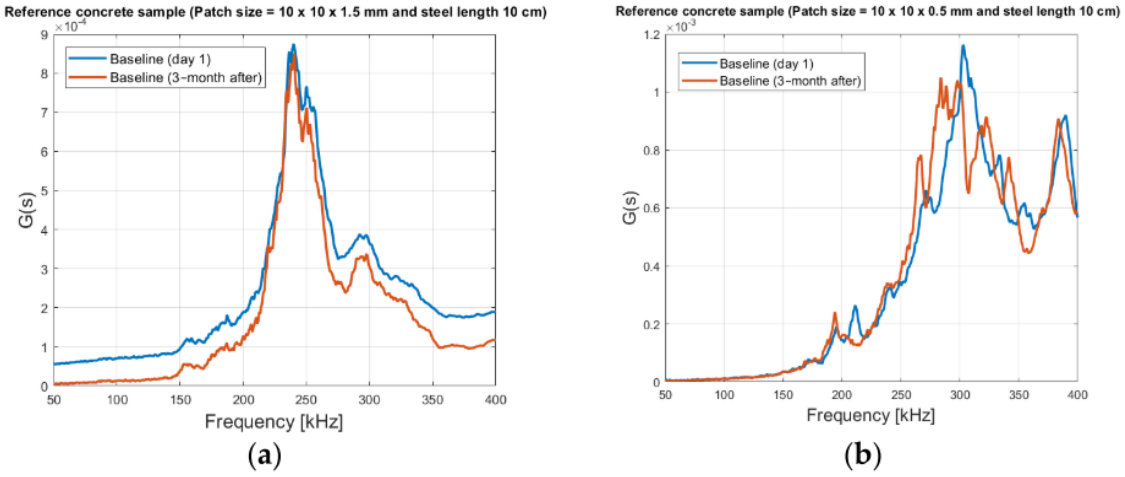

Figure 2. 23 Reference Concrete with Steel Rod of 10 cm Length: (a) Patch Size 10 × 10 × 1.5 mm, (b) Patch Size 10 × 10 × 0.5 mm (Hire, Hosseini and Moradi, 2021)

(Tamhane *et al.*, 2021) In order to preserve metal structures shielded by cathodic systems, the research presents a unique Electro-Mechanical Impedance (EMI) measurement technique for quantitative real-time monitoring of corrosion in sacrificial anodes. The study used circular zinc sacrificial anodes, each attached with a lead zirconate titanate (PZT) transducer, to highlight the importance of early-stage in-situ monitoring. One anode surface had to be polished, the PZT transducer had to be attached using instant adhesive, and the transducer had to be covered with weatherproof epoxy to protect it from the liquid electrolyte used in the experiments. The susceptance spectra of the PZT transducer were examined by the researchers using an impressed-current based accelerated corrosion device in order to evaluate variations in resonance frequency over time. The goal of the project was to measure corrosion automatically and incorporate the technique into Internet of Things (IoT)-based structural health monitoring systems. The PZT transducer's series resonance frequency significantly increased as the corrosion process advanced, and the observed nonlinearity was ascribed to partial delamination of the corrosion products made of zinc oxide.These findings validate the

EMI technique as an effective tool for real-time monitoring of sacrificial anodes, offering promising prospects for corrosion assessment and preventive maintenance.

(Tamhane *et al.*, 2022) The usefulness of Electro-Mechanical Impedance (EMI) monitoring for sacrificial anode corrosion protection for steel rebar in reinforced concrete structures is investigated in this research. In order to maintain the integrity of the infrastructure, sacrificial anodes are essential. This work focuses on evaluating anode health by measuring conductance spectra using root mean square deviation (RMSD). Two sacrificial anodes were used in the experimental setup, each implanted in a concrete block of 150 mm by 150 mm by 150 mm, and covered in hexagon-shaped conductive mortar with a resistance of 12,500 Ω cm. A three-dimensional ABS plastic cap was used to waterproof the anodes, and it was affixed with a two-component epoxy adhesive that required an hour to cure. By providing impressed current to the anodes during accelerated corrosion studies, changes in the RMSD of the conductance spectra were tracked over time to evaluate anode health. These results were compared with analytical models and finite element methods (FEM) to validate the findings, and resonance frequencies were observed to assess environmental impacts on corrosion. The study aimed to correlate RMSD values with the actual state of the anodes, focusing on zinc layer thickness changes due to corrosion. Results showed that RMSD values correlated well with experimental data, demonstrating that the EMI technique effectively monitors sacrificial anodes non-destructively, providing reliable assessments of corrosion severity and zinc layer thickness.

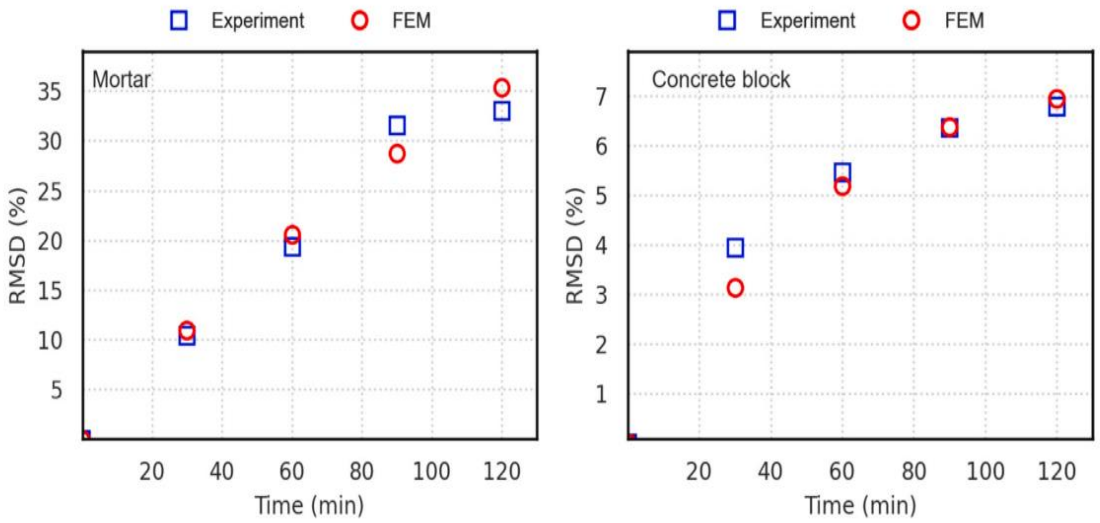

Figure 2. 24 Comparison of Experimentally Measured RMSD with FE Simulation Results: (a) 'Mortar' Specimen, (b) 'Concrete Block' Specimen (57.35 kHz Mode) (Tamhane et al., 2022)

(Morwal *et al.*, 2023) With an emphasis on the Electro-Mechanical Impedance (EMI) method using piezo sensors across a range of materials, including metallic, reinforced concrete (RC), and prestressed concrete (PC) structures, this paper provides an extensive overview of developments in corrosion monitoring techniques. The service life of these structures is seriously threatened by corrosion, which could result in technical failures. For this reason, efficient Structural Health Monitoring (SHM) is crucial to performance assessment and safety guarantee. Because it can enable real-time, non-destructive data collecting and processing, the EMI approach has grown in popularity. The review covers various configurations of piezo sensors, such as surface-bonded piezo sensors (SBPS) and embedded setups, which are crucial for accurate corrosion monitoring. High-strength epoxy adhesives are employed to bond piezoelectric lead zirconate titanate (PZT) patches to structures, ensuring precise measurements of mechanical impedance. The authors reviewed numerous studies using EMI to monitor corrosion, assessing different sensor configurations and their placement. They explored the correlation between structural mechanical impedance and admittance

measurements from piezo sensors, which are affected by corrosion damage. The review aims to guide researchers, academicians, and practitioners in choosing suitable sensor configurations and methodologies for monitoring chloride-induced corrosion in both metallic and concrete structures. The paper highlights that different piezo sensor configurations offer varying performance during different corrosion phases: the EPS configuration is more effective during initiation, while the SBPS configuration provides more accurate data during propagation. It also underscores the need for further research on equivalent structural parameters like stiffness and damping to better understand corrosion impacts.

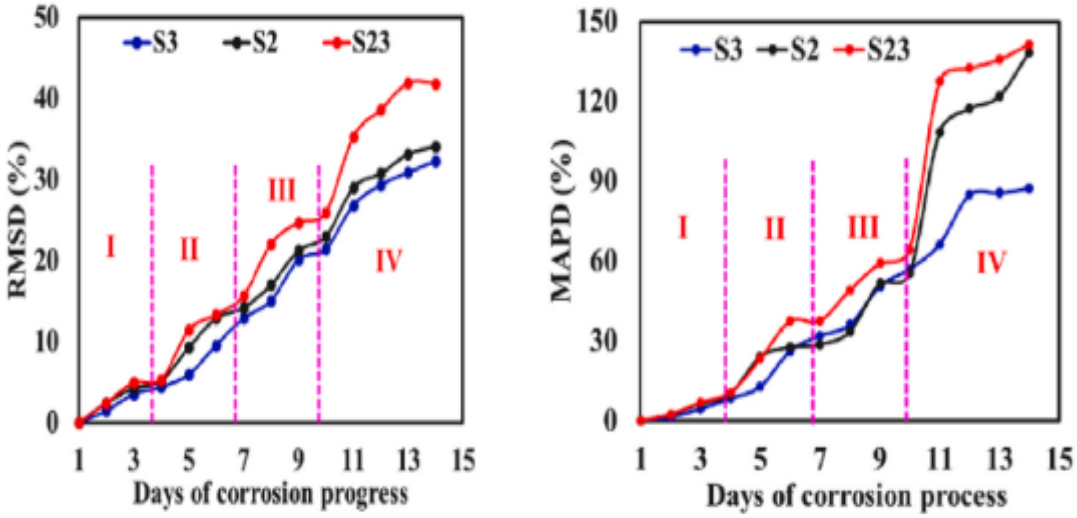

Figure 2. 25 RMSD and MAPD Indices During Corrosion Progression *(Morwal et al., 2023)*

2.7 RESEARCH GAPS

- Reliance on periodic inspections and visual assessments, lacking timely or accurate insights.
- Inadequate monitoring of dynamic interactions between anodes and concrete environments.
- Absence of real-time, non-destructive monitoring using advanced sensors like PZT transducers.
- Limited understanding of long-term anode performance under varying conditions.

CHAPTER 3 METHODOLOGY

This chapter details the characteristics of the materials used in the study. The study's primary objective is to monitor the effectiveness of sacrificial anode cathodic protection (SACP) systems using PZT (lead zirconate titanate) sensors. The aim is to assess the health monitoring and lifetime of the SACP systems. This involves evaluating the system's condition and estimating its lifespan. The chapter also covers the chemical and physical properties of the materials used.

3.1 MATERIAL USED

3.1.1 Cement

Ordinary Portland Cement (OPC) was utilized as the binder for preparing the specimens, in accordance with IS: 8112-1989. For this study, OPC-43 grade cement was selected for casting the specimens. The specific brand used was Shree, which is readily available in the market. The properties and characteristics of the cement, including setting time, workability, and strength development, were taken into account during the experimentation and evaluation phases. The chemical composition of the cement, as provided by the manufacturer, is presented in Table 3.1

Table 3. 1 Physical and Chemical Properties of OPC 43 cement

Properties	**Values**
Chemical Properties	
Silica (SiO_2)	21-25%
Alumina (Al_2O_3)	4-6%
Iron Oxide (Fe_2O_3)	2-3%
Calcium Oxide (CaO)	60-67%
Magnesium Oxide (MgO)	1-4%
Sulphur Trioxide (SO_3)	1-3%

Loss on Ignition (LOI)	1-3%
Physical Properties	
Fineness	225-280 m^3/kg
Setting Time	Initial: 30-90 minutes
	Final: 220-360 minutes
Soundness	Le Chatelier Expansion: <10mm
Compressive Strength (at 28 days)	41-45 MPa
Bulk Density	1.13-1.19 g/cm^3
Specific Gravity	3.16

3.1.2 Coarse Aggregates

Nominal Size: The coarse aggregates used in the study were crushed gravel with a nominal size of 12.5 mm, indicating that the maximum particle size was 12.5 mm, in accordance with IS 383:2016.

Specific Gravity: The specific gravity of the 12.5 mm aggregates was found to be 2.71. Specific gravity measures the density of a substance compared to the density of water, meaning these aggregates are 2.71 times denser than water, as per IS 2386 (Part 3): 2016.

Water Absorption: The water absorption rate for the 12.5 mm aggregates was recorded at 1.39%. This value represents the percentage of water the aggregates can absorb relative to their weight when immersed in water, following IS 2386 (Part 3): 2016.

The specific gravity and water absorption characteristics of the coarse aggregates are crucial for designing and proportioning concrete mixes. These properties influence the relative density, volume, and water content of the aggregates, which in turn affect the workability, strength, and durability of the concrete mixture.

3.1.3 Fine Aggregates

The fine aggregates used in the study were river sand classified under Zone-II according to Table 3.2. This classification indicates that the sand meets the required particle size distribution standards, making it suitable for concrete applications.

Specific Gravity: The specific gravity of the river sand was measured at 2.43. This means that the sand is 2.43 times denser than water, as per IS 2386 (Part 3): 2016.

Water Absorption: The water absorption rate for the river sand was found to be 1.8%, indicating that the sand can absorb 1.8% of its weight in water when immersed, as per IS 2386 (Part 3): 2016.

Fineness Modulus: The fineness modulus of the river sand was determined to be 3.14. This value, calculated by summing the cumulative percentages by mass retained on standard sieves (ranging from 150 microns to 4.75 mm) and dividing by 100, reflects the sand's particle size distribution. A fineness modulus of 3.14 indicates that the sand is moderately fine, as per IS 2386 (Part 1): 2016.

These characteristics specific gravity, water absorption, and fineness modulus are essential in the design of concrete mixes. They influence the relative density, volume, and grading of the fine aggregates, which in turn affect the concrete's workability, strength, and durability.

Table 3. 2 Gradation of Fine Aggregates

I.S. Sieve	**Weight Retained (gm)**	**Percentage Weight Retained**	**Cumulative % of Weight Retained**	**Cumulative % of Weight Passing**	**Limit by IS 383 for Zone-II**
4.75mm	13	1.3	1.3	98.7	90 to 100
2.36mm	10	1	2.3	97.7	75 to 100
1.18mm	385	38.5	40.8	59.2	55 to 90
600µm	169	16.9	57.7	42.3	35 to 59
300µm	267	26.7	84.4	15.6	8 to 30
150µm	120	12	96.4	3.6	0 to 10
Pan	36	3.6	-	-	
Total	1000	100	282.9		
Fineness Modulus		2.829		Hence, Zone II	

3.1.4 Sodium Chloride (NaCl)

Analytical-grade sodium chloride was obtained for the experiment. This type of salt is specifically produced and refined to meet high purity standards for use in analytical chemistry, research, and laboratory experiments. Analytical-grade salts undergo rigorous purification and quality control processes to minimize impurities that could potentially interfere with experimental results. The sodium chloride was sourced from a reputable chemical supplier.

3.1.5 Water

Potable tap water was used, with NaCl concentrations of 1% and 3% by weight of cement, for casting and curing the specimens. The inclusion of NaCl in the water was essential for curing because, in regular water, chlorides from the concrete specimens could leach out through

osmosis. For all testing purposes, deionized water was used to prevent the influence of ions like Ca^{2+}, Al^{3+}, Na^{+}, and K^{+} on the tests.

3.1.6 Nichrome Mesh

The Nichrome mesh used in this study has a specification of 40 lines per inch, with a wire diameter of 0.23 mm. Nichrome, an alloy primarily composed of nickel and chromium, is well-known for its excellent resistance to oxidation and high temperatures. The mesh, characterized by 40 lines per inch, indicates that there are 40 openings per inch of the material, providing a specific level of permeability and strength. The wire diameter of 0.23 mm contributes to the structural integrity of the mesh, balancing strength with flexibility. This makes it an ideal material for applications requiring durability under thermal stress.

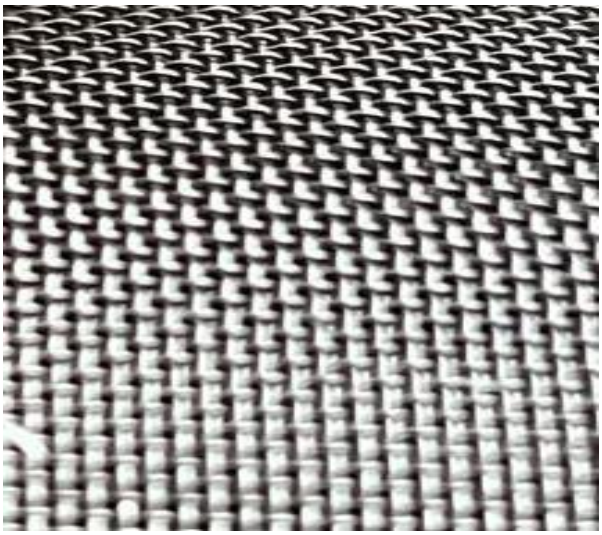

Figure 3. 1 Nichrome mesh 40 openings/inch wire dia of 0.23 mm

3.1.7 Steel

For the experimental purposes, HYSD steel bars with a diameter of 12 mm and a length of 360 mm were used, adhering to the specifications of IS 1786:2008. Detailed information about the physical and chemical properties of these steel bars, as provided by the manufacturer, can be found in Table 3.3.

Table 3. 3 Properties of steel bars used

Property	**Constituents**	**HYSD (Fe 550)**
Chemical Properties	Carbon	0.30%
	Sulphur	0.055%
	Phosphorus	0.055%
	Nitrogen	120ppm
Physical Properties	Minimum Yield Stress	500 N/mm^2
	Minimum Ultimate Tensile Strength	601 N/mm^2
	Minimum Elongation	12.0%

Figure 3. 2 Tata steel of 12mm fe550

3.1.8 Epoxy

For this study, Fevitite Rapid epoxy adhesive was used. This adhesive consists of two components: Resin and Hardener, which are mixed in a 1:1 ratio to ensure equal proportions. The adhesive was applied using a thin plate to coat the steel specimens, which were then allowed to dry for 24 hours. Additionally, the same epoxy was applied to the sides of the concrete specimens during the preparation for the BIEM experiment.

3.2 Experiment Conducted

3.2.1 PZT Transducer

The PZT transducer used in this study is a Lead Zirconate Titanate device with dimensions of 20 mm × 20 mm × 0.4 mm, specifically of the SP-5H grade (equivalent to Navy Type VI, as per US DOD MIL STD 1376). It features a silver electrode with high-quality, fired-on silver electrodes, which are suitable for soldering. The transducer is designed with wrap-around electrodes and is poled across its thickness, with the polarity clearly marked. The device includes lead wires for connection: a red wire soldered to the positive face and a black wire to the negative face, each made of PTFE-coated, 6-inch-long, 28/7/36 type wire.

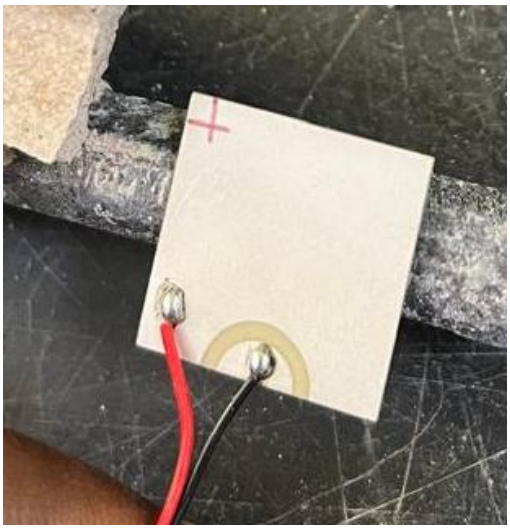

Figure 3. 3 Lead Zirconate Titanate device 20mm x 20mm x 0.4 mm SP-5H grade(Sparkler Piezoceramics Pvt Ltd.)

3.2.2 Sacrificial Zinc Anode

Sacrificial zinc anodes are vital in protecting metal structures from corrosion, particularly in challenging environments like marine settings. They function by undergoing oxidation, sacrificing themselves to shield the protected metal, thus significantly prolonging the structure's lifespan. The effectiveness of these anodes is often tested in artificial seawater conditions to mimic real-world scenarios, ensuring they can reliably prevent corrosion over time. Advanced techniques, such as impedance monitoring with PZT transducers, are used to

detect changes in conductance spectra, allowing for precise damage assessment and lifespan prediction. Additionally, zinc anodes have been shown to reduce chloride content on the surface of reinforcing steel in concrete structures, addressing one of the primary causes of corrosion. By lowering chloride concentration, they help maintain the structural integrity of reinforced concrete, making sacrificial zinc anodes indispensable in corrosion protection and infrastructure longevity.

In our experiment, we are using two types of zinc anodes for the protection of structures: Anode A and Anode B. To monitor the health and effectiveness of these anodes, PZT transducers were employed. These transducers allowed to track changes in impedance, providing valuable data on the condition and performance of the anodes over time.

Figure 3. 4 Anode A

Figure 3. 5 Anode B with PZT

3.2.3 Finding Peak Conductance at Frequency Range Using PZT on Anode

PZT ON Zinc Mass of Anode

PZT transducers were placed directly on the Zinc mass to find the peak conductance at a specific frequency range. This setup helps in assessing the condition and effectiveness of the sacrificial zinc anode over time.

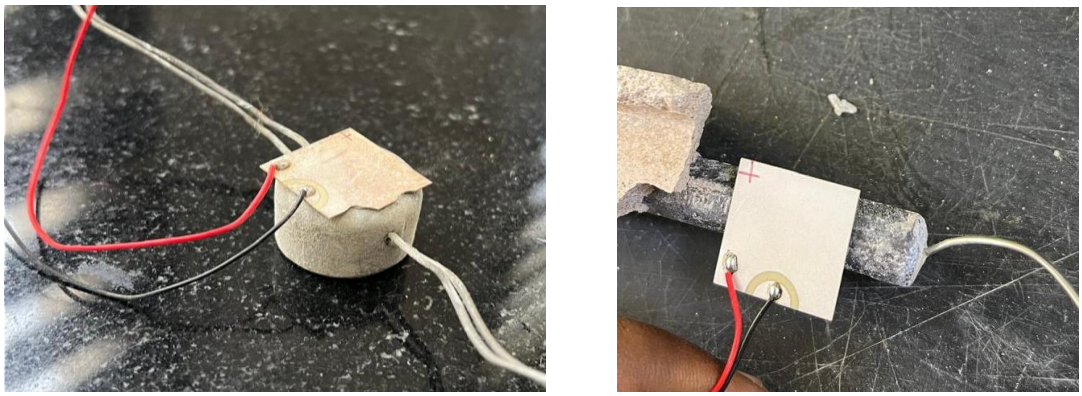

Figure 3. 6 PZT on Zinc mass of Anode A & B

PZT ON Conductive Motar

PZT transducers are positioned on the Anodes to find the peak conductance at a frequency range. This method was performed to check effectiveness of PZT to detect the health of the anode

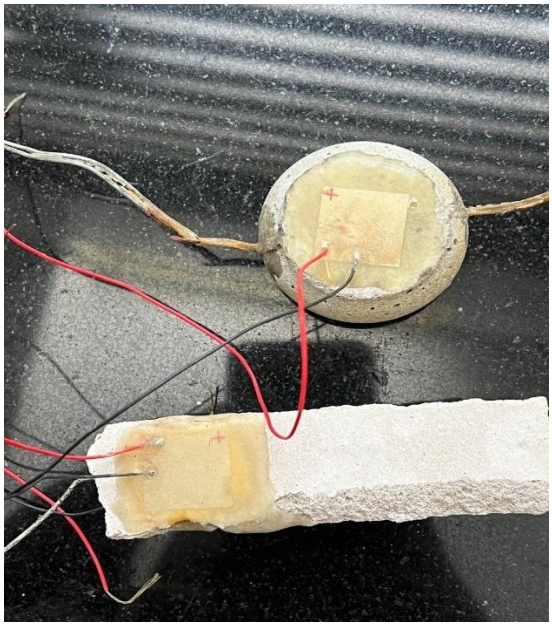

Figure 3. 7 PZT on anode surface of Anode A & B

PZT ON CONDUCTIVE MOTAR IMMERSED IN WATER

PZT transducers are positioned on the Anode that is immersed in water to find the peak conductance at a frequency range.

Figure 3. 8 PZT on immersed anode surface of Anode A & B

TESTING

1) Frequency Range of Conductance

The test was conducted to find the frequency range of conductance and to ensure that PZT transducers placed on the Zinc mass and those positioned on the Anode surface provide the same frequency range for peak conductance values. This verification is crucial for validating the consistency and reliability of PZT measurements across different locations on the Zinc mass or Anode surface.

2) Accelerated Corrosion Experiment

The electro-mechanical impedance (EMI) technique is an effective method for monitoring the condition of sacrificial anodes during accelerated corrosion experiments. This technique utilizes piezoelectric transducers, such as PZT (Lead Zirconate Titanate) transducers, which are bonded to or embedded in the anode material. The transducers generate mechanical vibrations that propagate through the material, allowing the measurement of electrical impedance across a range of frequencies. The experimental setup involved applying a constant current of 0.47 A to induce accelerated corrosion, which is significantly higher than typical natural corrosion rates. This method allows researchers to observe the effects of corrosion in a shorter time frame, facilitating a better understanding of the degradation process. Throughout the experiment, the impedance of the PZT transducer was measured at 30-minute intervals, providing valuable data on the conductance spectra.

$$RMSD(\%) = \sqrt{\frac{\sum_{i=1}^{N}(G1_i - G0_i)^2}{\sum_{i=1}^{N}(G0_i)^2}} X100$$

- **G0i**: Baseline conductance value at frequency index iii (uncorroded state).
- **G1i**: Post-corrosion conductance value at frequency index iii (corroded state).
- **N**: Total number of frequency points in the given frequency range.
- **i**: Frequency index corresponding to a particular frequency within the range.

Root mean square deviation (RMSD) of the spectra were studied to monitor anode's state-of-health, reflecting changes in corrosion dynamics. Additionally, the potential of EMI techniques for real-time, non-destructive monitoring of sacrificial anodes, which can significantly enhance the maintenance strategies for reinforced concrete structures. By understanding the corrosion behavior and the effectiveness of the sacrificial anodes, service life of critical infrastructure can be evaluated

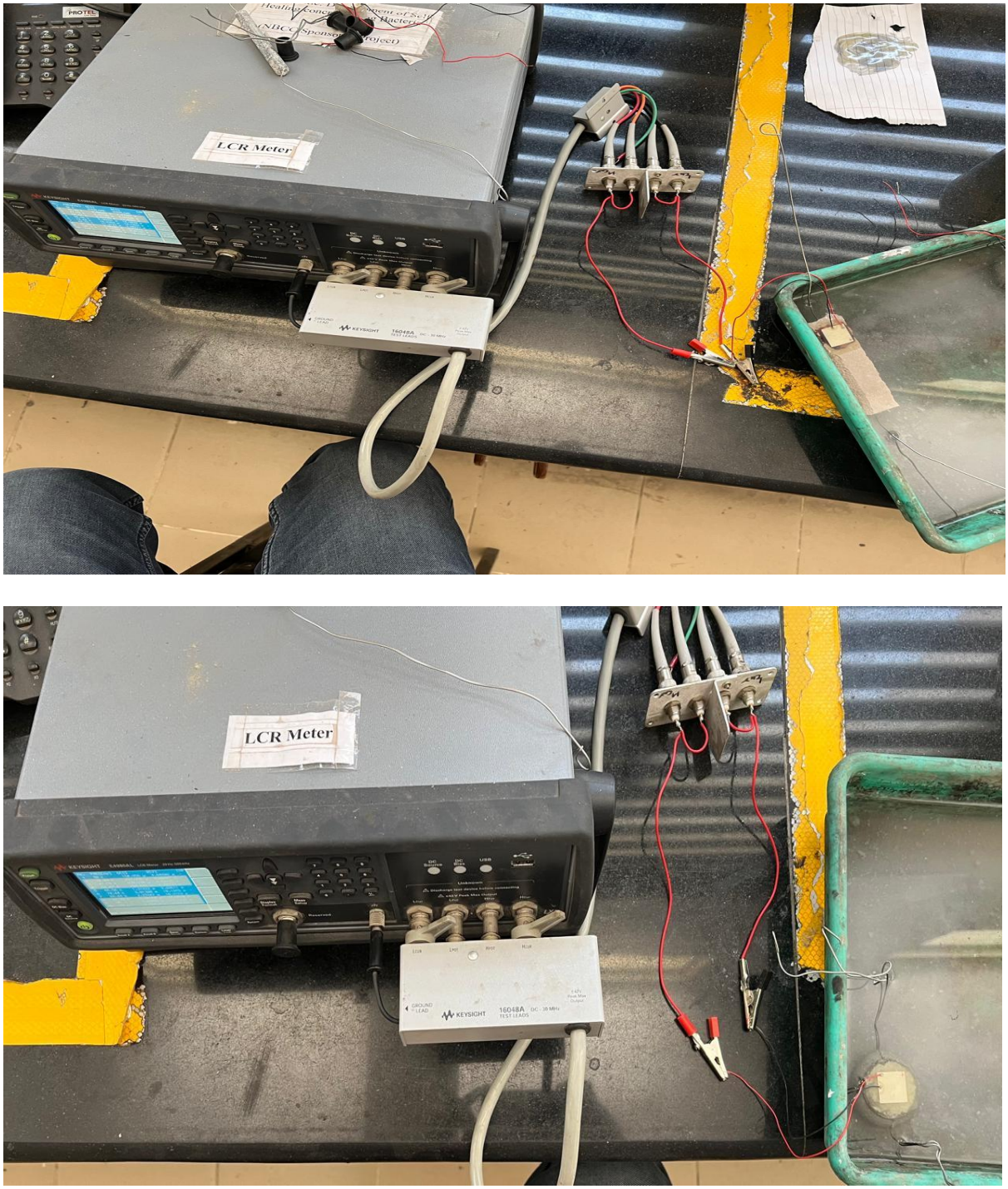

Figure 3. 9 Accelerated Corrosion Experiments on Anode A & B

3.2.4 PZT on anode embedded in concrete slab

Specimen Preparation

Concrete specimens were cast using Ordinary Portland Cement (OPC) of grade 43, in accordance with IS 8112-1989. To induce varying levels of corrosion within the concrete, NaCl (sodium chloride) was added at a concentration of 3% by weight of cement to the concrete mix.

The concrete specimens, measuring 300 mm × 300 mm × 80 mm, included four HYSD (High Yield Strength Deformed) steel bars, each with a diameter of 12 mm. These bars were embedded in each specimen, spaced 200 mm apart with a 25 mm cover from the bottom face. After 24 hours of casting, the specimens were demolded and then cured for 28 days in the respective NaCl solutions. This curing process facilitated the development of the desired corrosion conditions within the concrete.

To protect the exposed ends of the steel bars from corrosion, they were masked with epoxy and covered with a heat shrink sleeve. These protective measures aimed to isolate the exposed steel surfaces and prevent direct contact with the corrosive environment, allowing for a focused evaluation of corrosion effects within the concrete specimens. Controlled conditions were established through specific concrete mix proportions, NaCl concentrations, steel bar arrangements, and corrosion protection measures, which were used to study the corrosion behavior and assess the performance of the concrete specimens.

3.2.5 Procedure for Casting the Specimens:

1. **Preparation:** Gather the necessary materials and equipment, such as cement, sand, coarse aggregates, water, mould forms, reinforcement, mixing equipment (e.g., a concrete mixer or mixing tray), trowels, and a level.
2. **Mould Setup:** Place the mould forms on a casting bed, clean them of any debris or dirt, and coat them with a thin layer of oil to facilitate easy demolding.
3. **Reinforcement Placement:** Position the steel bars within the mould forms according to the design specifications, ensuring proper spacing of 200 mm and a cover of 25 mm from the bottom. Shown in Figure 3. 10

Figure 3. 10 4 Steel bar of 12mm were placed and are connected through tie wire

4. **Mixing:** Prepare the M40 concrete mix design by accurately proportioning cement, sand, and coarse aggregates. First, thoroughly mix the dry materials. Gradually add water while mixing until a uniform consistency is achieved, using a concrete mixer to ensure proper blending of the ingredients.
5. **Pouring:** Transfer the concrete mix into the oiled moulds, compacting in 3 layers. Use a shovel and scoop to distribute the concrete evenly within the moulds.
6. **Compaction:** Compact the mix within the moulds using a vibrating table to eliminate air voids and ensure proper compaction. Continue vibrating until air bubbles stop rising to the surface.
7. **Finishing:** Smooth the surface of the concrete using a trowel and a screed board after compaction. Shown in Figure 3. 11

Figure 3. 11 Concrete M40 was filled upto 80mm

8. **Demolding:** Carefully remove the specimens from the moulds after 24 hours. Gently tap the sides of the moulds with a pry bar to release the concrete slabs and loosen the nuts to open the mould properly.
9. **Curing:** Cure the cast specimens for 28 days, maintaining a moist environment. Use NaCl water with the same concentration as in the mixed concrete for curing.
10. **Drilling:** Drill a hole in the center of the slab to the size of the zinc anode embedded in conductive mortar, ensuring the depth levels with the steel bars inside while maintaining a safe distance from the internal steel. Shown in Figure 3. 12

Figure 3. 12 Drilled a hole to place anode at the center to the level of steel

11. **PZT Sensor Placement:** Attach the PZT sensor onto the surface of the conductive mortar (in which the zinc anode is embedded) and cover the PZT wires with a heat shrink sleeve to protect them. Shown in Figure 3. 13

Figure 3. 13 Anode is placed in the Drilled area

12. **Zinc Anode Placement:** Place the zinc anode (embedded in conductive mortar) into the drilled hole in the slab and cover it with additional mortar to secure it in place. Shown in Figure 3. 13

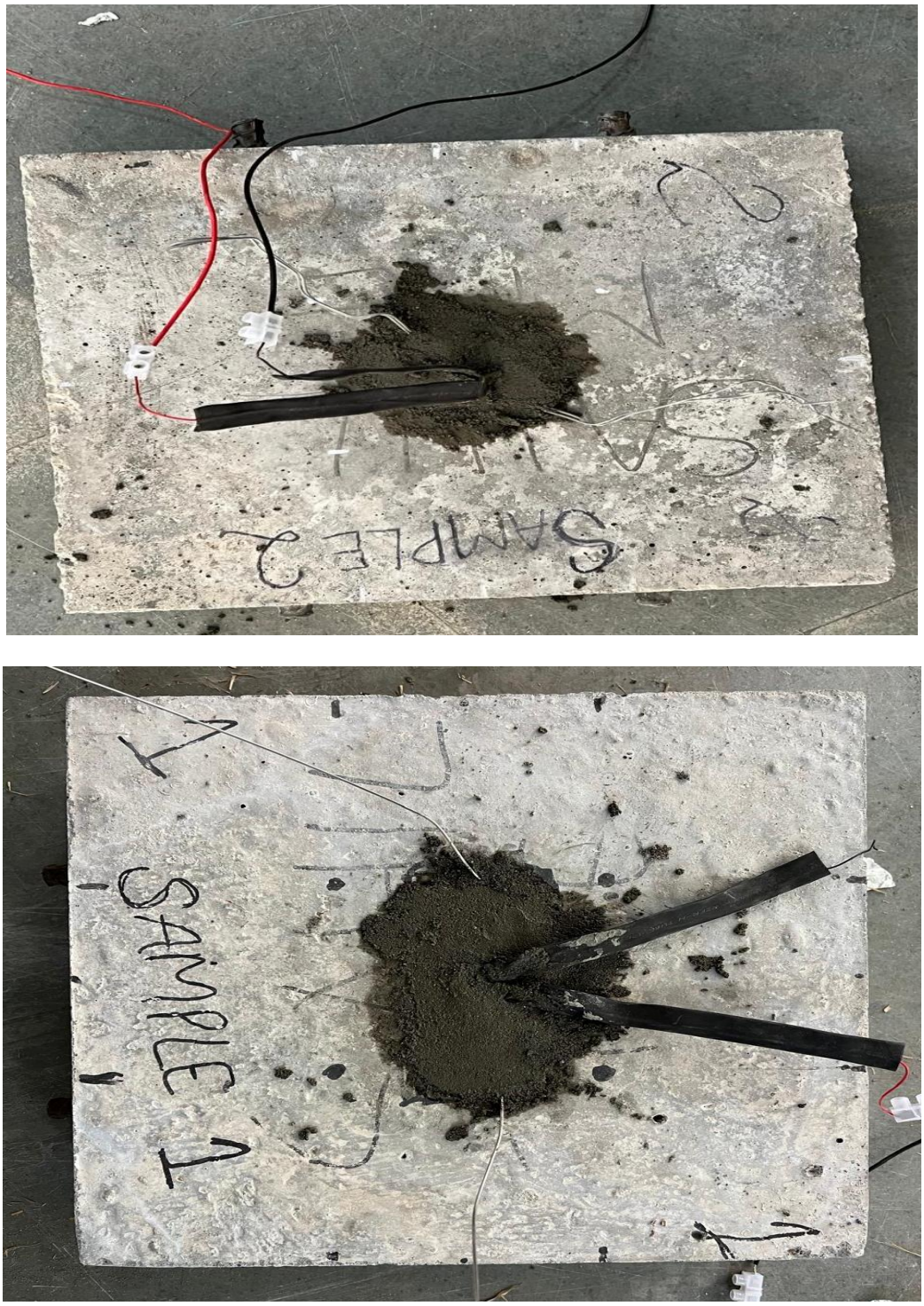

Figure 3. 14 Covered the anode with mortar

3.2.6 Half-Cell Potential

The half-cell potential method is a widely used electrochemical technique for assessing the corrosion potential of steel embedded in concrete. This method involves measuring the electrical potential difference between a reference electrode and the steel reinforcement within the concrete. A copper/copper sulfate (Cu/CuSO4) or silver/silver chloride (Ag/AgCl) electrode typically serves as the reference, providing a stable reference potential. During the procedure, the reference electrode is placed on the surface of the concrete while making an electrical connection to the steel reinforcement. The potential difference between the reference electrode and the steel is then measured using a high-impedance voltmeter.

The measured potential indicates the likelihood of corrosion activity and is interpreted according to standard criteria, such as those outlined in ASTM C876. A potential more positive than -200 mV (Cu/CuSO4) suggests a low probability of corrosion, whereas a potential between -200 mV and -350 mV indicates an uncertain probability. A potential more negative than -350 mV points to a high probability of active corrosion.

The half-cell potential method offers several advantages, including its non-destructive nature, allowing for the assessment of corrosion potential without damaging the concrete structure. It facilitates early detection of corrosion, enabling timely maintenance and repairs that can extend the structure's lifespan. Additionally, this method is versatile, suitable for both laboratory and field use, making it applicable to various structures such as bridges, buildings, and other concrete constructions. Employing the half-cell potential method helps engineers and maintenance professionals effectively monitor the condition of steel reinforcement in concrete, ensuring structural integrity and longevity.

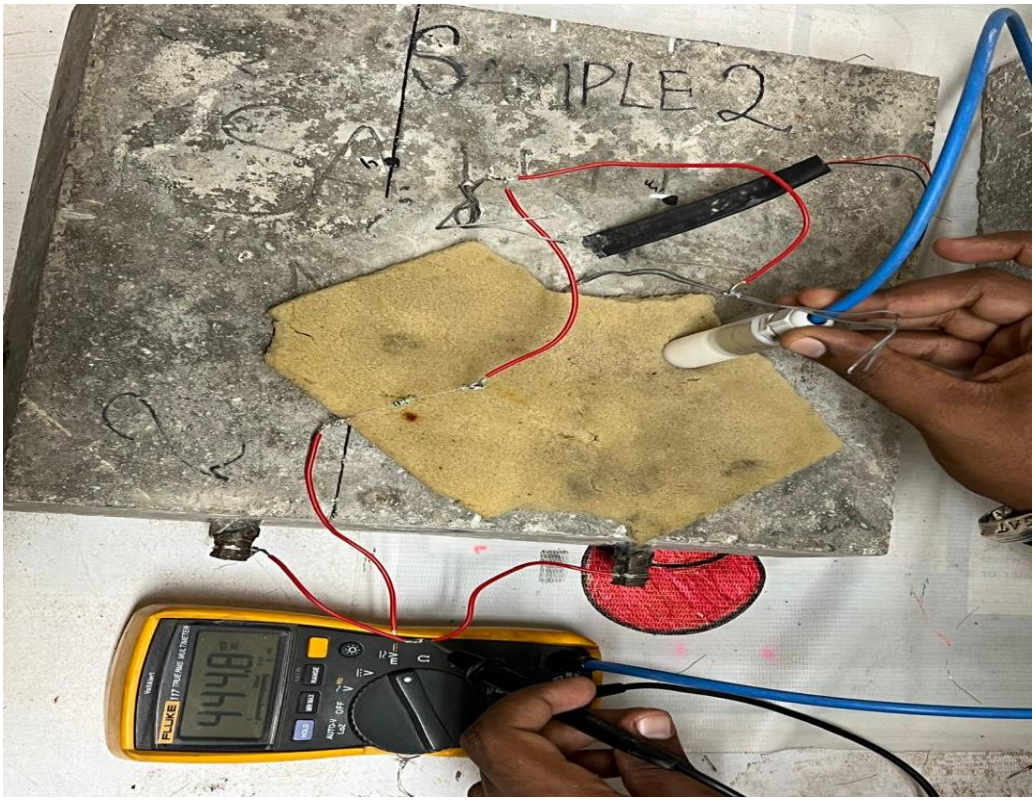

Figure 3. 15 Half cell potential using multi-meter and Ag/AGCl/0.5M KCl reference electrode

3.2.7 Linear Polarization Resistance (LPR)/ Corrosion Rate (CR)

Linear Polarization Resistance (LPR) is a widely utilized electrochemical method for determining the corrosion rate of metallic materials. This technique operates on the principle that when a metal is exposed to a corrosive environment, it experiences electrochemical reactions, leading to the flow of electric current. As outlined in BS EN ISO 14038-2:2020, LPR measures the resistance to polarization by applying a small perturbation in potential and monitoring the resulting current response.

The significance of LPR lies in its capability to provide a rapid, non-destructive, and quantitative evaluation of the corrosion rate of metals. This method allows for continuous monitoring of corrosion processes, enabling early detection and intervention, which is crucial for preventing significant material degradation and ensuring the longevity of structures and components.

Figure 3. 16 Linear Polarization Resistance (LPR)

3.2.8 Health monitoring of anode with PZT through LCR meter

The health monitoring of a sacrificial anode embedded in conductive mortar was conducted using a PZT transducer and an LCR meter. The wires of the PZT transducer, attached to the conductive mortar encasing the anode, were connected to the LCR meter. The LCR meter provided different frequencies and measured the conductance of the anode at these frequencies. By identifying the specific frequencies at which the conductance was highest, critical areas of the anode's performance were recorded. These conductance values were then used to determine the Root Mean Square Deviation (RMSD%), which provides insights into the degradation and effectiveness of the sacrificial anode over time.

$$\Delta m = F \times z \times M \times I \times T$$

- **Δm**: Mass loss of the sacrificial anode due to corrosion.
- **I**: Current passing through the cell (impressed current in accelerated corrosion experiments).
- **M**: Molecular weight of the reactive species (e.g., zinc in the case of a zinc sacrificial anode).
- **T**: Total time duration for which the current flows in the cell, starting from t=0t = 0t=0.
- **F**: Faraday's constant, which is approximately 96,485 coulombs per mole of electrons.
- **z**: Valency (number of electrons involved in the reaction) of the reactive species.

Additionally, using Faraday's law of electrolysis, the mass loss of the anode in grams can be calculated. This law relates the amount of substance that undergoes oxidation or reduction at an electrode to the amount of electric charge passing through the circuit. By calculating the mass loss, we gain further insights into the rate of corrosion and overall health of the anode. This method allows for a detailed and quantitative assessment of the anode's health, ensuring timely maintenance and replacement to maintain the integrity of the reinforced concrete structure.

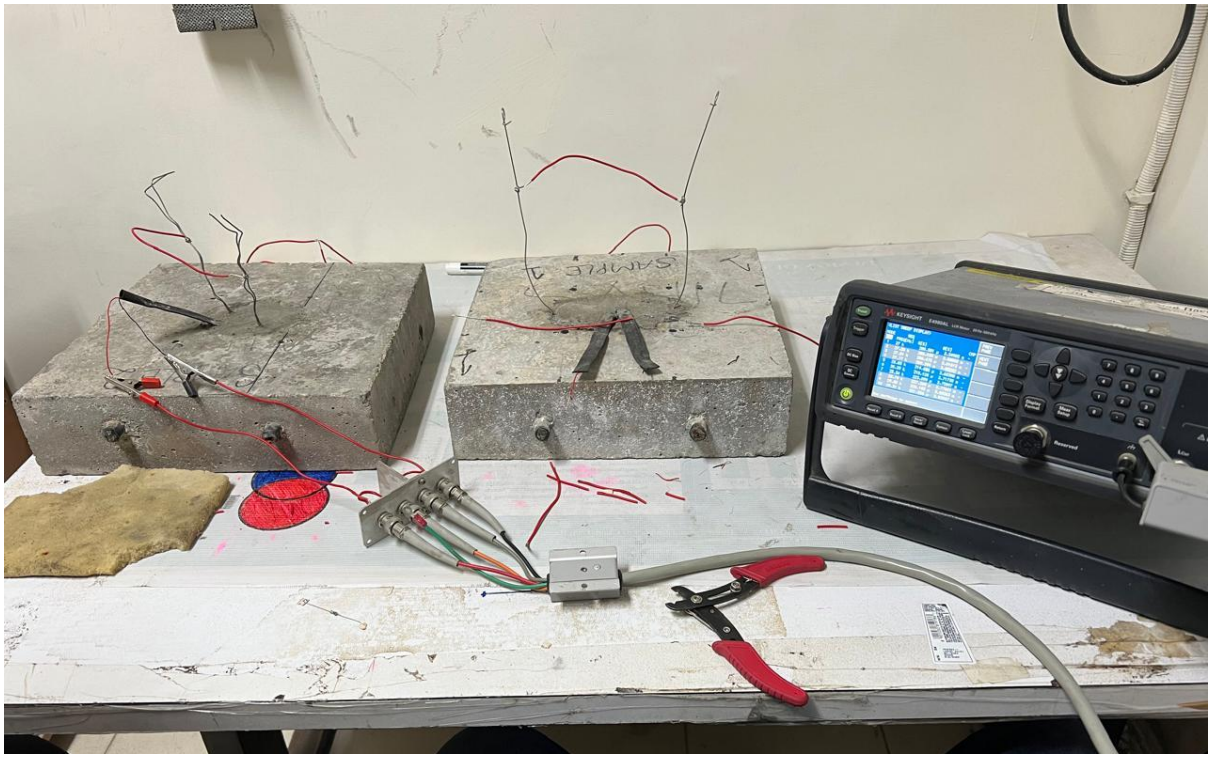

Figure 3. 17 Health monitoring of anode through LCR meter

3.2.9 GAP Test

The Galvanic Anode Performance (GAP) test is an innovative method designed to evaluate the longevity of galvanic anodes (GAs) used in reinforced concrete structures. This test is crucial as many GAs fail prematurely, often within a few months, leading to significant repair costs and structural issues. The GAP test aims to address this problem by providing a reliable assessment of GA performance over time. In the GAP test, the anode is embedded in bedding mortar, simulating real-world conditions, while a cathode made of corrosion-resistant mesh represents the rebars in concrete structures. The test examines several critical factors, including the selection of cathode material, the ratio of cathode to anode, the applied potential, and the type and level of electrolyte used.

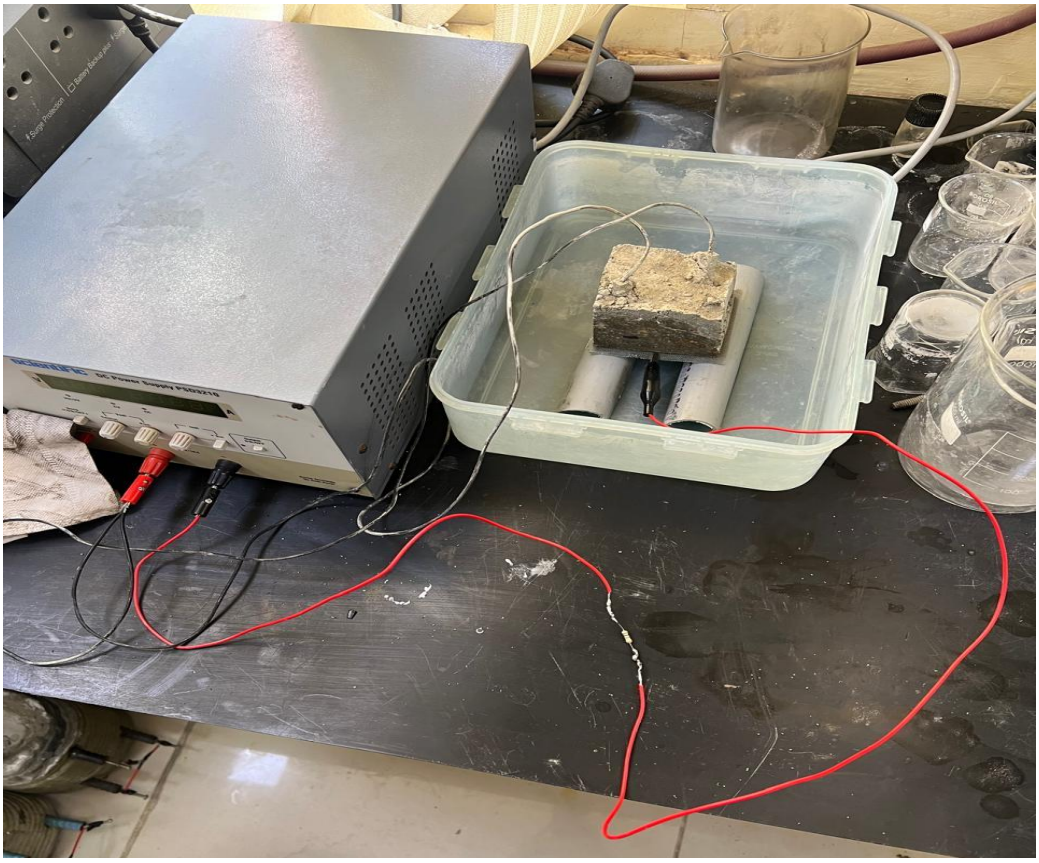

Figure 3. 18 GAP test setup

By conducting the GAP test, researchers can identify potential failure mechanisms, such as the pH and pore volume of the encapsulating mortar, which can lead to premature failures. This method not only helps in understanding the behavior of GAs under various conditions but also assists engineers in estimating their service life, ultimately contributing to more effective maintenance strategies for reinforced concrete structures.

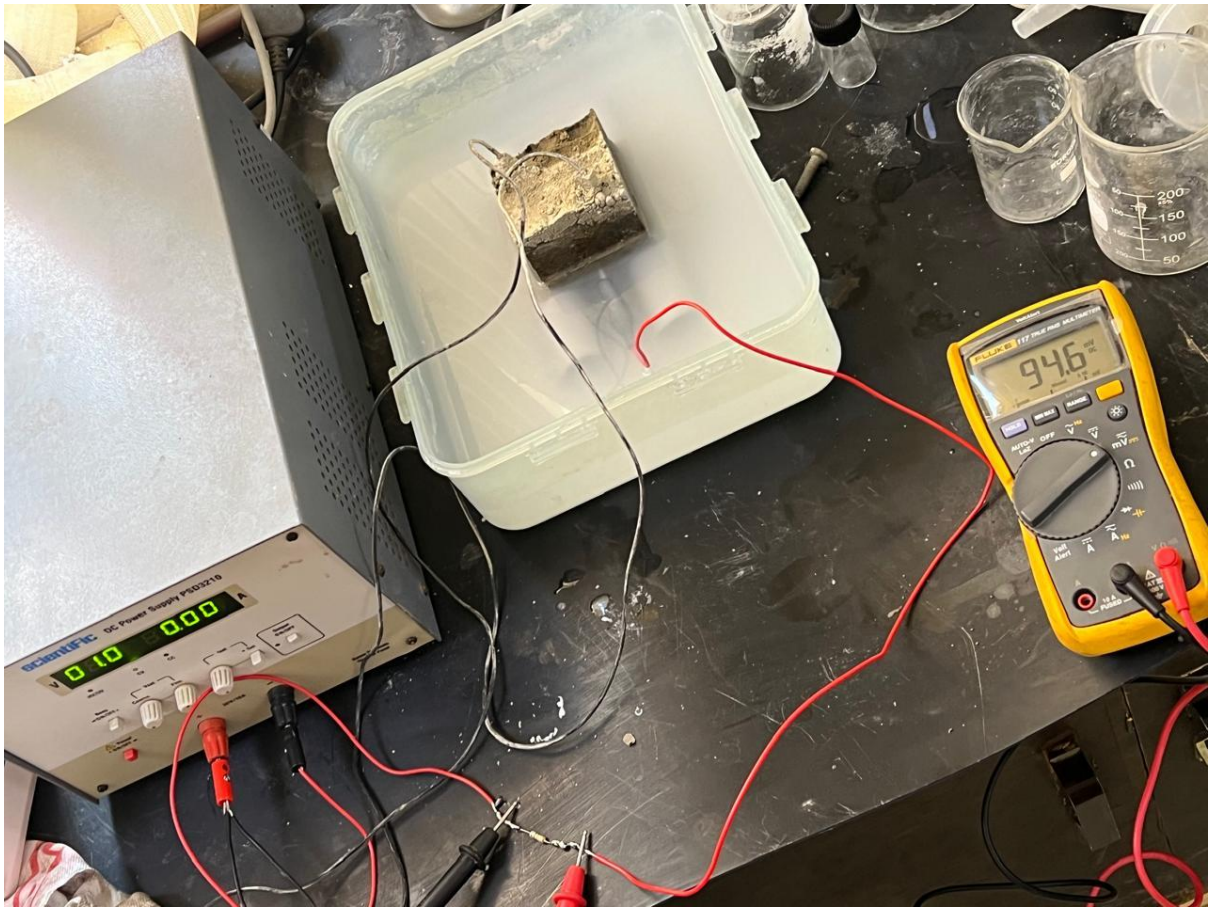

Figure 3. 19 Multi meter is used to take the potential of the Anode

CHAPTER 4 RESULTS AND DISCUSSION

This Chapter provides an in-depth examination of the long-term viability and effectiveness of sacrificial anodes and their role in protecting reinforced concrete structures from corrosion. Through a series of tests, including galvanic anode performance, frequency range analysis, accelerated corrosion experiments, 100 mV depolarization tests, and Life Span analysis using RMSD%, this chapter offers a comprehensive evaluation of how these anodes perform over time under different conditions. The findings reveal critical insights into the behavior of sacrificial anodes, the impact of corrosion on reinforced concrete, and the effectiveness of cathodic protection systems.

4.1 Validation of Conductance Frequency Range Consistency for PZT Transducers on Zinc Mass and Anode Surface

This test was performed to find the frequency range of conductance and to ensure that PZT transducers placed on the Zinc mass and those positioned on the Anode provide the same frequency range for peak conductance values for Both Anode. This verification is crucial for validating the consistency and reliability of PZT measurements across different locations on the Zinc mass or Anode.

ANODE A

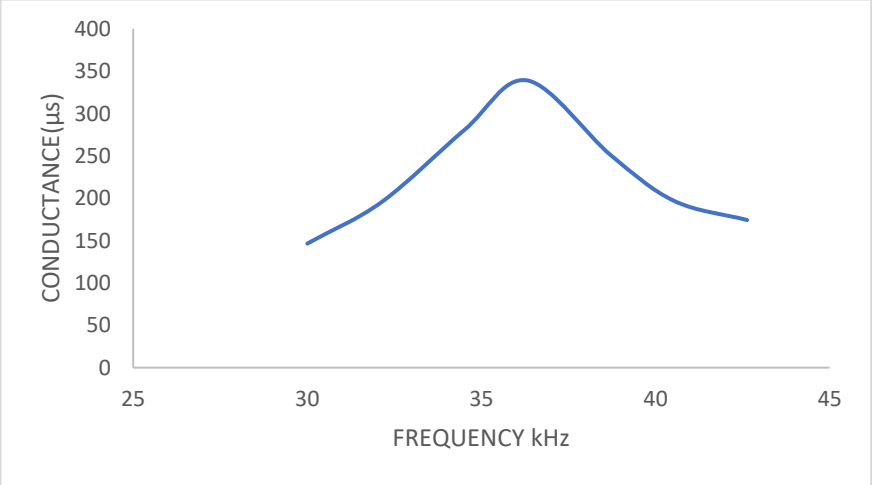

Figure 4. 1 PZT ON ZINC MASS OF ANODE A

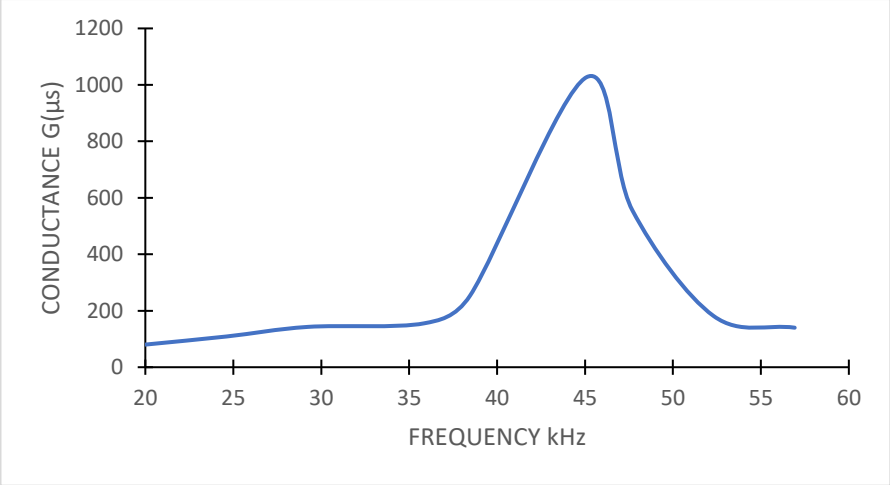

Figure 4. 2 PZT ON Surface of ANODE A

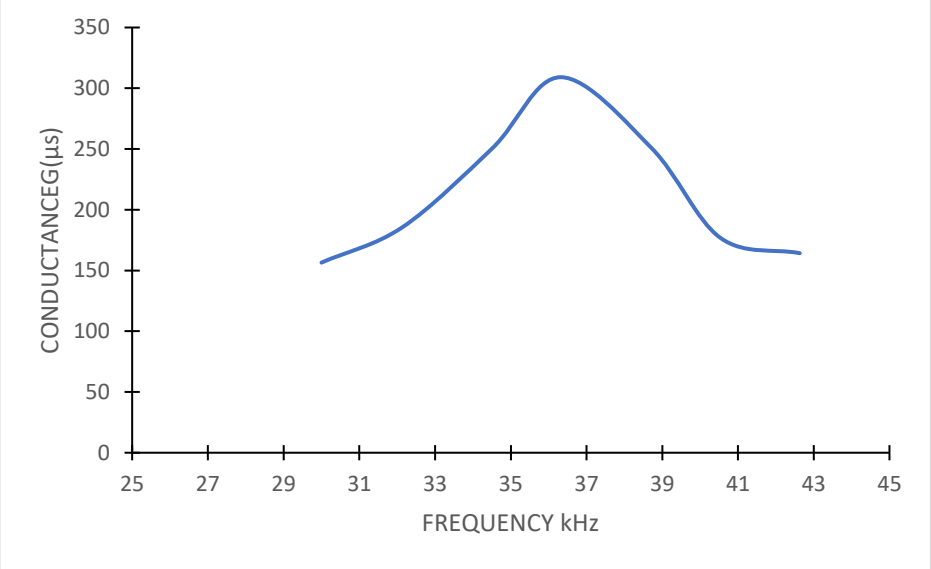

Figure 4. 3 PZT ON ANODE SURFACE AND IMMERSED IN WATER

ANODE B

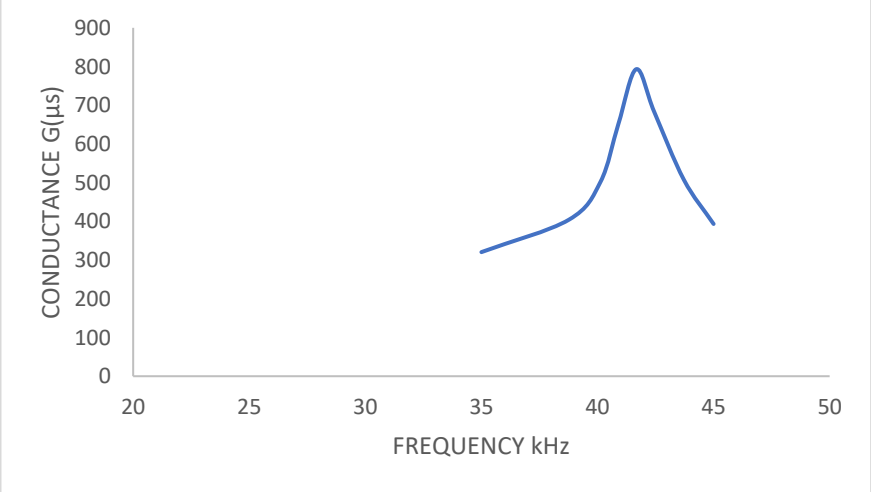

Figure 4. 4 PZT ON ZINC MASS OF ANODE B

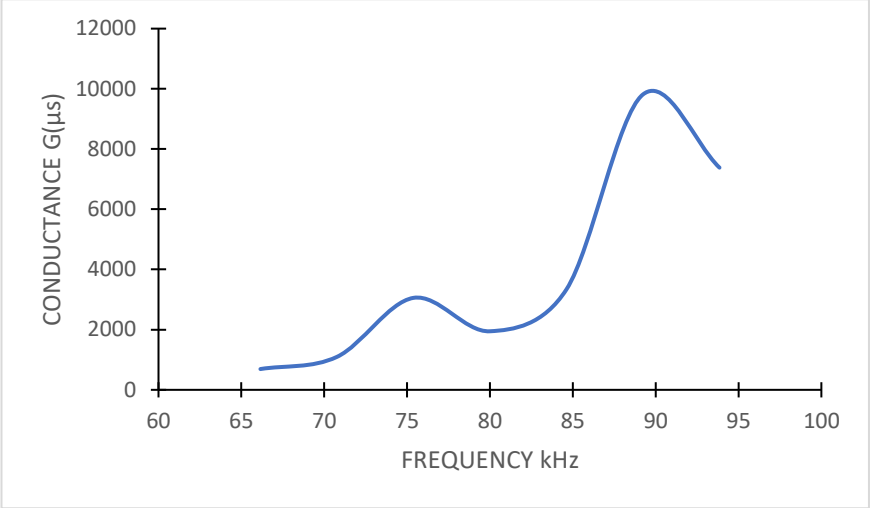

Figure 4. 5 PZT ON SURFACE OF ANODE B

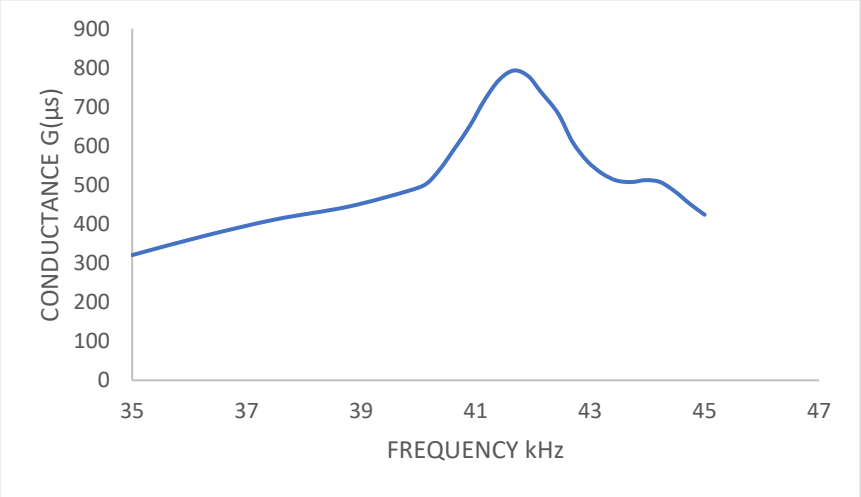

Figure 4. 6 PZT ON SURFACE OF ANODE B AND IMMERSED IN WATER

The conductance measurements for PZT (Lead Zirconate Titanate) in various configurations reveal distinct resonance behaviors. When PZT is placed on the zinc mass (Anode B), the conductance peaks at 41.67 kHz, indicating this as the optimal frequency for maximum conductance. On the anode surface (Anode B), the peak shifts higher to 45.08 kHz, suggesting a different resonance compared to the anode. However, when the PZT is placed on the Anode surface and immersed in water, the conductance peak reverts to 41.67 kHz, similar to the anode condition, implying that immersion activates the PZT similarly to its activation on the anode. In the case of PZT with Anode A, the anode configuration shows a peak at 36.32 kHz, while

on the surface, multiple resonance peaks are observed at 75.38 kHz and 89.23 kHz, differing from the Anode B measurements. Upon immersion, the surface with Anode A also shows a peak at 36.32 kHz, consistent with the anode condition. These findings suggest that immersion in water has a significant impact on the activation and resonance of PZT, aligning its behavior with that observed on the anode.

4.2 Accelerated Corrosion Experiments

Evaluating the performance of Anode A and Anode B to determine their effectiveness and durability in corrosion protection systems. This comparison aims to identify the more reliable anode under challenging conditions, ensuring optimal protection and longevity of structures.

ANODE A

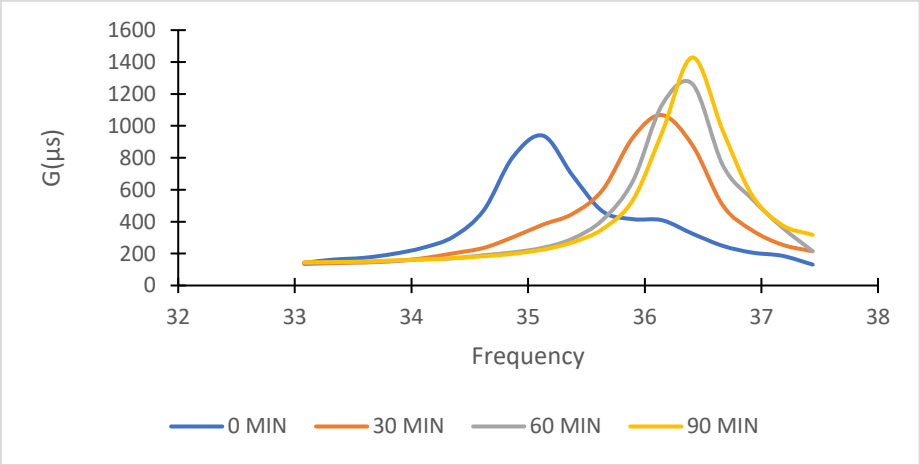

Figure 4. 7 Experimental results for conductance spectra for ANODE A

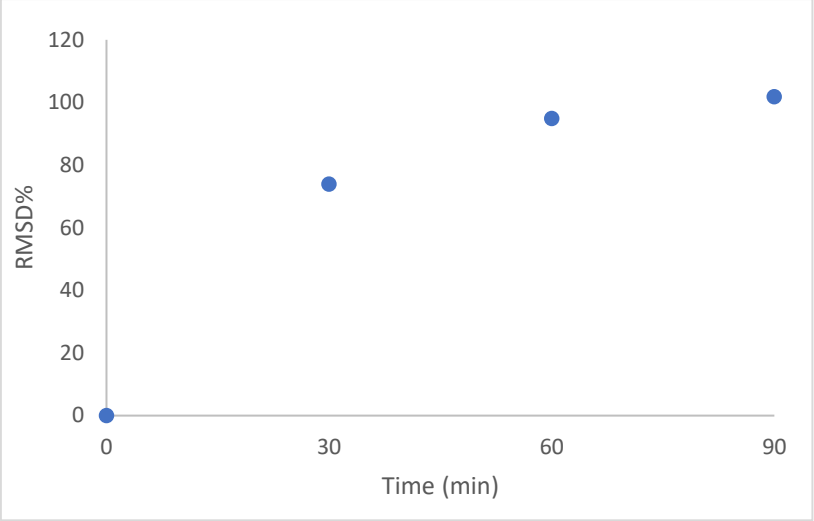

Figure 4. 8 Time V/S RMSD % ANODE A

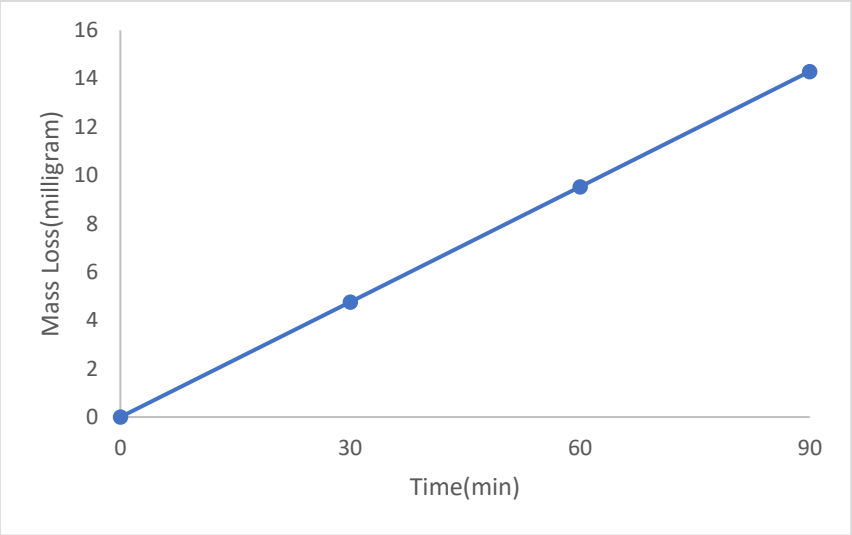

Figure 4. 9 Time V/S Mass loss ANODE A

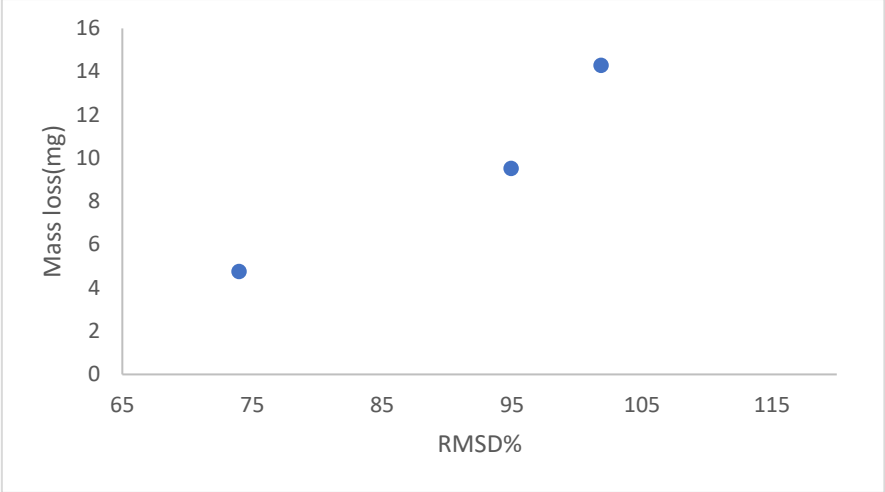

Figure 4. 10 RMSD% V/S Mass loss ANODE A

ANODE B

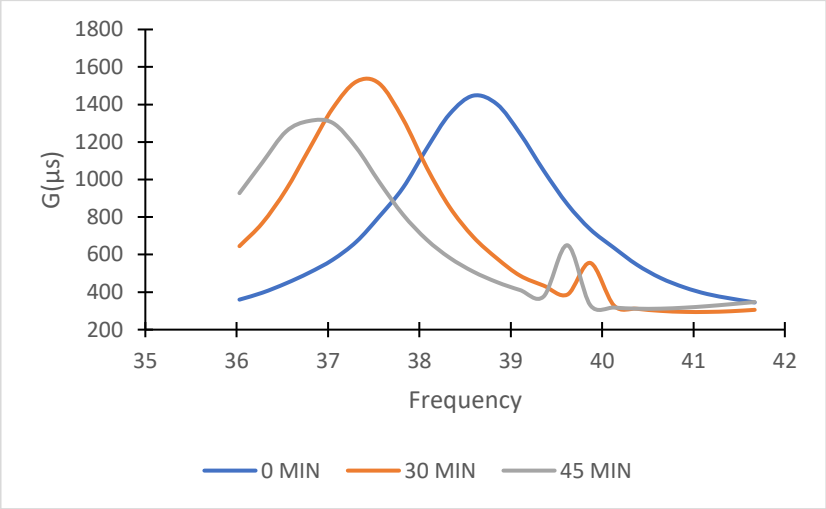

Figure 4. 11 Experimental results for conductance spectra for ANODE B

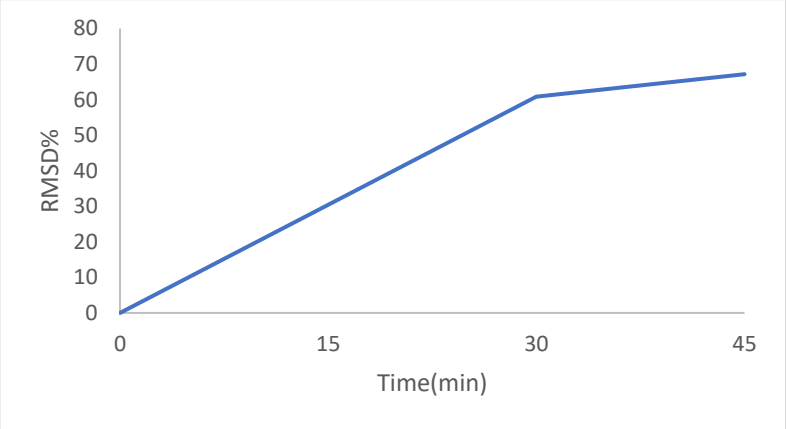

Figure 4. 12 Time V/S RMSD % ANODE B

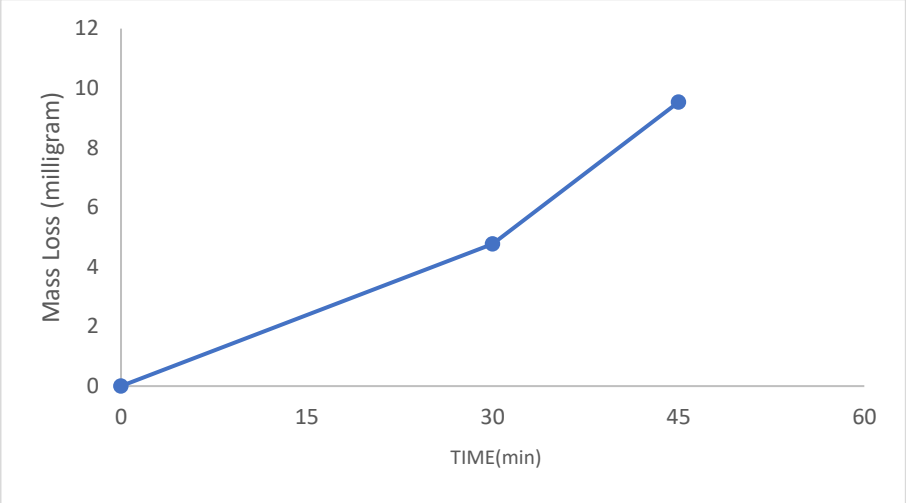

Figure 4. 13 Time V/S Mass loss ANODE B

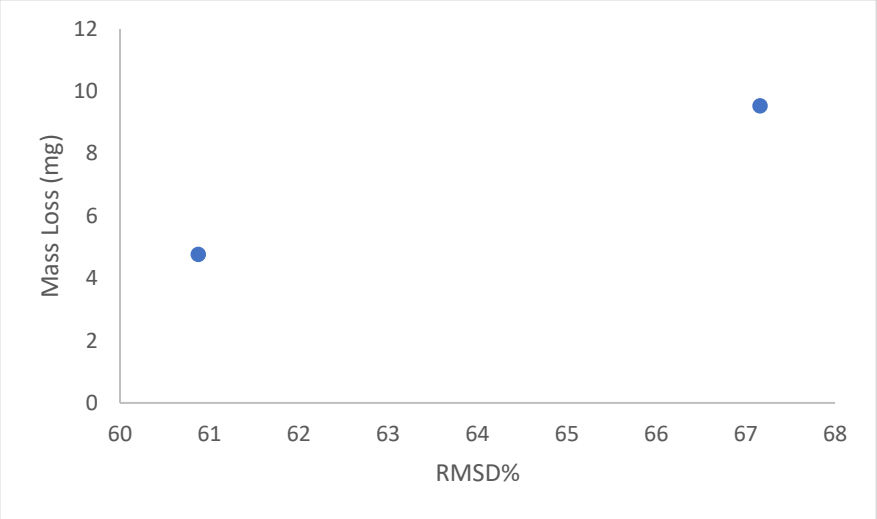

Figure 4. 14 Mass loss V/S RMSD% ANODE B

Table 4. Mass Loss with Time

ANODE A				**ANODE B**			
Time (T)	**RMSD%**	**Mass Loss Δm(milligrams)**	**zinc oxide**	**Time (T)**	RMSD%	**Mass Loss Δm(milligrams)**	**zinc oxide**
30	73.9716	4.7658	5.9502	30	60.87331474	4.7658	5.9502
60	94.9362	9.5316	11.9004	45	67.15820978	9.5316	11.9004
90	101.8517	14.2974	17.8506				

The performance differences between the Anode B and Anode A anodes when submerged in a NaCl solution with a current of 0.47A. The **Anode B anode** shows suboptimal performance, as evidenced by its tie wire breaking after just 45 minutes. This premature failure is indicative of the anode's inability to withstand the applied conditions for an extended period. The frequency vs. conductance graph for Anode B reveals that the peaks occur at different locations with increasing frequency, suggesting instability in its response. This erratic behavior further highlights the Anode B anode's unsuitability for sustained use under these conditions, leading to its early breakdown.

Anode A performs significantly better. The conductance graph for Anode A shows a consistent increase in conductance with rising frequency, indicating stability and robustness. This steady increase suggests that Anode A can maintain its structural integrity and performance over time, even in the challenging environment of a NaCl solution with a constant current. The accompanying data, including RMSD% (Root Mean Square Deviation) and mass loss, further reinforces these observations. The RMSD% for Anode B increases over time, signaling a degradation in performance, while the mass loss data shows that Anode B is losing material more rapidly. On the other hand, Anode A's RMSD% values and mass loss data indicate greater resistance to degradation, with more stable performance over time.

Overall, the data strongly supports the conclusion that **Anode A** is the more reliable and durable anode material under these test conditions, while **Anode B** fails to meet the necessary performance standards.

The conductance data over different time intervals (0, 30, 60, and 90 minutes) during an accelerated corrosion experiment in mortar highlights the progression of corrosion and its impact on the material’s electrical properties. Initially, at 0 minutes, the conductance peak occurs at 35.13 kHz with a value of 938.322 μS, representing the mortar’s state before significant corrosion. As time progresses to 30 minutes, the conductance peak increases to

1067.51 µS at a slightly higher frequency of 36.15 kHz, indicating the onset of corrosion and the early changes in the material's structure. At 60 minutes, the peak conductance further rises to 1261.81 µS at 36.41 kHz, reflecting more advanced corrosion where the rebar's protective layer deteriorates, leading to increased conductivity within the system. By 90 minutes, the conductance reaches its highest value of 1429.36 µS at the same frequency, signifying extensive corrosion and significant degradation of the rebar and mortar interface. The shift in peak conductance to higher frequencies along with the increasing conductance values suggest that corrosion progressively alters the mortar's properties, enhancing its conductivity and affecting its resonant frequency. These findings underscore the critical role of monitoring conductance in assessing the extent of corrosion in reinforced concrete structures.

Figure 4. 15 Progressive change in color of electrolyte due to corrosion of the sacrificial (Anode A)

You have not discussed anything about RMSD and Mass loss relationship. Highlight this that how much percentage has been observed under accelerated condition

4.3 100mV Depolarisation test on anode embedded Slab

The 100 mV depolarization test results using the half-cell potential method assess the effectiveness of cathodic protection in mitigating corrosion risk for steel reinforcement in concrete. By comparing potential readings with and without disconnection, engineers can determine if the 100 mV criterion is met, indicating sufficient corrosion protection. The

observed potential drop within 24 hours of disconnection confirms the protective system's adequacy and the stability of the steel reinforcement environment. This evaluation is essential for ensuring the structural integrity and longevity of concrete structures, thereby preventing premature degradation and reducing maintenance costs.

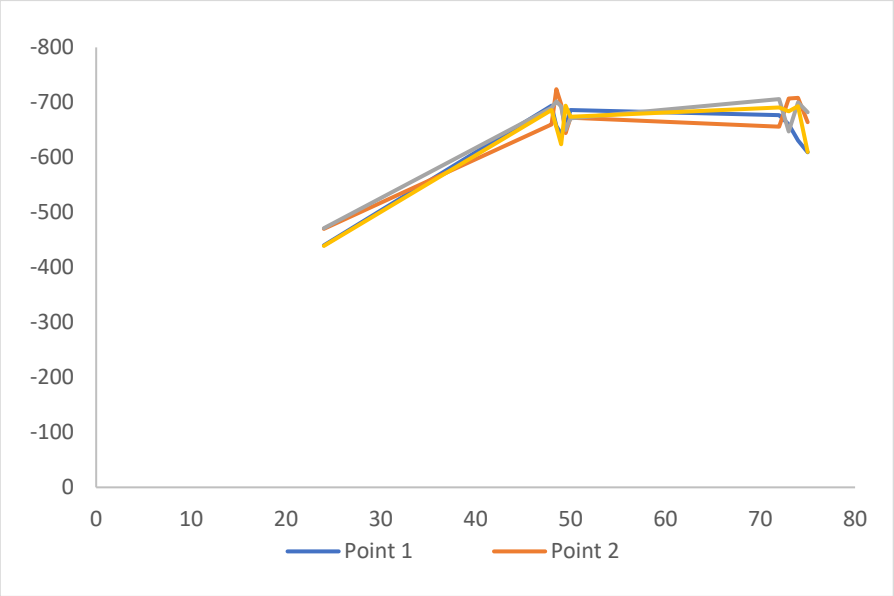

Figure 4. 16 ON-Potential reading of slab with time

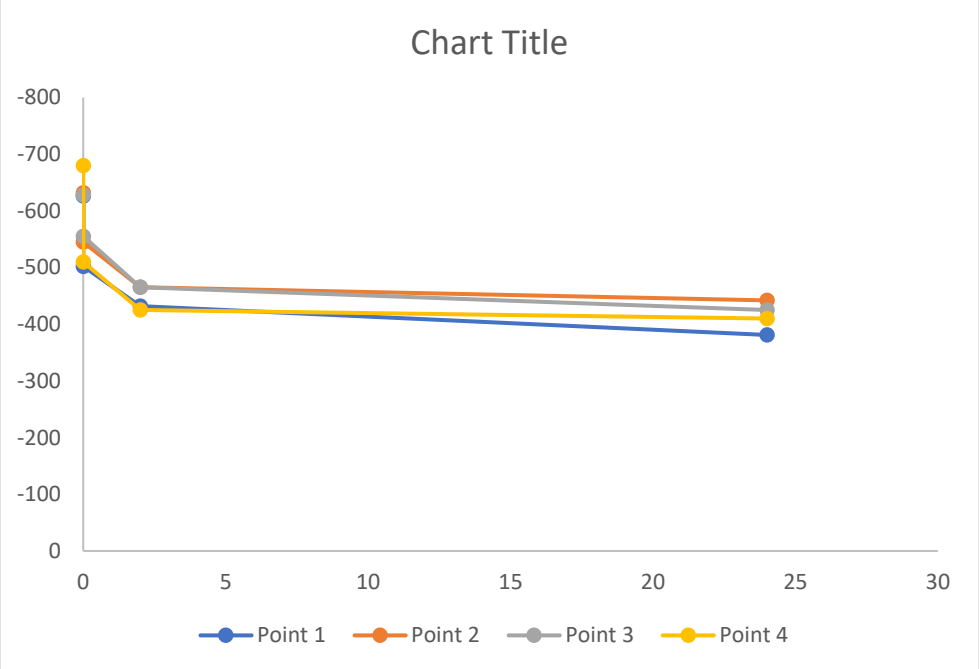

Figure 4. 17 100mV Depolarization after a week

The 100 mV depolarization test results from the half-cell potential method demonstrate the effectiveness of cathodic protection in reducing the corrosion risk for steel reinforcement embedded in concrete. Figure 4. 18 presents potential readings without disconnection, showing how the electrical potential difference between the reference electrode and the steel changes over time under continuous polarization. These readings help establish a baseline for assessing potential shifts that indicate adequate corrosion protection. In contrast, Figure 4. 19 details the potential measurements taken with disconnection, highlighting the depolarization effect after the protective current is removed. The significant potential drop observed from the initial readings to the 24-hour measurements demonstrates that the 100 mV depolarization criterion is met. This criterion is crucial in verifying the effectiveness of cathodic protection, as a reduction of at least 100 mV in potential within 24 hours of disconnection signifies adequate corrosion prevention. The fulfilment of this criterion confirms a low likelihood of active corrosion, as evidenced by the potential readings shifting to more positive values, indicating a stable and protective environment for the steel reinforcement. By using the half-cell potential method, engineers can effectively monitor and ensure the structural integrity and longevity of concrete structures, preventing costly repairs and extending their lifespan.

4.4 Linear Polarization Resistance (LPR)/ Corrosion Rate (CR)

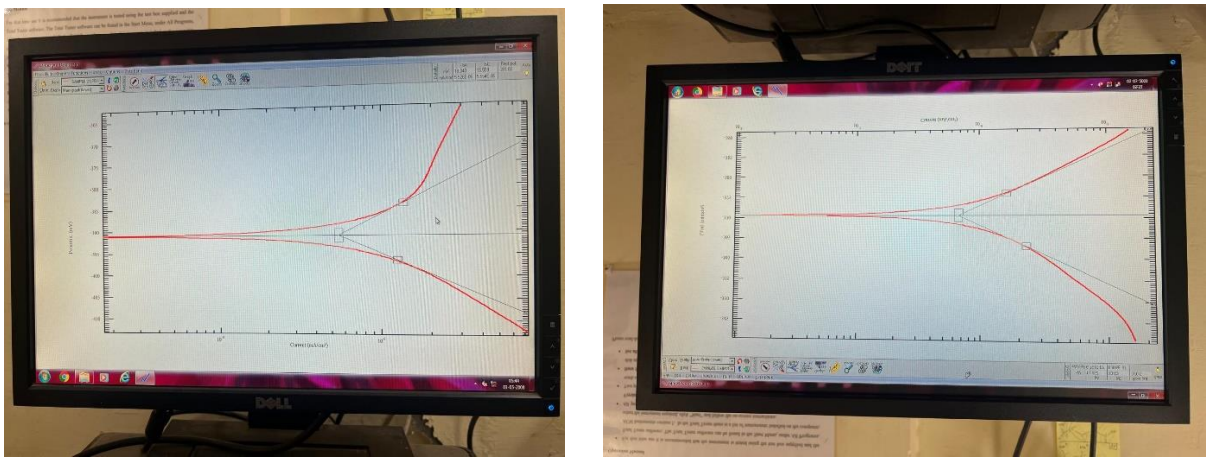

Figure 4. 20 Initial and Final Tafel point graph (LPR)

After the Initial LPR Test, which showed a relatively high corrosion rate of 0.048086 mm/year, a sacrificial anode (Anode A) was embedded in the slab. The presence of this sacrificial anode significantly altered the electrochemical behavior of the steel. As a more reactive metal, Anode A corrodes preferentially, sacrificing itself to protect the steel. This protective mechanism shifts the steel to a cathodic state, drastically reducing its corrosion rate. In the Final LPR Test, this change is evident: the corrosion rate drops to 0.008468 mm/year, which is much lower than in the Initial LPR Test. Furthermore, the Linear Polarization Resistance (LPR) increased substantially, and the corrosion current density (Icorr) decreased, confirming a substantial reduction in the steel's susceptibility to corrosion. This demonstrates that the sacrificial anode effectively mitigated the corrosion process by altering the electrochemical dynamics of the system, proving the anode's role in enhancing the steel's durability.

4.5 Life Span of Anode

In sacrificial anode cathodic protection (SACP), monitoring RMSD% (Root Mean Square Deviation percentage) is crucial for evaluating the anode's degradation and effectiveness. Initially, the anode's RMSD% is low, reflecting its intact condition and effective protection. As the anode corrodes, RMSD% increases due to material loss and changes in the resonant frequency detected by the PZT (Lead Zirconate Titanate) transducer. This rising RMSD% indicates ongoing degradation and reduced effectiveness in protecting the rebar. In advanced stages, although RMSD% may stabilize or slightly decrease as the anode nears the end of its life, it still provides valuable insights into the anode's condition. The correlation between RMSD% and mass loss (Δm) confirms that increasing RMSD% parallels the physical degradation of the anode. Thus, RMSD% is an effective indicator for assessing when maintenance or replacement is needed to ensure continued corrosion protection.

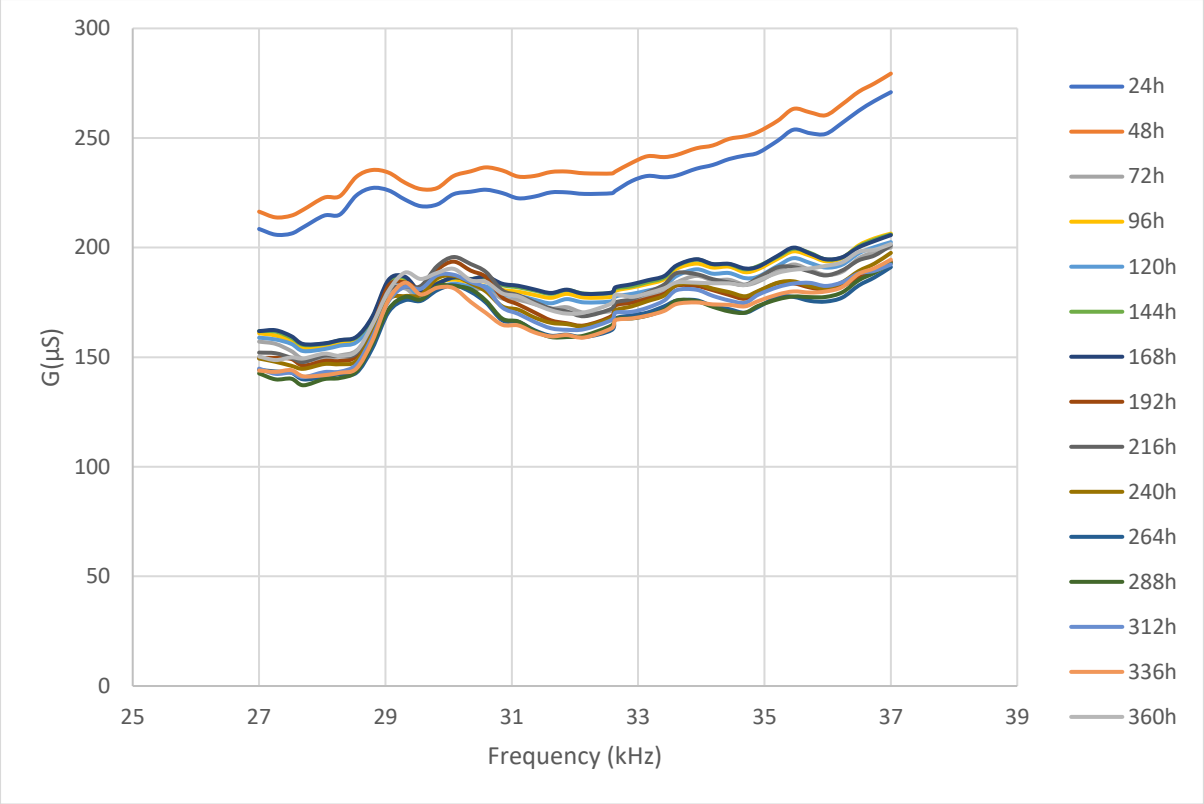

Figure 4. 21 CONDUCTANCE G(µS) using LCR meter

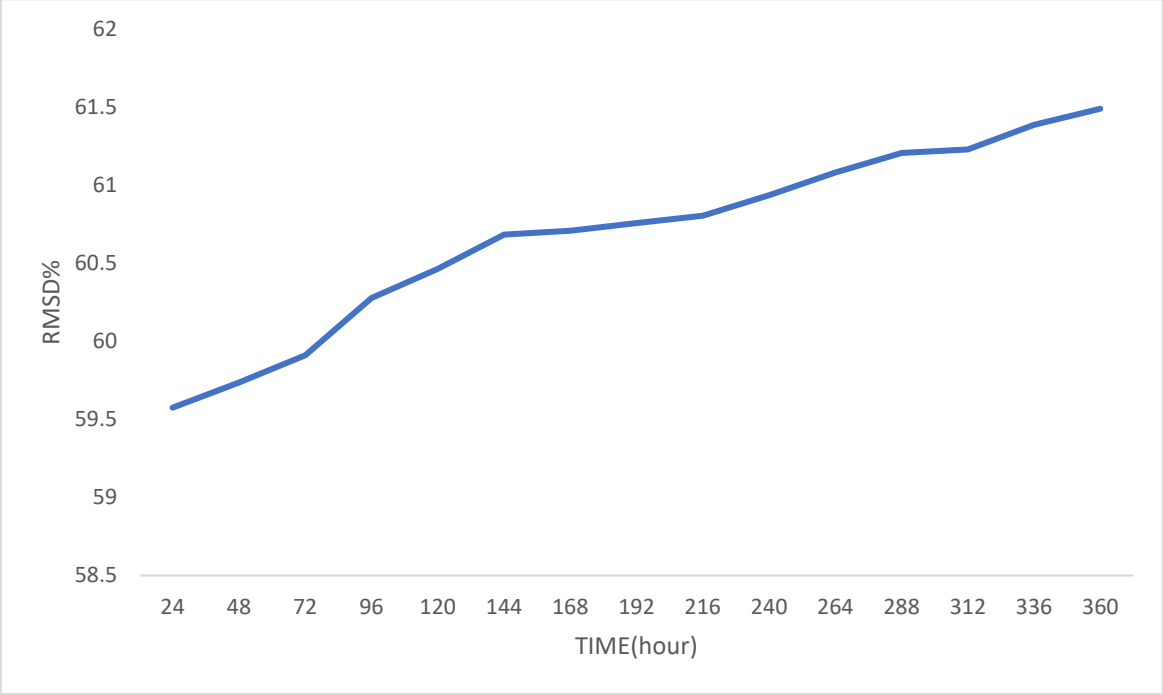

Figure 4. 22 Time V/S RMSD %

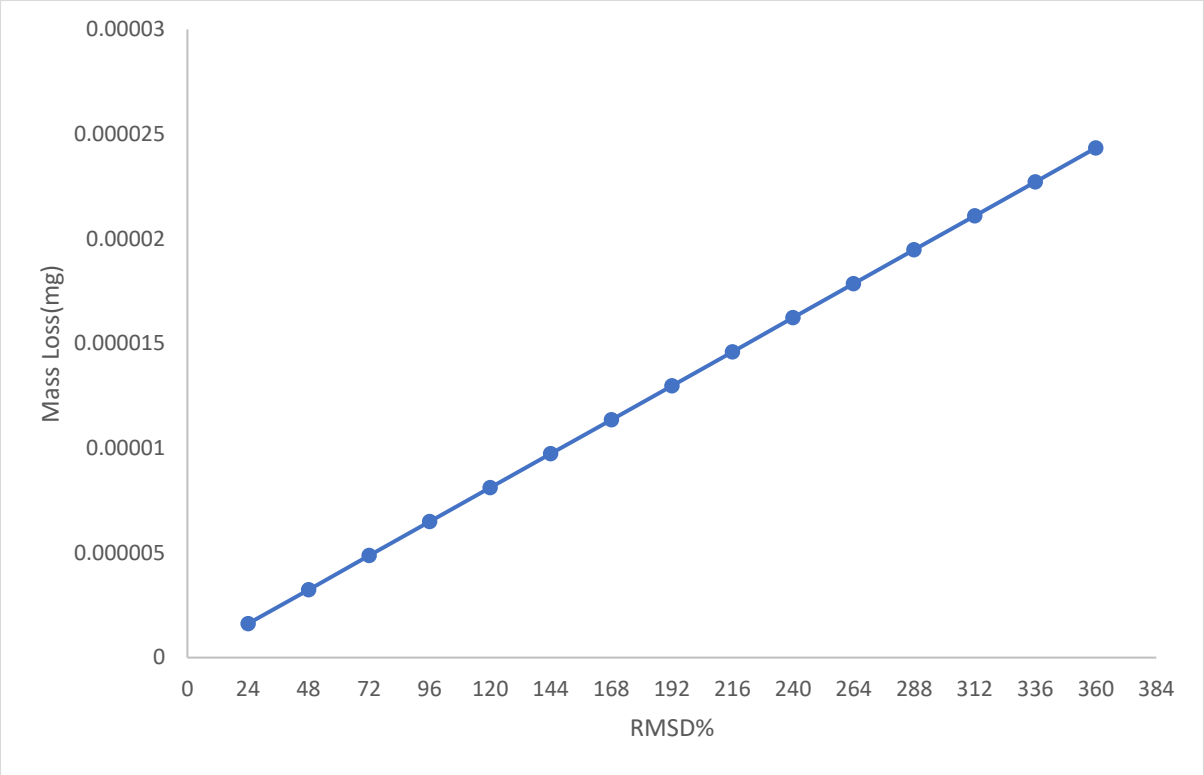

Figure 4. 23 Time V/S Mass Loss

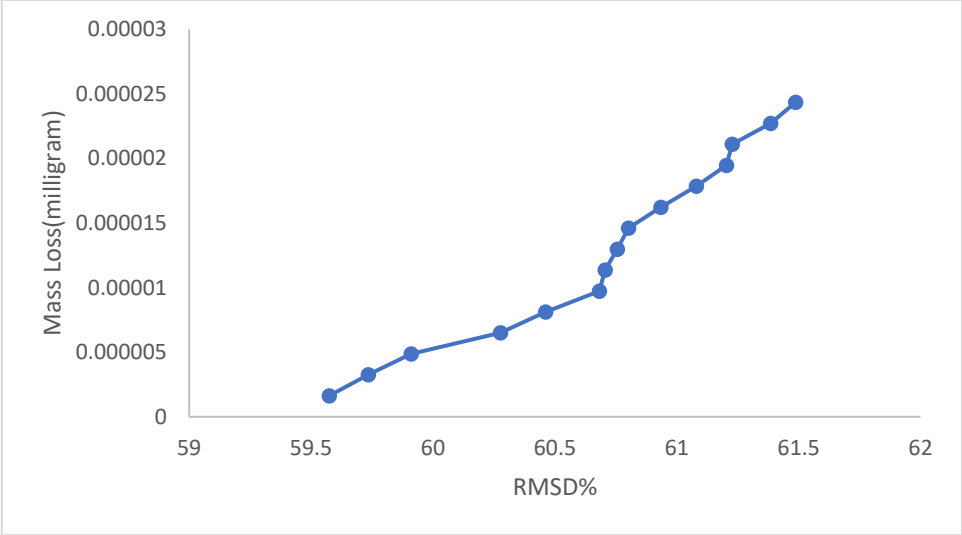

Figure 4. 24 RMSD% V/S Mass Loss

Table 4. 1 Mass Loss with RMSD% & Time

Time	RMSD%	Δm (milligrams)
0	0	0
24	59.57429	0.001622
48	59.73483	0.003245
72	59.9098	0.004867
96	60.27685	0.00649
120	60.46176	0.008112
144	60.68249	0.009734
168	60.70602	0.011357
192	60.75547	0.012979
216	60.80248	0.014602
240	60.93469	0.016224
264	61.07996	0.017846
288	61.20356	0.019469
312	61.22747	0.021091
336	61.38444	0.022714
360	61.48708	0.024336

In sacrificial anode cathodic protection (SACP), monitoring RMSD% provides critical insights into the anode's degradation and overall effectiveness of the protection system.

At the initial stage, when the sacrificial anode is first introduced, it begins its role of protecting the rebar by corroding preferentially. The anode's material is relatively intact at this point, so the RMSD% is low. This low value signifies that the PZT (Lead Zirconate Titanate) transducer is detecting the resonant frequency of an anode that remains in good condition, indicating minimal degradation and effective initial protection.

As the anode continues to function, it corrodes over time, leading to material loss and structural changes such as increased porosity. The resulting shift in the anode's material properties causes a change in the resonant frequency detected by the PZT transducer. Consequently, RMSD% starts to increase. This increase reflects the extent of corrosion and the ongoing degradation of

the anode. An increasing RMSD% at this stage confirms that the anode is actively sacrificing itself to protect the rebar, with the anode's material progressively consumed.

In the advanced stages of anode degradation, the RMSD% continues to rise. This increase signifies substantial material loss and a significant shift in the resonant frequency due to the anode's deteriorated condition. The rising RMSD% indicates that the anode has undergone extensive corrosion and is progressively becoming less effective in protecting the rebar.

Eventually, as the sacrificial anode approaches the end of its useful life, the RMSD% might stabilize or show a slight decrease. This stabilization or decrease occurs because the anode has been largely consumed, resulting in reduced material to cause further frequency changes. Although the anode's effectiveness in providing protection might diminish, the RMSD% still provides valuable information about the extent of degradation and the overall condition of the anode.

The graphs clearly show that as the RMSD% increases, there is a corresponding and progressive increase in the mass loss (Δm) of the sacrificial anode. This relationship underscores the connection between the resonant frequency shift and the physical degradation of the anode material. As the anode sacrifices itself to protect the rebar, it undergoes material loss, which is reflected in both the rising RMSD% and the increased mass loss. This parallel increase confirms that RMSD% is an effective indicator of the anode's condition and provides a quantitative measure of its ongoing degradation. This information can be crucial for determining the optimal time for maintenance or replacement to ensure continuous protection of the rebar.

4.6 Long-term viability of galvanic anodes

Analysing the output current of the galvanic anode over time to evaluate its effectiveness in providing corrosion protection and to determine its remaining service life. Monitoring these

changes helps assess the anode's long-term performance and informs maintenance decisions to ensure continued protection of the rebar.

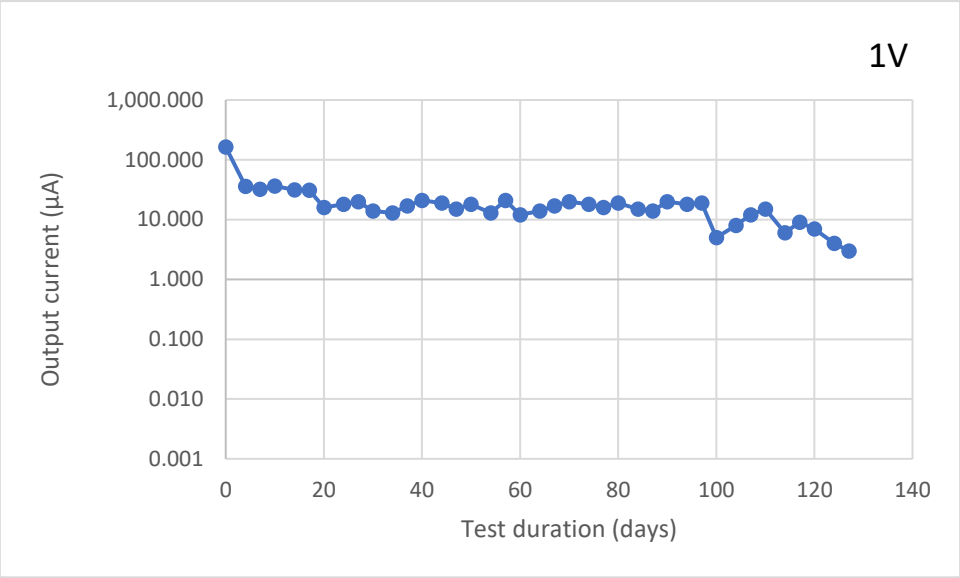

Figure 4. 25 Performance of galvanic anodes evaluated using GAP test

The graph illustrates the output current (in microamperes) over a 127-day period for a galvanic anode under a 1V potential. Initially, there is a sharp decrease in the output current, dropping from 163.8 µA on day 0 to 36.02 µA by day 4. This rapid decline likely reflects the initial high rate of corrosion as the anode begins to protect the embedded rebar. After this initial drop, the current stabilizes somewhat, fluctuating between 10 µA and 36 µA for the majority of the test duration. This relatively stable period indicates that the anode is still actively supplying current, though at a reduced rate compared to the initial days.

From around day 100 onward, there is a noticeable decline in current, with values falling as low as 5 µA by day 100 and continuing to decrease, reaching just 3 µA by the end of the test on day 127. This decline suggests that the anode may be nearing the end of its service life, as it can no longer maintain the higher current levels necessary for effective corrosion protection. The overall trend of the graph indicates that while the galvanic anode remains functional for a

significant portion of the test period, its performance becomes less stable toward the later stages of the test.

This data highlights the importance of monitoring current output over time to assess the long-term viability of galvanic anodes in providing adequate protection against corrosion. The anode shows a high initial activity that gradually tapers off, indicating that the process of protecting the underlying metal is dynamic and subject to changes over time. These observations can help inform decisions about the design and maintenance of structures that rely on galvanic anodes for corrosion protection.

4.7 Optimal time to replace a sacrificial anode

1. Output Current: The output current is a direct measure of the anode's effectiveness in providing protection. A significant and sustained decline in current over time indicates that the anode is losing its ability to protect the structure. For example, if the output current drops below a threshold value that is considered effective for the system, it is a signal that replacement may be necessary.

2. RMSD%: RMSD% reflects the anode's material degradation. An increasing RMSD% indicates that the anode's structural integrity is compromised. If RMSD% reaches a level where it suggests substantial material loss or degradation (e.g., nearing the highest recorded values), it is a sign that the anode's effectiveness is diminishing.

3. Mass Loss (Δm): Tracking mass loss provides insight into how much of the anode material has been consumed. If mass loss accumulates to a point where the anode has significantly eroded (e.g., if Δm approaches the maximum allowable or expected consumption level), it indicates that the anode is nearing the end of its useful life.

Replacement Timing: Typically, an anode should be replaced when output current drops below the minimum required level, RMSD% shows significant degradation, and mass loss

indicates substantial material consumption. Monitoring these indicators regularly ensures timely replacement, preventing inadequate protection and extending the lifespan of the structure.

CHAPTER 5 CONCULSIONS

The study investigates the long-term effectiveness of galvanic anodes in reinforced concrete structures by employing various testing and measurement techniques. The findings provide valuable insights into corrosion protection mechanisms, emphasizing the need for continuous monitoring to maintain the integrity and durability of these structures.

1. Initial High Protection Activity: The sharp decrease in output current observed in the galvanic anode tests indicates a high rate of initial corrosion protection, which stabilizes over time before declining as the anode nears the end of its service life.
2. Importance of Continuous Monitoring: The study emphasizes the need for continuous monitoring of galvanic anodes to ensure sustained corrosion protection, especially as the anode's effectiveness decreases over time.
3. Frequency Analysis Insights: Conductance measurements reveal that the placement and immersion conditions of PZT (Lead Zirconate Titanate) significantly impact its resonance behavior, with immersion aligning PZT’s response with that observed on the anode.
4. Comparison of Anode Materials: The Anode A anode outperforms the Anode B anode in accelerated corrosion experiments, demonstrating greater stability and resistance to degradation, making it a more reliable material for long-term corrosion protection.
5. RMSD% as a Degradation Indicator: The use of RMSD% as an indicator effectively tracks the degradation of sacrificial anodes over time, offering valuable insights into the anode's condition and its ability to protect the underlying rebar.
6. Conductance as a Corrosion Measure: Conductance data over different time intervals highlights the progressive nature of corrosion in reinforced concrete, with increasing conductance values indicating more advanced stages of corrosion.

7. Effectiveness of Cathodic Protection: The 100 mV depolarization test results confirm that cathodic protection is effective in minimizing corrosion risk, with potential readings shifting to more positive values, indicating a stable and protective environment for steel reinforcement.
8. Challenges of Anode B Anode: The Anode B anode exhibited suboptimal performance under test conditions, failing to meet the necessary standards for sustained use, as evidenced by its early failure and erratic conductance behavior.
9. Life Span Prediction: Monitoring RMSD% allows for predicting the life span of sacrificial anodes, with increasing RMSD% signaling progressive degradation and a nearing end of the anode's useful life.
10. Impact of Corrosion on Structural Integrity: The study reinforces the critical importance of using advanced monitoring techniques to assess the extent of corrosion and ensure the structural integrity of reinforced concrete structures, ultimately prolonging their lifespan

CHAPTER 6 REFERENCES

Aslam, R. *et al.* (2022) 'A comprehensive review of corrosion inhibitors employed to mitigate stainless steel corrosion in different environments', *Journal of Molecular Liquids*. Elsevier B.V. Available at: https://doi.org/10.1016/j.molliq.2022.119992.

Astuti, P. *et al.* (2019) 'Application of sacrificial anode cathodic protection for partially repaired RC beams damaged by corrosion', *Proceeding of 4th International Symposium on Concrete and Structures (CSN2019)*, (January), pp. 284–291.

Büchler, M. (2020) 'On the Mechanism of Cathodic Protection and Its Implications on Criteria Including AC and DC Interference Conditions', *Corrosion*, 76(5), pp. 451–463. Available at: https://doi.org/10.5006/3379.

Byrne, A., Norton, B. and Holmes, N. (2015) 'State-of-the-art review of cathodic protection for reinforced concrete structures'.

Deshpande, P. *et al.* (2021) 'Impressed current cathodic protection (ICCP) of mild steel in association with zinc based paint coating', *Materials Today: Proceedings*, 50, pp. 1660–1665. Available at: https://doi.org/10.1016/j.matpr.2021.09.145.

Elyoussfi, A. *et al.* (2023) 'Corrosion inhibitors of alloys and metals in acidic solution: A bibliometric analysis from 2010 to 2022', *International Journal of Corrosion and Scale Inhibition*, 12(2), pp. 722–740. Available at: https://doi.org/10.17675/2305-6894-2023-12-2-19.

Farh, H.M.H., Ben Seghier, M.E.A. and Zayed, T. (2023) 'A comprehensive review of corrosion protection and control techniques for metallic pipelines', *Engineering Failure Analysis*, 143. Available at: https://doi.org/10.1016/j.engfailanal.2022.106885.

Farhana Zainal, F. *et al.* (2020) 'Corrosion Control by Using Aluminium as Sacrificial Anode Cathodic Protection (SACP) in Geopolymer Reinforced Concrete', *IOP Conference Series: Materials Science and Engineering*, 864(1). Available at: https://doi.org/10.1088/1757-

899X/864/1/012039.

Farooq, A. *et al.* (2019) 'Evaluating the performance of zinc and aluminum sacrificial anodes in artificial seawater', *Electrochimica Acta*, 314, pp. 135–141. Available at: https://doi.org/10.1016/j.electacta.2019.05.067.

Goyal, A. *et al.* (2018) 'A Review of Corrosion and Protection of Steel in Concrete', *Arabian Journal for Science and Engineering*. Springer Verlag, pp. 5035–5055. Available at: https://doi.org/10.1007/s13369-018-3303-2.

Goyal, A. *et al.* (2020) 'Potential and current distribution across different layers of reinforcement in reinforced concrete cathodic protection system- A numerical study', *Construction and Building Materials*, 262, p. 120580. Available at: https://doi.org/10.1016/j.conbuildmat.2020.120580.

Goyal, A., Pouya, H.S. and Ganjian, E. (2023) 'Electrochemical Performance of Concrete Conductive Anode Paint Used as an Impressed Current Anode Material', 35(7), pp. 1–14. Available at: https://doi.org/10.1061/JMCEE7.MTENG-15550.

Goyal, A., Sadeghi, H. and Ganjian, E. (2019) 'Performance assessment of specialist conductive paint for cathodic protection of steel in reinforced concrete structures', *Construction and Building Materials*, 223, pp. 1083–1094. Available at: https://doi.org/10.1016/j.conbuildmat.2019.07.344.

Harahap, S. *et al.* (2023) 'Comparison between sacrificial anode cathodic protection and impress current cathodic protection in concrete structures: A review', *Xvii Mexican Symposium on Medical Physics*, 2947(April 2018), p. 090001. Available at: https://doi.org/10.1063/5.0154303.

Hire, J.H., Hosseini, S. and Moradi, F. (2021) 'Optimum pzt patch size for corrosion detection in reinforced concrete using the electromechanical impedance technique', *Sensors*, 21(11). Available at: https://doi.org/10.3390/s21113903.

Jawad, M.N., Amouzad Mahdiraji, G. and Hajibeigy, M.T. (2020) 'Performance improvement of sacrificial anode cathodic protection system for above ground storage tank', *SN Applied Sciences*, 2(12), pp. 1–8. Available at: https://doi.org/10.1007/s42452-020-03823-7.

Krishnan, N. *et al.* (2021) 'Long-term performance and life-cycle-cost benefits of cathodic protection of concrete structures using galvanic anodes', *Journal of Building Engineering*, 42(February), p. 102467. Available at: https://doi.org/10.1016/j.jobe.2021.102467.

Lambert, P. *et al.* (2015) 'Dual function carbon fibre fabric strengthening and impressed current cathodic protection (ICCP) anode for reinforced concrete structures', *Materials and Structures/Materiaux et Constructions*, 48(7), pp. 2157–2167. Available at: https://doi.org/10.1617/s11527-014-0300-0.

Liu, P. *et al.* (2020) 'Corrosion monitoring of the reinforced concrete by using the embedded annular piezoelectric transducer', *Journal of Materials Research and Technology*, 9(3), pp. 3511–3519. Available at: https://doi.org/10.1016/j.jmrt.2020.01.088.

Martinelli-orlando, F., Mundra, S. and Angst, U.M. (no date) 'Mechanism of cathodic protection of iron and steel in porous media', (August 2023).

Morwal, T. *et al.* (2023) 'Monitoring chloride-induced corrosion in metallic and reinforced/prestressed concrete structures using piezo sensors-based electro-mechanical impedance technique: A review', *Measurement: Journal of the International Measurement Confederationfile:///C:/Users/DELL/Downloads/sacp.pdf*, 218(February), p. 113102. Available at: https://doi.org/10.1016/j.measurement.2023.113102.

Oleiwi, H.M. *et al.* (2018) 'An experimental study of cathodic protection for chloride contaminated reinforced concrete', *Materials and Structures/Materiaux et Constructions*, 51(6), pp. 1–11. Available at: https://doi.org/10.1617/s11527-018-1273-1.

Polder, R. and Peelen, W. (2018) 'Cathodic protection of steel in concrete-experience and overview of 30 years application', in *MATEC Web of Conferences*. EDP Sciences. Available

at: https://doi.org/10.1051/matecconf/201819901002.

Poltavtseva, M., Ebell, G. and Mietz, J. (2015) 'Electrochemical investigations of carbon - based conductive coatings for application as anodes in ICCP systems of reinforced concrete structures', (7), pp. 627–634. Available at: https://doi.org/10.1002/maco.201407680.

Quale, G. *et al.* (2017) 'Cathodic protection by distributed sacrificial anodes - A new cost-effective solution to prevent corrosion of subsea structures', *NACE - International Corrosion Conference Series*, 2(March), pp. 949–963.

Sadeghi, K., Musa, M.K. and Nassrullah, H.M. (2019) 'Corrosion problems in RC structures : An overview of causes , mechanism, effects, controls and evaluation', *Academic Research International*, 10(2), pp. 15–28.

Shi, W. *et al.* (2019) 'Corrosion investigation of reinforced concrete based on piezoelectric smart materials', *Materials*, 12(3). Available at: https://doi.org/10.3390/ma12030519.

Syaiful, M., Sujitha, B. and Vedalakshmi, R. (2014) 'Light-weight cementitious conductive anode for impressed current cathodic protection of steel reinforced concrete application', *CONSTRUCTION & BUILDING MATERIALS*, 71, pp. 167–180. Available at: https://doi.org/10.1016/j.conbuildmat.2014.08.032.

Talakokula, V. *et al.* (2016) 'Diagnosis of carbonation induced corrosion initiation and progression in reinforced concrete structures using piezo-impedance transducers', *Sensors and Actuators, A: Physical*, 242, pp. 79–91. Available at: https://doi.org/10.1016/j.sna.2016.02.033.

Tamhane, D. *et al.* (2021) 'Smart cathodic protection system for real-time quantitative assessment of corrosion of sacrificial anode based on electro-mechanical impedance (EMI)', *IEEE Access*, 9, pp. 12230–12240. Available at: https://doi.org/10.1109/ACCESS.2021.3051953.

Tamhane, D. *et al.* (2022) 'Performance evaluation of electro-mechanical impedance based

state of health estimation of sacrificial anodes in reinforced concrete structures', *Construction and Building Materials*, 342(May). Available at: https://doi.org/10.1016/j.conbuildmat.2022.128034.

Verma, C. *et al.* (2018) 'An overview on plant extracts as environmental sustainable and green corrosion inhibitors for metals and alloys in aggressive corrosive media', *Journal of Molecular Liquids*. Elsevier B.V., pp. 577–590. Available at: https://doi.org/10.1016/j.molliq.2018.06.110.

Wang, D. *et al.* (2010) 'Experimental and numerical study on damage detection in I-type steel beam based on PZT admittance signals', *Proceedings of the 12th International Conference on Engineering, Science, Construction, and Operations in Challenging Environments - Earth and Space 2010*, 41096(March 2015), pp. 2369–2375. Available at: https://doi.org/10.1061/41096(366)219.

Wang, F. *et al.* (2020) 'A comparative investigation on cathodic protections of three sacrificial anodes on chloride-contaminated reinforced concrete', *Construction and Building Materials*, 246, pp. 1–10. Available at: https://doi.org/10.1016/j.conbuildmat.2020.118476.

Zabihi-Samani, M. *et al.* (2018) 'Simulation of the Behavior of Corrosion Damaged Reinforced Concrete Beams with/without CFRP Retrofit', *Civil Engineering Journal*, 4(5), p. 958. Available at: https://doi.org/10.28991/cej-0309148.

Preston, J. (2019) TN23 Cathodic Protection for New Structures. Bordon, UK: Corrosion Prevention Association